ΠΑΝΕΠΙΣΤΗΜΙΟ ΘΕΣΣΑΛΙΑΣ
ΠΟΛΥΤΕΧΝΙΚΗ ΣΧΟΛΗ
ΤΜΗΜΑ ΜΗΧΑΝΟΛΟΓΩΝ ΜΗΧΑΝΙΚΩΝ ΒΙΟΜΗΧΑΝΙΑΣ
ΕΡΓΑΣΤΗΡΙΟ ΘΕΡΜΟΔΥΝΑΜΙΚΗΣ & ΘΕΡΜΙΚΩΝ ΜΗΧΑΝΩΝ

Μεταπτυχιακή Εργασία

ΕΝΕΡΓΕΙΑΚΗ ΠΡΟΣΟΜΟΙΩΣΗ ΜΕΤΑΒΑΤΙΚΗΣ ΛΕΙΤΟΥΡΓΙΑΣ ΣΥΣΤΗΜΑΤΟΣ ΤΡΙ-ΣΥΜΠΑΡΑΓΩΓΗΣ ΣΥΝΔΥΑΣΜΕΝΟΥ ΚΥΚΛΟΥ ΜΕ ΚΑΥΣΗ ΦΥΣΙΚΟΥ ΑΕΡΙΟΥ

υπό

ΟΛΥΜΠΙΑΣ ΖΩΓΟΥ
Διπλωματούχου Μηχανολόγου Μηχανικού Α.Π.Θ., 1988

Υπεβλήθη για την εκπλήρωση μέρους των

απαιτήσεων για την απόκτηση του

Μεταπτυχιακού Διπλώματος Ειδίκευσης

Βόλος, Ιούνιος 2007

Η έγκριση της μεταπτυχιακής εργασίας από το Τμήμα Μηχανολόγων Μηχανικών Βιομηχανίας της Πολυτεχνικής Σχολής του Πανεπιστημίου Θεσσαλίας δεν υποδηλώνει αποδοχή των απόψεων του συγγραφέα (Ν. 5343/32 αρ. 202 παρ. 2).

Εγκρίθηκε από τα Μέλη της Πενταμελούς Εξεταστικής Επιτροπής:

Πρώτος Εξεταστής (Επιβλέπων)	Δρ. Αναστάσιος Σταμάτης Επίκουρος Καθηγητής, Τμήμα Μηχανολόγων Μηχανικών Βιομηχανίας, Πανεπιστήμιο Θεσσαλίας
Δεύτερος Εξεταστής	Δρ. Νικόλαος Βλάχος Καθηγητής, Καθηγητής, Τμήμα Μηχανολόγων Μηχανικών Βιομηχανίας, Πανεπιστήμιο Θεσσαλίας
Τρίτος Εξεταστής	Δρ. Κωνσταντίνος Παπαδημητρίου Καθηγητής, Τμήμα Μηχανολόγων Μηχανικών Βιομηχανίας, Πανεπιστήμιο Θεσσαλίας
Τέταρτος Εξεταστής	Δρ. Ερρίκος Σταπουντζής Αναπληρωτής Καθηγητής, Τμήμα Μηχανολόγων Μηχανικών Βιομηχανίας, Πανεπιστήμιο Θεσσαλίας
Πέμπτος Εξεταστής	Δρ. Γεώργιος Λυμπερόπουλος Αναπληρωτής Καθηγητής, Τμήμα Μηχανολόγων Μηχανικών Βιομηχανίας, Πανεπιστήμιο Θεσσαλίας

Ευχαριστίες

Από τη θέση αυτή θα ήθελα να ευχαριστήσω τον επιβλέποντα, Επίκουρο Καθηγητή κ. Αναστάσιο Σταμάτη, για την εμπιστοσύνη και καθοδήγησή του στην εκπόνηση της μεταπτυχιακής εργασίας μου, καθώς και τα υπόλοιπα μέλη της Συμβουλευτικής Επιτροπής, Καθηγητή Νικόλαο Βλάχο για τις πολύτιμες συμβουλές του, και Καθηγητή Κων/νο Παπαδημητρίου για τις ωφέλιμες υποδείξεις του. Θα ήθελα επίσης να ευχαριστήσω τα μέλη της Εξεταστικής Επιτροπής Αναπληρωτές Καθηγητές Ερρίκο Σταπουντζή και Γεώργιο Λυμπερόπουλο για τις εν γένει υποδείξεις τους που συνέβαλαν στη βελτίωση της παρουσίασης της εργασίας αυτής.

Ολυμπία Ζώγου

ΕΝΕΡΓΕΙΑΚΗ ΠΡΟΣΟΜΟΙΩΣΗ ΜΕΤΑΒΑΤΙΚΗΣ ΛΕΙΤΟΥΡΓΙΑΣ ΣΥΣΤΗΜΑΤΟΣ ΤΡΙ-ΣΥΜΠΑΡΑΓΩΓΗΣ ΣΥΝΔΥΑΣΜΕΝΟΥ ΚΥΚΛΟΥ ΜΕ ΚΑΥΣΗ ΦΥΣΙΚΟΥ ΑΕΡΙΟΥ

Ολυμπία Ζώγου

Πανεπιστήμιο Θεσσαλίας, Τμήμα Μηχανολόγων Μηχανικών Βιομηχανίας, 2007

Επιβλέπων Καθηγητής: Δρ. Αναστάσιο Σταμάτης, Επίκουρος Καθηγητής

Περίληψη

Η συμπαραγωγή ηλεκτρικής – θερμικής – ψυκτικής ισχύος διεισδύει όλο και περισσότερο στην παγκόσμια αγορά ενέργειας. Στην εργασία παρουσιάζεται η χρήση της δυναμικής προσομοίωσης στο σχεδιασμό συστημάτων συμπαραγωγής. Παραδοσιακά ο σχεδιασμός αυτών των συστημάτων γίνεται με βάση τυπικές τιμές των χαρακτηριστικών μόνιμης λειτουργίας τους. Η δυναμική προσομοίωση εισάγεται με στόχο την βελτίωση του σχεδιασμού των συστημάτων συμπαραγωγής, ώστε να λαμβάνει υπόψη τις ημερήσιες και εποχιακές διακυμάνσεις της παραγωγής και ζήτησης ηλεκτρικής, θερμικής και ψυκτικής ισχύος. Το σύστημα συμπαραγωγής που μελετάται βασίζεται σε συνδυασμένο κύκλο αεριοστροβίλου – ατμοστροβίλων, με ενδιάμεση απομάστευση ατμού διεργασίας, καθώς και εκμετάλλευση θερμικής ισχύος σε διάφορα επίπεδα θερμοκρασιών. Για την ανάπτυξη του μοντέλου δυναμικής προσομοίωσης συμπαραγωγής χρησιμοποιήσαμε τα ενεργειακά δεδομένα του Νοσοκομείου του Βόλου. Παρουσιάζεται αναλυτικά το σύστημα συμπαραγωγής καθώς και τα επιμέρους δομικά στοιχεία (components) του ενεργειακού συστήματος. Επίσης παρουσιάζονται και σχολιάζονται αποτελέσματα από την ενεργειακή προσομοίωση στη διάρκεια ενός τυπικού μετεωρολογικού έτους καθώς και οι θερμοδυναμικοί συντελεστές που επηρεάζουν τον σχεδιασμό και την βελτιστοποίηση του. Τέλος παρουσιάζεται μία συγκριτική παραμετρική ανάλυση διαφορετικού μεγέθους συστημάτων, καθώς και μια απλή οικονομική ανάλυση της απόδοσής τους με στόχο την κατάδειξη της βέλτιστης λύσης.

TABLE OF CONTENTS

Abstract

This study demonstrates the use of transient simulation in the design of tri-generation systems. Traditionally, the in-use methodologies for the design of cogeneration systems are usually based on the system's steady state operation characteristics. Transient modelling is introduced as a means of supporting an improved cogeneration system design and optimization methodology. A hospital tri-generation system is selected as a case study for the development of the transient simulation. The development of the transient simulation model in the TRNSYS simulation environment is presented, along with a description of the component models employed. The details and results of a yearly simulation of the tri-generation system are presented and discussed, and yearly statistics are carried out and certain indices are evaluated to aid the design process. Finally is presented a comparative parametric analysis of different size of systems, as well as a simple economic analysis of their output aiming at the most optimal solution.

List of Figures

List of Tables

Nomenclature

Symbol	Units	Meaning
C	-	Losses factor
D	-	Steam
e_H	-	Carnot factor
e	kJ/kg	Specific Flow Exergy
e_D	-	Exergy factor of steam (Carnot factor)
EHR	-	Electrical to Heat ratio
EUF	-	Energy Utilisation Factor
hi	kJ/kg	Specific enthalpy at state i
HRSG		Heat Recovery Steam Generator
m	kg/s	Mass flow rate
pi	MPa	Pressure at state i
Pel	kW	Electrical Power
PHR		Power-to-heat ratio
P_T	kW	Turbine Power
Q_{Cond}	kJ	Condensation Energy
Q_F	kJ	Energy supplied by fuel
Q_H	kJ	Thermal energy
r (pi)	kJ/kg	Condensation enthalpy at pressure pi
R	-	Exhaust gases
SPP	y	Simple Payback Period of investment
T	K	Temperature

Greek Symbols

σ	-	Ratio of electrical-to heat energy output
η	-	Efficiency
η_m	-	Mechanical .efficiency
n_s	-	Isentropic efficiency
η_{exp}	-	Total exploitation factor
η_{el}	-	Electrical efficiency = electrical output [kW] / fuel input [kW]

Overall efficiency Useful thermal + electrical output [kW] / fuel input [kW]

1 Introduction

During the operation of a conventional power plant, large quantities of heat are rejected in the atmosphere either through the cooling circuits (steam condensers, cooling towers, water coolers in Diesel or Otto engines, etc.) or with the exhaust gases. Most of this heat can be recovered and used to cover thermal needs, thus increasing the (energetic) efficiency from 30-50% of a power plant to 80-90% of a cogeneration system. A comparison between cogeneration and the separate production of electricity and heat from the point of view of efficiency is given in Figure 1, based on typical values of efficiencies.

Cogeneration first appeared in late 1880.s in Europe and the U.S.A. During the early parts of the 20th century most industrial plants generated their own electricity using coal-fired boilers and steam turbine generators. Many of the plants used the exhaust steam for industrial processes. It has been estimated that as much as 58% of the total power produced by on-site industrial power plants in the U.S.A. in the early 1900's was cogenerated.

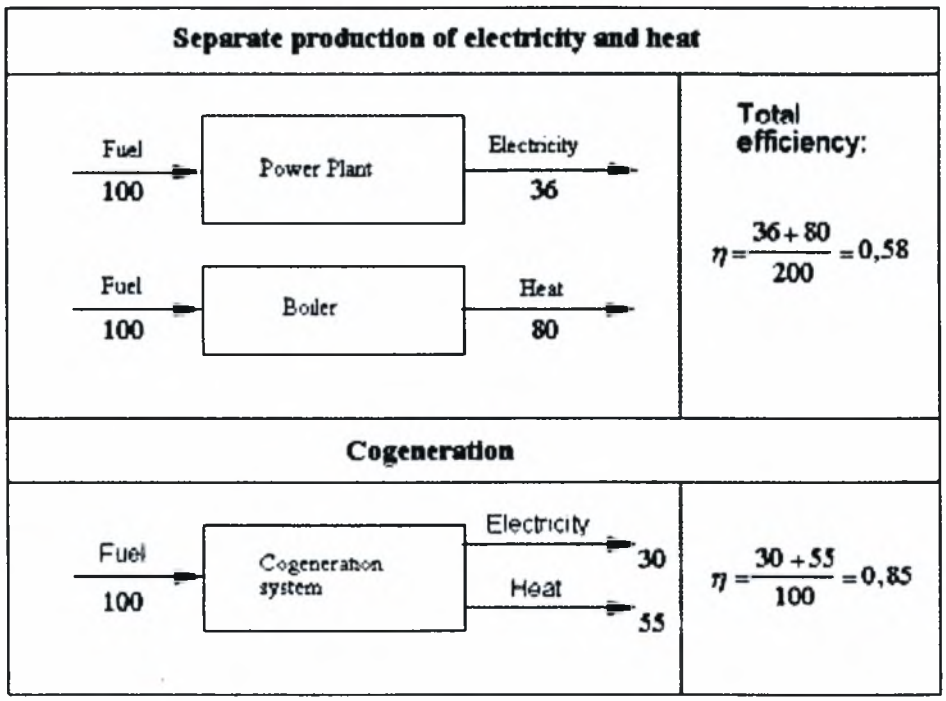

Figure 1 Efficiency comparison between cogeneration and separate production of electricity and heat. (Numbers below arrows represent units of energy in typical values).

In cogeneration systems, the efficiency of energy conversion increases to over 80% as compared to an average of 30–35% in conventional fossil fuel fired electricity generation systems [1].

Cogeneration is the most efficient way of energy conversion. Its wider use has various positive impacts on the economy, the environment, the responsible use of resources and security of energy supply. Cogeneration (CHP) produces 10% of all electricity and around 10% of heat in the EU-25. Figure 2 presents CHP as a share of national power production in the EU-15. Based on the above, EU has a strong political will to increase the share of cogeneration in the coming years.

Cogeneration is the simultaneous production of both heat and power from the same plant. The prime mover converts fuel (chemical) to mechanical energy and then to electrical energy and produces heat for applications. It allows greater energy efficiency and cost effectiveness by utilisation of energy that would have been otherwise wasted [2].

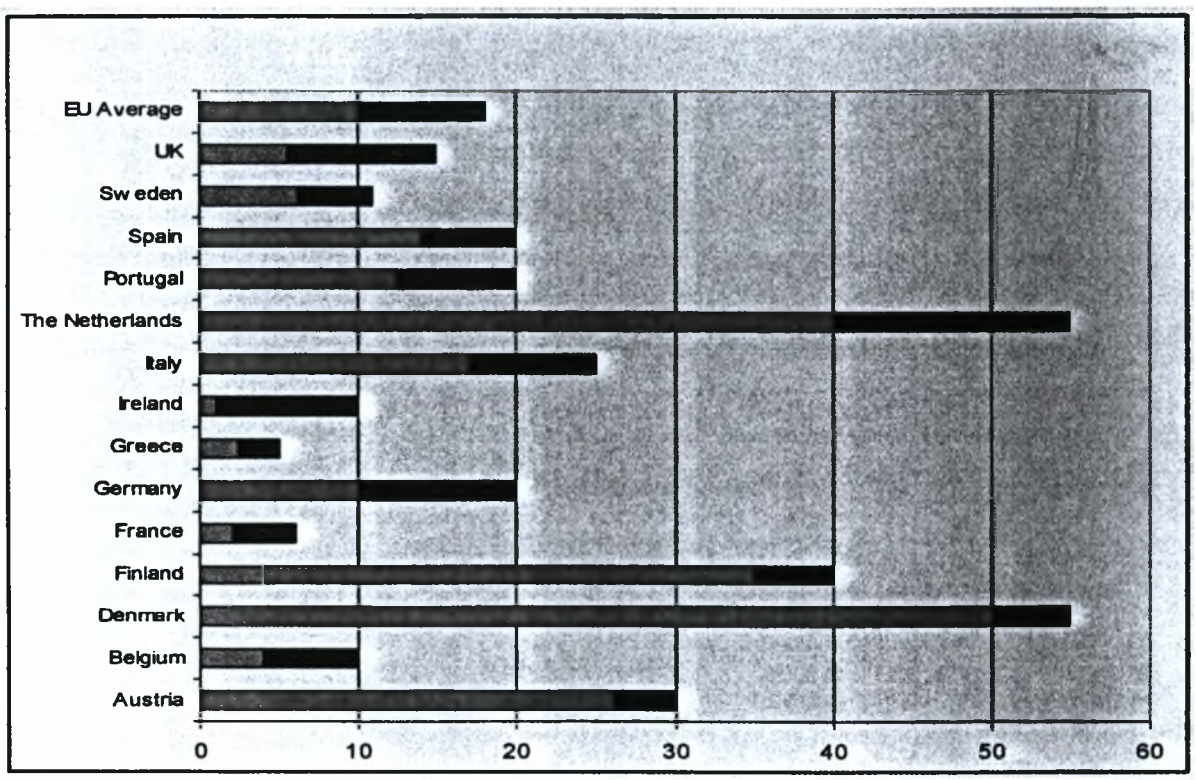

Figure 2 CHP as a share of national power in the EU-15 (blue bar: 1999- violet bar: estimated increase in 2010) (source: COGEN Europe [3]).

Cogeneration can be applied anywhere a facility has need of two or more energy uses. Energy uses are described as electricity, hot water, steam, chilled water, space heating, chemical bath heating, air conditioning and just about any other need that requires energy input. As a rough guide, cogeneration is likely to be suitable where there is a fairly constant heat demand for at least 4500 hours in the year.

The most typical use is a facility needs electricity and hot water. Obviously, electricity is universal in its use, and rarely would we find a cogeneration system in operation that would not have electricity as one of its energy products. Hot water applications are found everywhere, both in commercial and

industrial applications. Residential use is also an area where cogeneration can be successfully applied if the user is large enough or if the technology to provide suitable cogeneration is available.

Typical water heating applications are the following [4]

Hotels: Guest room water for bathing and showering; laundry service; kitchen service for dish washing; swimming pool heating; spa heating.

Restaurants: kitchen service for dishwashing; lavatory hot water.

Hospitals: patient room-bathing and showering, therapeutic pools, spas, swimming pools, kitchen service, laundry service.

Health and fitness facilities: swimming-pool heating, spa heating, showers and lavatory service.

Municipalities: swimming-pool heating, spa heating, lavatory and shower service.

Nursing homes and care facilities: patient showering and bathing, therapeutic pools, spas, kitchen service, laundry service.

Metal-plating factories: hot chemical baths

Food-processing plants: hot water for cooking, cleaning, lavatory service.

Residential: swimming-pool heating, spa heating, lavatory water for showering and bathing, kitchen and laundry service.

As can be seen, any facility that has a need for hot water is a potential user of the benefits of cogeneration. There is another practical use for cogeneration when hot water is not needed in the facility to any great degree: cooling in the form of air conditioning or refrigeration. The hot water generated by cogeneration can be used to make chilled water by absorption-chilling.

When central electric power plants and reliable utility grids were constructed and the costs of electricity decreased, many industrial plants began purchasing electricity and stopped producing their own. Thus, on-site industrial cogeneration accounted for only 15% of total U.S. electricity generation by 1950 and dropped to about 5% by 1974.

Other factors that contributed to the decline of industrial cogeneration were the increasing regulation of electric generation, low energy costs which represent a small percentage of industrial costs, advances in technology such as packaged boilers, availability of liquid or gaseous fuels at low prices, and tightening environmental restrictions. The aforementioned trend in cogeneration started being inverted after the first dramatic rise of fuel costs in 1973. Systems that are efficient and can utilise alternative fuels have become more important in the face of price rises and uncertainty of fuel supplies.

In addition to decreased fuel consumption, cogeneration results in a decrease of pollutant and CO_2 emissions. So, it promotes a healthier environment by reducing emissions to the atmosphere and helping to prevent climate change. For these reasons, governments in Europe, U.S.A. and Japan are taking an active role in the increased use of cogeneration. Methods of stimulating the use of cogeneration are seen in three major forms: (i) regulations or exemption from regulations, (ii) monetary incentives, and (iii) financial support of research and development. They are described in [5].

Table 1 Characteristics and parameters of prime movers in CHP systems (adapted from [6])

	Steam turbines	Diesel engines	Spark ignition engines	Gas turbines	Micro-turbines	Stirling engines	Fuel cells	Combined Cycle
Capacity range	50kW-500MW	5kW-20MW	3kW-5MW	250kW-50MW	15-200 kW	1kW-1.5MW	5kW-2MW	50 kW – 500 MW
Fuel used	Any	Gas, distillate oils, biogas	Gas, biogas, liquid fuels,	Gas, propane, distillate oils, biogas	Gas, propane, distillate oils, biogas	Gas, alcohol, butane, biogas	Hydrogen, gaseous hydrocarbons	Gas, propane, distillate oils, biogas
Efficiency electrical (%)	25-40	35-45	25-42	25-42	15-30	25-40	37-60	35-55
Efficiency overall (%)	60-80	65-90	70-92	65-87	60-85	65-85	85-90	73-90
Power to heat ratio	0.1-0.5	0.8-2.4	0.5-0.7	0.2-0.8	1.2-1.7	1.2-1.7	0.8-1.1	0.4-1.2
Output heat temperature	Up to 350	350-600	400-700	Up to 600	Up to 600	60-200	260-570	Up to 350
Noise	Loud	Loud	Loud	Loud	Fair	Fair	Quiet	Loud
Part load performance	Poor	Good	Good	Fair	Fair	Good	Good	Fair
Life cycle (year)	25-35	20	20	20	10	10	10?	20
Average investment cost ($/kW)	1000-2000	340-1000	800-1600	450-950	900-1500	1300-2000	2500-3500	400-500
Operating and maintenance costs ($/kWh)	0.004	0.0075-0.015	0.0075-0.015	0.0045-0.0105	0.01-0.02	N/A	0.007-0.05	0.004 - 0.009

Research, development and demonstration projects realised during the last 25 years led to a significant improvement of the technology, which now is mature and reliable (Table 1). Most cogeneration systems can be characterised either as topping systems or as bottoming systems. In topping systems, a high temperature fluid (exhaust gases, steam, 600-1200°C) drives an engine to produce electricity, while low temperature heat (200 – 600°C) is used for thermal processes or space heating (or cooling). In bottoming systems, high temperature heat (1000-1200°C) is first produced for a process (e.g. in a

furnace of a steel mill or of glass-works, in a cement kiln) and after the process hot gases (500 – 600°C) are used either directly to drive a gas-turbine generator, if their pressure is adequate, or indirectly to produce steam in a heat recovery boiler, which drives a steam-turbine generator [4].

More details on the existing categories of cogeneration systems are compiled in Table 1, (adapted from [4]). Another classification of the cogeneration system is based on the size of the engine:

a) Small units with a gas engine (15 - 1000 kW) or Diesel engine (75 - 1000 kW).

b) Medium power systems (1 - 6 MW) with gas engine or Diesel engine.

c) High power systems (higher than 6 MW) with Diesel engine Table 1

1.1 Steam turbine systems

Central electricity power stations traditionally use steam as the working fluid, with maximum steam temperatures of the order of 600 °C, and temperatures of heat rejection at 35-40 °C. For such a cycle to be used in cogeneration, steam exit temperatures must be increased by imposing a back pressure on the turbine expansion, which of course reduces the amount of available work (i.e. electricity). Thus, any cogeneration system based on steam cycles needs to be designed as a whole, as it is almost impossible to "add on" a waste heat utilization system on an existing steam turbine installation.

A further constraint on the combined steam system is the fluctuating balance between the heat and power demands which require fairly complex controls for steam pass-out, dump condenser etc. A well matched heat/power ratio over long periods can make a steam power-based conversion system extremely efficient in energy terms, as evidenced by the use of such systems for electricity and community heating in the colder regions of the world. The Figure 3 below presents the basic principles of cogeneration with steam turbine cycles.

Case (a) refers to a conventional device based on a steam cycle, where we seek maximization of produced electric power. Thus, steam expansion reaches the lowest possible backpressure which corresponds to the ambient temperature (e.g. absolute pressure of 0.04 bar corresponds to 30°C condensation temperature). Case (b) refers to a cogeneration installation with steam expansion against a higher backpressure that corresponds to a higher condensation temperature. In this way, the rejected condensation heat may be brought to the temperature level of a specific practical application.

For example, expansion against a backpressure of 2 bar corresponds to a condensation temperature of 120 °C, which is suitable for space heating, whereas expansion against a backpressure of 20 bar would

produce 211 °C steam, suitable for a variety of industrial processes. Based on the water saturation curve, Table 2 presents corresponding pairs of backpressure and temperature levels.

$$P_{el} = n_m \; n_{Gen} \; m \; \Delta h_T \qquad (1.1)$$

$$P_{el} = n_m \; n_{Gen} \; m \; \Delta h_T^{\bullet} \qquad (1.2)$$

$$Q_{Cond} = m \; r(P_2) \qquad (1.3)$$

$$Q_{Cond} = 0 \qquad (1.4)$$

$$Q_{exp} = 0 \qquad (1.5)$$

$$Q_{exp} = m \; r^{\bullet}(P_2^{\bullet}) \qquad (1.6)$$

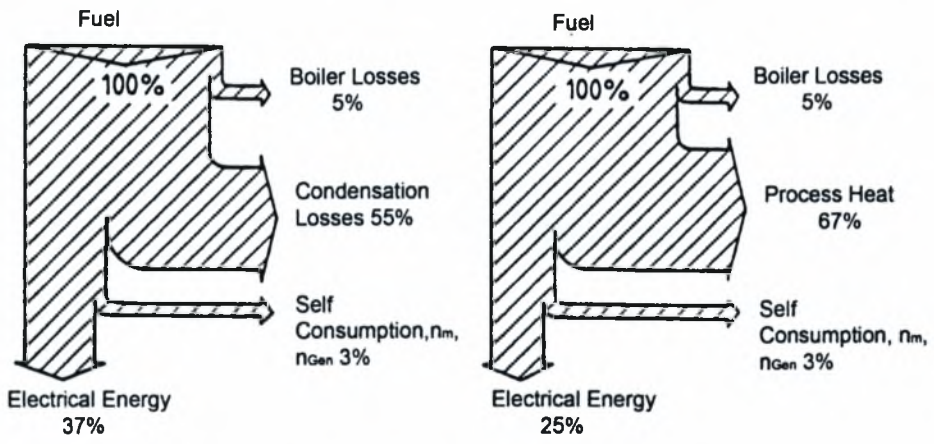

$n_{el} = 37\%$

$n_{exp} = 37\%$

(a)

$n_{el} = 25\%$

$n_{exp} = 92\%$

(b)

Figure 3 Basic steam turbine cycle cogeneration layouts. (a) With condenser (b) with backpressure [7]

Table 2 Thermodynamic coordinates of process steam that corresponds to the saturation curve.

Steam Pressure (bar)	2	3	5	10	15	20	30	40
Temperature °C	120	133	151	179	197	211	233	249

Naturally, cycle efficiency drops with increased backpressure, but the heat produced has a market value. The h-s diagrams of the simplified layouts of Figure 3, combined with the respective Sankey diagrams highlight the situation. By employing the notation of Figure 3 we can define the following ratio of electrical-to heat power output:

$$\sigma = \frac{P_{el}}{Q_H} = \frac{h_1 - h_2}{h_2 - h_3} = \frac{1}{\frac{1}{n_{el}} - 1} \qquad (1.7)$$

Table 3 below, shows the resulting dependence of EHR on the backpressure.

Table 3 Dependence of EHR on the backpressure in simple cogeneration layouts (live steam temperature 500°C, pressure 120 bar, boiler efficiency η_k=0.85).

backpressure (bar)	1	2	5	10	20	30	40	50
σ kW_{el}/kW_{th}	0.403	0.359	0.297	0.246	0.191	0.1550	0.128	0.100

A total exploitation factor can be defined here:

$$n_{exf} = \frac{P_{el} + \dot{Q}_H}{\dot{Q}_F} = \frac{\dot{Q}_H}{\dot{Q}_F}(\sigma + 1) \qquad (1.8)$$

which can reach values as high as 90%.

Of course, exergy levels of thermal and electrical power produced are quite differing, and thus the assessment of real system efficiency must comprise also exergy balances:

$$\dot{E}_F = \dot{m}_F e_F = P + \varepsilon_H \dot{Q}_H + \dot{m}_R e_R + \Delta \dot{E}_{vv} + \sum \Delta \dot{E}_v \qquad (1.9)$$

where $\varepsilon_H=(T_H-T_L)/T_H$ the Carnot factor of heat produced, $m_R e_R$ the flow rate times specific exhaust exergy, ΔE_{vv} the combustion inefficiency and $\Sigma\Delta E_v$ the sum of exergy losses for all cycle parts (see Figure 4).

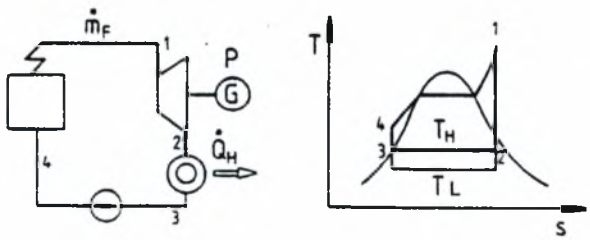

Figure 4 Schematic of steam turbine cogeneration cycle and T-s diagram for the explanation of exergy balances

The power generation capacity of steam, based on its temperature is expressed by the Carnot factor:

$$\varepsilon_D = \frac{T_D - T_L}{T_D} \qquad (1.10)$$

Thus, the overall exergy balance takes the form:

$$C\varepsilon_D \dot{Q}_D = \dot{m}_F e_F C\varepsilon_D \eta_D = \frac{P}{\eta_T} + \varepsilon_H \dot{Q}_H \quad (1.11)$$

or

$$\dot{E}_B = \frac{1}{C\varepsilon_D \eta_D}\left(\frac{P}{\eta_T} + \varepsilon_H \dot{Q}_H\right) \quad (1.12)$$

where $Q_D=m_F(h_1-h_4)$ the heat output of the combined process, η_D the energetic efficiency of the steam boiler and $\eta_T=P/m_F(e_1-e_2)$ the exergetic efficiency of electricity production. C is a factor that takes into account energy consumption of the condensate pumps as well as the exergy requirements for the preheating of condensate before entrance to the steam boiler. The exergetic efficiency and the Electricity to Heat Ratio of the cogeneration process are given by the respective relations:

$$n_E = \frac{P+\varepsilon_H \dot{Q}_H}{\dot{E}_B} = \frac{C\varepsilon_D \eta_D(\sigma + \varepsilon_H)}{\frac{\sigma}{\eta_T} + \varepsilon_H} \quad (1.13)$$

$$\sigma = \frac{C\varepsilon_D - \varepsilon_H}{\frac{1}{\eta_T} - C\varepsilon_D} \quad (1.14)$$

Their interdependence is shown in Figure 1. The simplest possible cogeneration process layout in steam turbine cycles has already presented in Figure 3. Due to the strong degree of coupling induced by the need for condensation of the total steam mass flow in the specific concept, the electricity to heat ratio tends to remain fairly constant, with only small perturbations possible with a variation of the live steam temperature.

However, a variable electricity to heat ratio is necessary in most industrial applications of cogeneration. For this reason, more complex cycles are employed (Figure 6 c,d), with steam takeoff from intermediate turbine stages. These variants allow a wide variation of the electricity to heat ratio to match transient variation of demand.

Even the variant b has a certain capability of variation of EHR, at a penalty of a reduced total exploitation factor. Variant c is capable of a complete decoupling of electricity and heat output. In the specific layout, the turbine power and the available heat power output are given by the respective relations:

$$P_T = \dot{m}(h_1-h_2) + \left(\dot{m}-\dot{m}^*\right)(h_2-h_3) \qquad (1.15)$$

$$\dot{Q}_H = \dot{m}^*(h_2-h_5) \qquad (1.16)$$

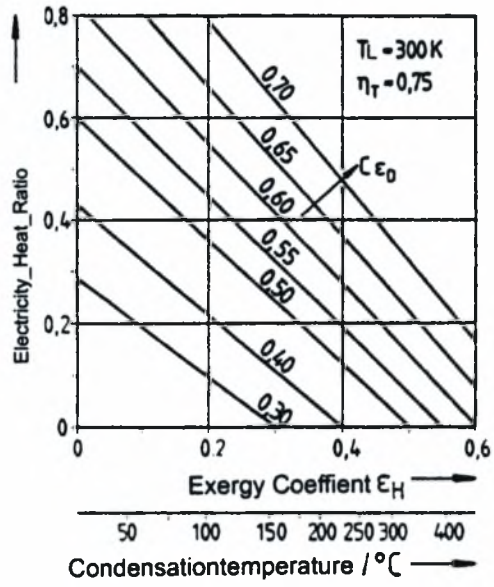

Figure 5 Electricity to heat ratio of the ideal Rankine cycle cogeneration process with η_{II}=0.75

The electricity to heat ratio is given, respectively, by the following relation:

$$\sigma = \frac{P_T}{\dot{Q}_H} = \frac{(h_1-h_2)+(1-x)(h_2-h_3)}{x(h_2-h_5)} \qquad (1.17)$$

This ratio can be directly modified by varying the percentage of steam takeoff x=m*/m

In practice, heat can be drawn from the system at different temperature levels, as shown in Figure 8.

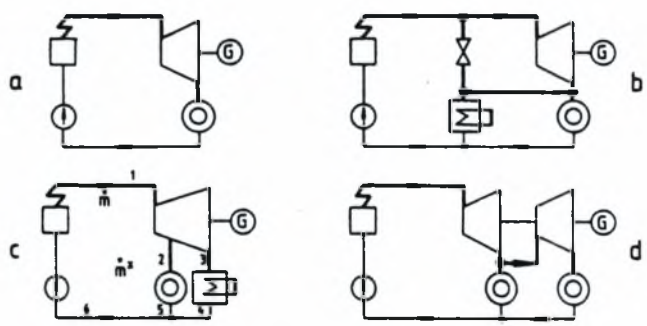

Figure 6 Different variants of Rankine cycle cogeneration systems: (a) basic backpressure layout (b) backpressure layout with additional throttling and condensation capability (c) condensation layout with intermediate steam takeoff (d) backpressure layout with intermediate steam takeoff.

With this type of layouts it is possible e.g. alternatively to produce exclusively 390 MW_{el} of electrical power or, respectively, the production of less (360 MW_{el}) electricity with an additional heat output of 295 MW_{th}.

Even the large nuclear power plants are very appropriate for cogeneration of process heat. In order to realize the differentiation of production of electricity and power in such a system, a process steam generator is usually added to the cycle (Figure 7).

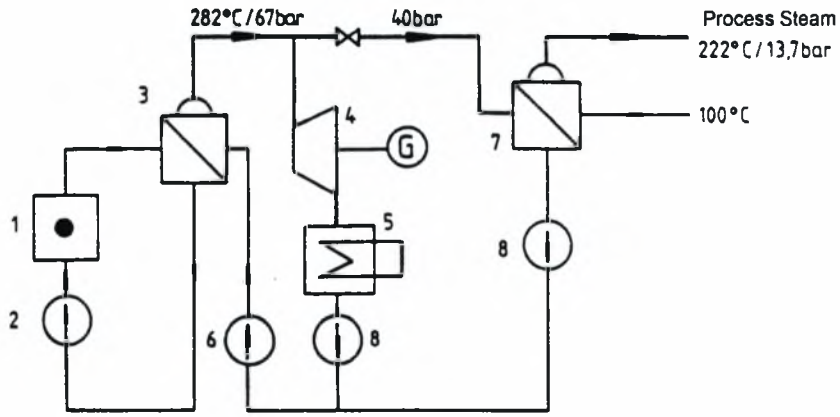

Figure 7 Cogeneration of process steam from pressurized water nuclear reactor. (1) Nuclear reactor (2) Main cooling medium pump (3) Steam generator (4) Steam turbine (5) Condenser (6) Water pump (7) Process steam heat exchanger (8) Condensate pump

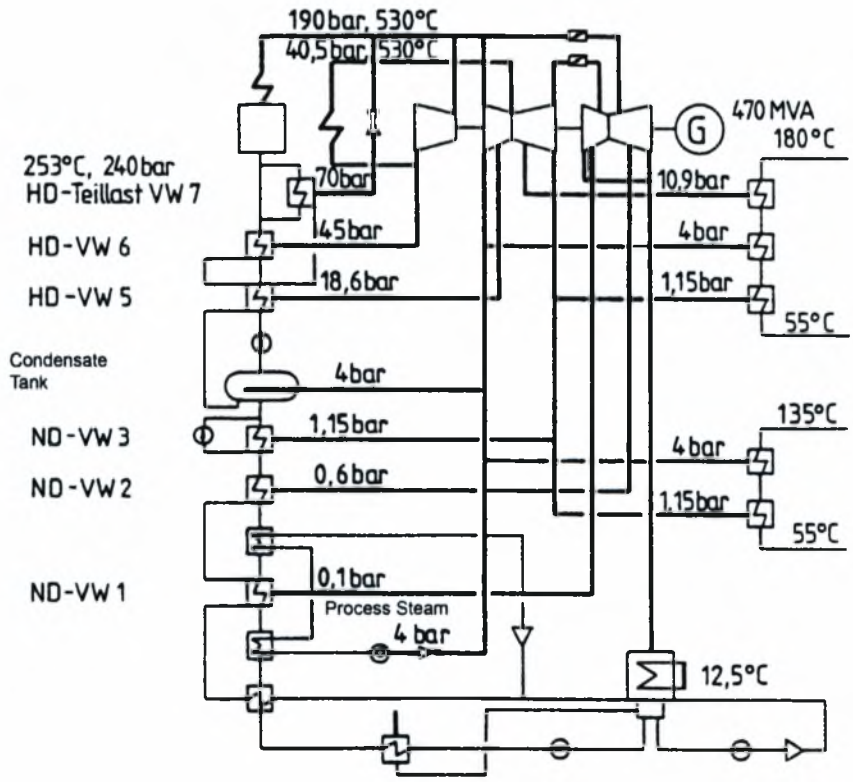

Figure 8 Layout of modern cogeneration power plant which produces electricity, process steam and district heating

1.2 Gas-turbine systems

Industrial (Table 4) gas turbine engines typically operate with exhaust gas temperatures of 500-600 °C, thus apparently offering ready access to large temperature differences in an exhaust gas heat exchanger. Unfortunately, the power output of the engines is quite sensitive to the back pressure of such an exchanger, unlike the situation of a spark ignition reciprocating engine [8]. Retrofitting of an exhaust gas heat exchanger could jeopardize the safety of the engine by overheating the turbine. It is therefore desirable that, in a cogeneration system, the two sections of the system are designed initially together, so that the overall performance in terms of both power and heat is optimized.

Gas turbines either in a simple cycle or in a combined cycle are the most frequently used technology in recent cogeneration systems of medium to high power. Their electric power output ranges from a few hundred kilowatts to several hundred megawatts. On the other side of the spectrum, recent research and development aims at the construction of micro turbines, which have a power output of a few kilowatts.

Gas turbines have been developed as either heavy-duty units for industrial and utility applications, or as lightweight, compact and efficient aircraft engines. These engines are modified for stationary applications, in which case they are called "aero derivative turbines". In general, they are capable of faster start-ups and rapid response to changing load. Both gas turbine designs have been successfully used for cogeneration having as main advantages low initial cost, high availability, fast and low-cost maintenance, fuel-switching capabilities, high quality heat which can easily be recovered, and high efficiencies in larger sizes. In addition, the commercial availability of packaged units helped in their widespread applications. A gas turbine can operate either in open cycle or in a closed cycle.

Figure 9 summarizes the main possible layouts of cogeneration systems based on gas turbines. This variety is possible due to the high exhaust temperature levels of the gas turbine (400 – 500 °C).

As seen in the different layouts of Figure 9, there exist various points that are appropriate to extract heat in a gas-turbine cycle. In the example of the simple open gas turbine cycle, we can calculate the electricity-to-heat ratio as follows:

$$\sigma = \frac{P_{el}}{\dot{Q}_H} = \frac{(T_3 - T_4) - (T_2 - T_1)}{T_4 - T_5} \qquad (1.18)$$

This simplification is reasonable due to the very high air-to-fuel ratio of the gas turbine that is dictated by the high temperature fatigue limits of the first turbine stage. A typical Sankey diagram of this type of process is presented at Figure 10. In this example, the following characteristic temperature values

are assumed: T_1=20°C, T_2=150°C, T_3=800°C, T_4=450°C, T_5=150°C. Based on these values, we can calculate an electricity to heat ratio value of σ=0.73 kWh_{el}/kWh_{th} and a total exploitation factor of the order of 80%.

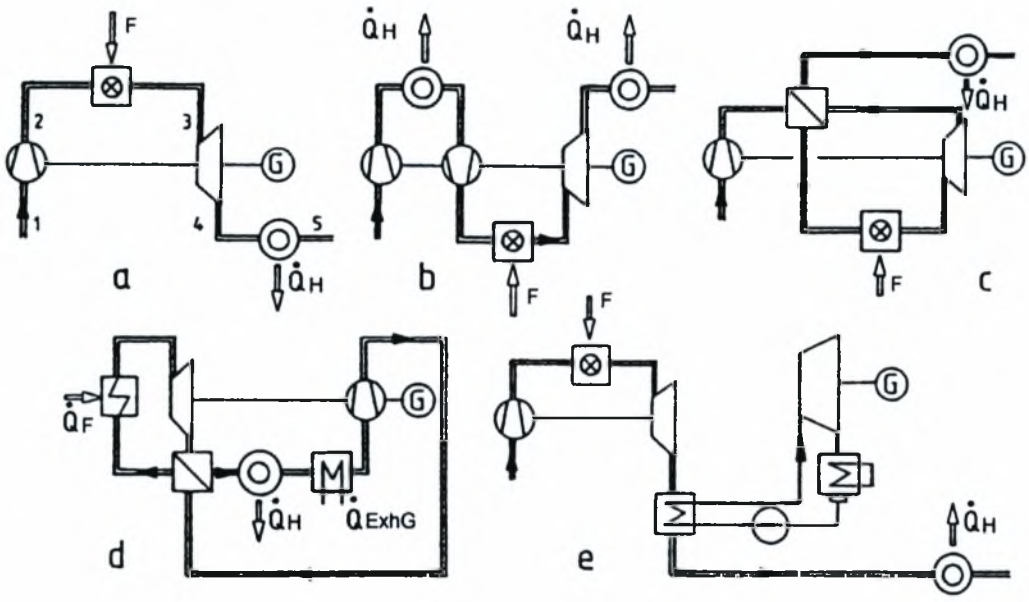

Figure 9 Gas turbine cogeneration systems layouts (a) open gas turbine cycle (b) open gas turbine cycle with two compressors and intercooler (c) open gas turbine cycle with recuperator (d) closed gas turbine cycle (e) combined gas-turbine – steam turbine cycle.

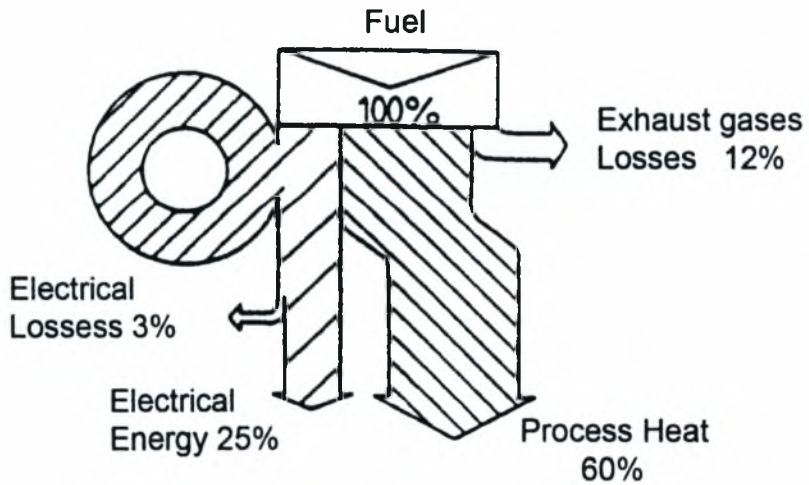

Figure 10 Sankey diagram of an open gas-turbine cycle with exploitation of exhaust gas heat

If one employs additional heat sources in more complex layouts, it is possible to match the year-round electricity and heat requirements of a small community or a factory. An example installation of this kind that can be fuelled by diesel fuel or natural gas is presented in Figure 11. If needed, heat production can be further increased by additional heating. Efficiency in the production of electricity can be raised by the introduction of a recuperator. The specific installation is capable of producing a total of 27 MW_{el} and 63 MW_{th}. The EHR lies at around 0.43 and the total fuel exploitation factor reaches 78%. Such a layout can be readily modified to produce process steam for industrial applications.

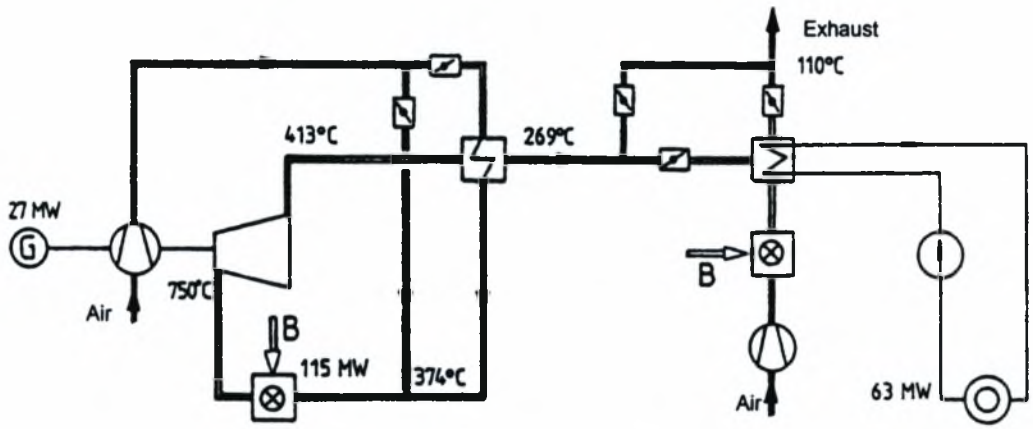

Figure 11 Open gas-turbine cycle cogeneration process example

In closed gas-turbine cycle systems we can take heat (mainly for space heating) downstream the regenerator (Figure 9d). Also, there is an additional capability to take heat for distance heating, by means of an additional steam generator that can be placed in the exhaust duct (Figure 9e). Such layouts are now widely used in industry.

Chemical process industries are known for specific needs of large steam quantities for a variety of processes, as reactor heating, powering of compressors through steam turbines, steam as a reactant in chemical reactions, process steam needed for drying, evaporation, distillation and other processes.

The example of Figure 12, taken form a chemical industry, demonstrates the flexibility of the specific process, especially if an additional heat source is available for the heat recovery steam generator. Such layouts may easily match the industrial requirements for separate steam networks at different pressure levels. The existence of an additional steam generator ensures the availability of steam in any case, irrespective of the variation in electricity and heat loads.

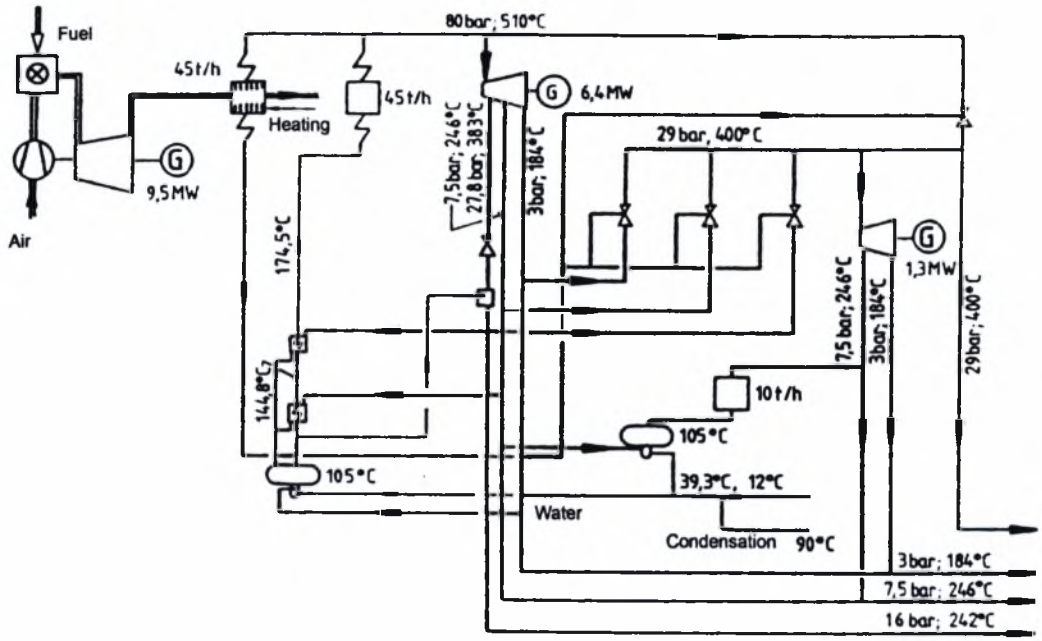

Figure 12 A combined gas-turbines – steam turbine process for the cogeneration of electricity and steam in a chemical industry

Table 4 Performance comparison of various Gas Turbine models [9]

Performance comparison of various Gas Turbine models						
Bastan VII (Turboméca)	Makila (Turboméca)	Hurricanne (GEC-AIsthom)	TGC 378 (Solar)	571 k (Allison)	PGT 10 (GE)	Bastan VII (Turboméca)
Production of Heat (kWh):						
without post-combustion	1950	2240	3570	3570	8480	16170
with air-assisted burner	8600	7870	10600	10600	26800	60700
with turbulence burner	13700	12000	15800	5800	40300	
Overall efficiency (power + heat production) (%)						
without post-combustion	71.0	76.8	79.0	70.0	78.4	77.7
with air-assisted burner	87.3	88.5	88.8	89.7	88.7	88.8
with turbulence burner	91.5	91.0	91.4	92.7	91.4	
Heat-to-Power ratio						
without post-combustion	2.49	2.03	2.13	1.83	1.50	1.45
with air-assisted burner	11.00	7.15	6.31	6.43	4.74	5.44
with turbulence burner	17.50	10.90	9.40	9.90	7.15	
Specific fuel consumption						
without post-combustion	2.10	1.64	1.55	1.51	1.49	1.54
with air-assisted burner	1.12	1.08	1.06	0.98	1.08	0.98
with turbulence burner	0.53	0.69	0.70	0.51	0.79	

1.3 Conventional reciprocating engines

The working fluids in conventional spark ignition or compression ignition reciprocating engines achieves temperatures of over 2000 °C, and exit from the engine at up to about 800 °C. Retrofitting of an exhaust gas heat exchanger to an existing engine is relatively simple, although it imposes a certain back pressure with consequent loss in power output. Access to a large temperature difference between the hot and the cold fluids across the heat exchanger is beneficial to the design of the exchanger. In addition to heat extraction from the exhaust gas, the heat from the engine cooling system may be put o a useful purpose with cogeneration. Electric efficiencies as high as 43% are possible with Otto cycle Natural Gas fuelled engines [10]. Even higher efficiencies are reported with Diesel engines or dual fuel engines. Emissions levels of natural gas fuelled engines are also quite favourable [11].

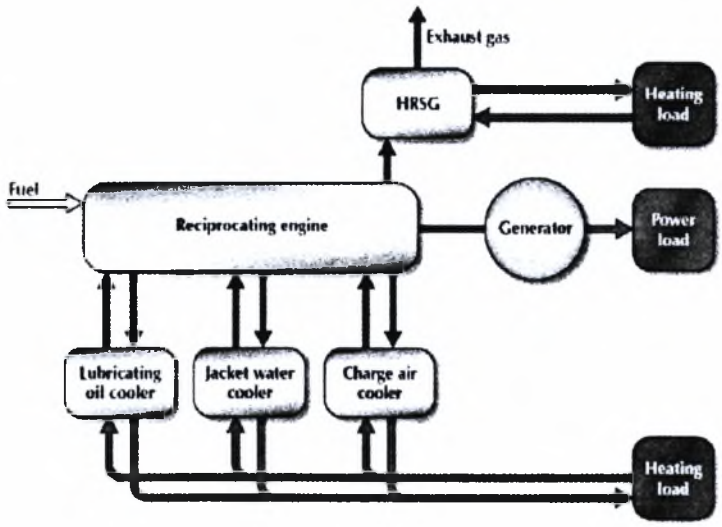

Figure 13 Reciprocating engine cogeneration system schematic

2 Literature Review

(The focus of this review is on specific applications of cogeneration and tri-generation and especially on the design methodologies in-use and the role of transient operation in the design procedures).

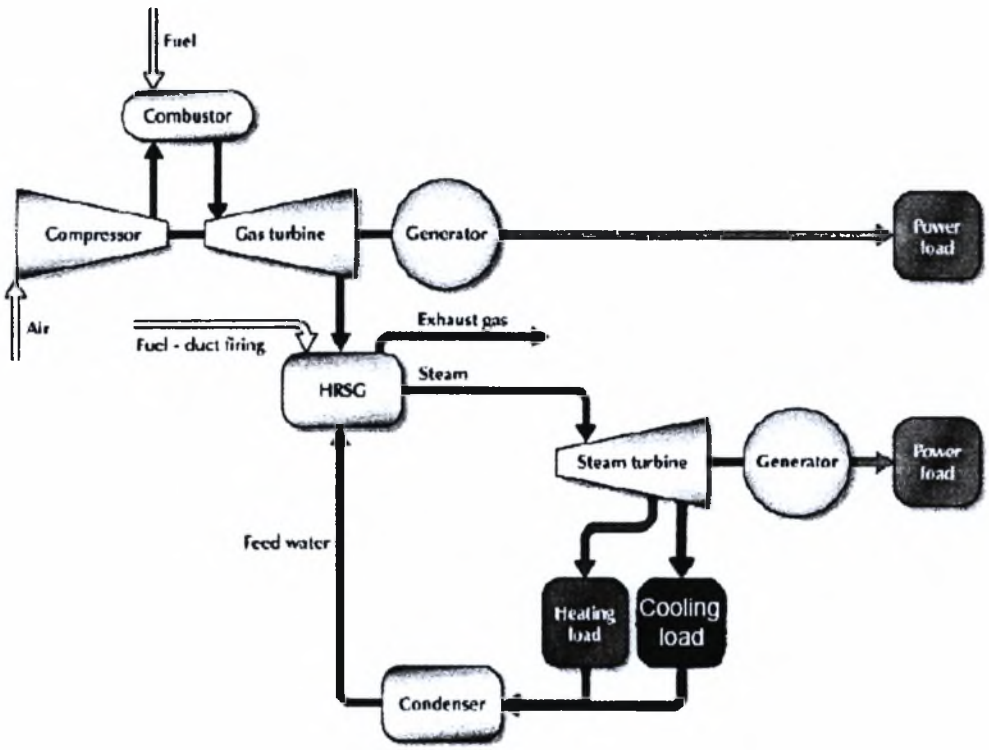

Figure 14 Joule-Rankine combined cycle tri-generation system with back pressure steam turbine

Cogeneration applications are usually classified with reference to the sector they appear:

utility sector

industrial sector

building sector (called also residential-commercial-institutional sector)

rural sector

Cogeneration opportunities in each sector and related information are mentioned in the following.

2.1 Cogeneration in the Utility Sector

Thermal power plants can either be built as or converted to cogeneration systems supplying with heat nearby cities or part of a city, industries, greenhouses, fisheries, water desalination plants (in particular

on islands or in countries with scarce water resources), etc. The distance of the users of heat from the plant and their dispersion are of crucial importance for the feasibility of the project.

When a city or a district is supplied with heat, the system is also called a district heating cogeneration system. In district heating applications, in addition to the distance and dispersion of users, the thermal power required and the annual number of degree - days are important parameters for the feasibility. In most of the cases the economic distance for transfer of heat does not exceed 10 km; in exceptional cases it may reach 30 km.

In hot climates, district cooling during the summer may also be economically feasible [12, 13]. In such cases, heat supplied by the plant is used to drive an absorption cooling or air-conditioning unit. It is possible to have central coolers and distribute cold water to the users or to have local units. In the second case there is no need of cold water network; the hot water or steam network is used throughout the year.

Two other applications, which can be mentioned here, are landfills and sewage treatment plants. In both cases, a fuel gas is produced, which can fuel a gas engine cogeneration unit. Another alternative for city wastes, instead of being buried in landfills, is to be burned in boilers of steam turbine cogeneration systems. The heat produced can serve near-by communities. In particular for the sewage treatment plants, heat is required for the digestion tanks.

2.2 Cogeneration in Industry

Many industrial processes require heat in order to be completed. They are classified according to the temperature level of the required heat:

Low temperature processes (lower than 100°C) e.g. drying of agricultural products, space heating or cooling, domestic hot water.

Medium temperature processes (100-300°C), e.g. processes in pulp and paper industry, textile industry, sugar factories, certain chemical industries, etc. In these processes heat is usually supplied in the form of steam.

High temperature processes (300-700°C), e.g. in the chemical industry.

Very high temperature processes (higher than 700°C), e.g. in cement factories, primary metal industries, glass works [14].

Significant cogeneration potential exists in the following industries:

food and beverage,

textile,

lumber,

pulp and paper,

chemicals,

petroleum refineries,

cement,

primary metals.

Lower but non-negligible potential exists also in the glass and ceramics industries. Trigeneration potential exists mainly in the food and beverage industry [15].

2.3 Cogeneration in the Building Sector

A combination of electrical and thermal load with level and duration appropriate for cogeneration often appears in buildings such as the following:

houses and apartment buildings,

hotels,

hospitals,

schools and universities,

office buildings,

stores, supermarkets, shopping centres,

restaurants,

swimming pools and leisure centres.

Cogenerated heat is used for domestic hot water, space heating or cooling, laundry facilities, dryers, swimming pool water heating. An indication of the electrical power required in various types of buildings is given in Table 5.

From the point of view of heating and cooling demands, three sub sectors can be identified: (a) hospitals and hotels, (b) apartment buildings, (c) office buildings

Each one of these sub sectors has its own profile. Other buildings (such as universities and stores) have load profiles which are combinations of the profiles of the three sub sectors. The feasibility study and especially the final design of a cogeneration system must be based on the load profiles of the particular building; peak or average load values are not sufficient, because they may lead to wrong results and decisions [16].

Feasibility studies have shown that in cold climates, like in north European countries, long space heating periods may make cogeneration economically viable. In hot climates, like in south European countries, space cooling in addition to space heating is necessary in most of the case in order for cogeneration to be economically feasible.

The availability of natural gas and of standardised packaged cogeneration units gave a boost to cogeneration applications in buildings in certain European countries (e.g. UK, The Netherlands) during the last decade. Packaged units for buildings have an electrical power output in the range 10-2000 kW and have the advantages of low cost, high power density, fast and easy installation (they are ready for connection with the electrical and piping network) and automatic operation with no need of continuous attendance by specialised personnel.

The units usually have a reciprocating internal combustion engine. Liquid fuels can be used, but the most frequent fuel is natural gas, which is clean, relatively cheap, and which does not require storage.

Table 5 Typical electrical load ranges in buildings.

Building	Electric Load (kW)
Restaurants	50-80
Apartment buildings	50-100
Supermarkets	90-120
Hotels	100-2000
Hospitals	300-1000
Shopping centres	500-1500
Schools, Universities	500-1500
Office buildings	500-2000

2.4 Open-cycle gas turbine cogeneration systems

Most of the currently available gas turbine systems operate on the open Brayton cycle (also called Joule cycle when irreversibilities are ignored): a compressor takes in air from the atmosphere and derives it at increased pressure through a diffuser to a constant-pressure combustion chamber, where fuel is injected and burned. Older and smaller units operate at a pressure ratio in the range of 15:1, while the newer and larger units operate at pressure ratios approaching 30:1. [8]. Pressure drop across

the combustor ranges between 1-2%. Combustion takes place with high excess air, to keep low combustor gas temperatures at turbine inlet, (up to a maximum of about 1300°C with film cooling) due to blade material limitations. This severely deteriorates cycle efficiency. The exhaust gases exit the combustor at high temperature and with oxygen concentrations of up to 15-16%. The high pressure and temperature exhaust gases enter the gas turbine producing mechanical work to drive the compressor and the load (e.g. electric generator). The exhaust gases leave the turbine at a considerable temperature (450-600°C), which makes high-temperature heat recovery ideal. This is effected by a heat recovery boiler of single-pressure or double-pressure, for more efficient recovery of heat. Triple-pressure is also possible but not very usual, because it makes the system more complex and expensive, which is not always justified. The steam produced can have high quality (i.e. high pressure and temperature), which makes it appropriate not only for thermal processes but also for driving a steam turbine thus producing additional power.

Instead of producing steam, the exhaust gases after the turbine can be used directly in certain thermal processes, such as high-temperature heating and drying.

In any of the aforementioned applications, it is possible to increase the energy content and temperature of the exhaust gases by supplementary firing. For this purpose, burners are installed in the exhaust gas boiler, which use additional fuel. Usually there is no need of additional air, since the oxygen content in the exhaust gases is significant, as mentioned above.

Cogeneration systems with open cycle gas turbines have an electrical power output usually in the range 100 kW - 100 MW, not excluding values outside this range. A variety of fuels can be used: natural gas, light petroleum distillates (e.g. gas oil, Diesel oil), products of coal gasification. The use of heavier petroleum distillates (fuel oil) in mixtures with light ones is under investigation and it may prove successful. Also, non-commercial fuel gases, produced during the catalytic cracking of hydrocarbons in petroleum refineries, are used as fuels in gas turbines. However, attention has to be paid to the fact that the turbine blades are directly exposed to the exhaust gases. Consequently, the combustion products must not contain constituents causing Open-cycle gas turbine cogeneration systems corrosion (such as chemical compounds of sodium (Na), potassium (K), calcium (Ca), vanadium (Va), sulfur (S)) or erosion (solid particles larger than a certain size). In order to prevent these effects, there may be need of fuel treatment or exhaust gas treatment before they enter the turbine.

The installation time for gas turbine cogeneration systems of up to 7 MWe is about 9-14 months, and it may reach two years for larger systems. The reliability and annual average availability of gas turbine systems burning natural gas are comparable to those of steam turbine systems. Systems burning liquid

fuels or gaseous by-products of chemical processes may require more frequent inspection and maintenance, which results in lower availability. The life cycle is 15-20 years and it may be critically affected by a low quality fuel or poor maintenance.

Manufacturers normally specify the capacity (power output) and performance of a gas turbine at ISO standard conditions: 15°C, 60% relative humidity, at sea level. In addition, the performance is typically specified without pressure losses in the inlet and exhaust ducts. The capacity of the turbine decreases as ambient temperature or altitude increases. The capacity may decrease by about 2-4% for each 300m increase in altitude. Partial load has a strong effect on efficiency: decreasing load causes a decrease in electrical efficiency. As with the steam turbines, it is necessary to consult the manufacturer for performance maps or graphs of each particular gas turbine [3]. If a gas turbine system is to operate over long periods of time in an environment of high temperature, pre-cooling of the inlet air may be economically feasible. Mechanical, evaporative or absorption chillers may be used; the final choice will be dictated by a feasibility study. It is interesting to note that absorption chillers may operate with turbine exhaust gas heat as the main source of energy.

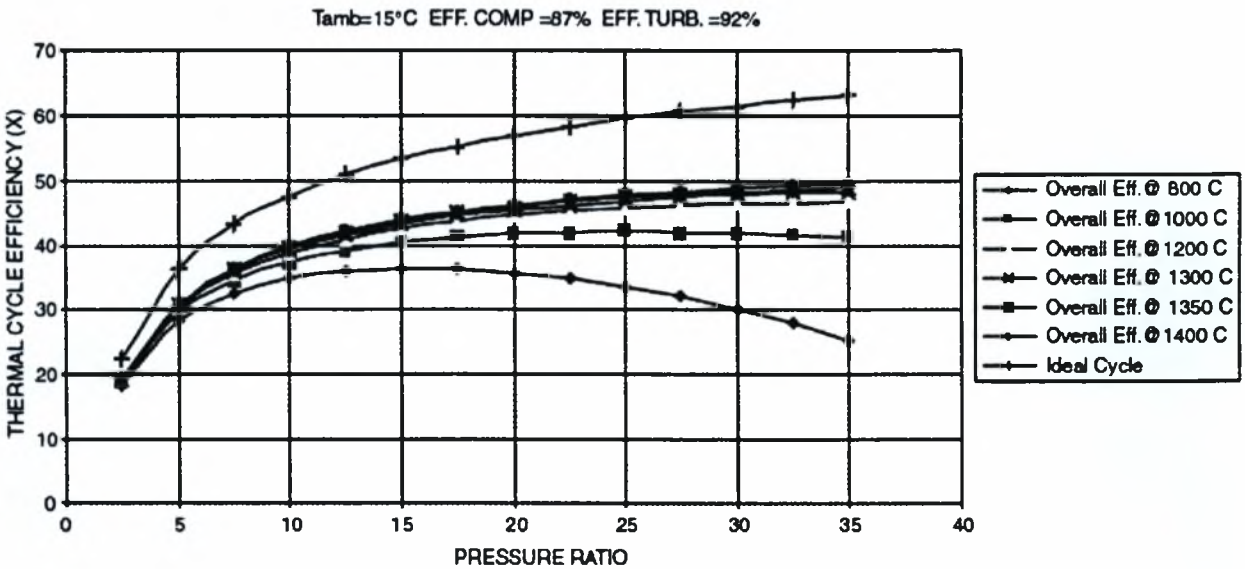

Figure 15 Effect of pressure ratio and gas turbine inlet temperature on powerplant thermal efficiency [17]

The nominal electrical efficiency (i.e. the efficiency at rated power) of small-to-medium gas turbine systems is usually in the range of 25-35%. Larger systems built recently have reached electrical efficiencies of 40-42% by means of high temperature of exhaust gases at the turbine inlet (1200-1400 °C). The total efficiency is typically in the range of 60-80%. The power-to-heat ratio (PHR) is in the range 0.5-0.8.

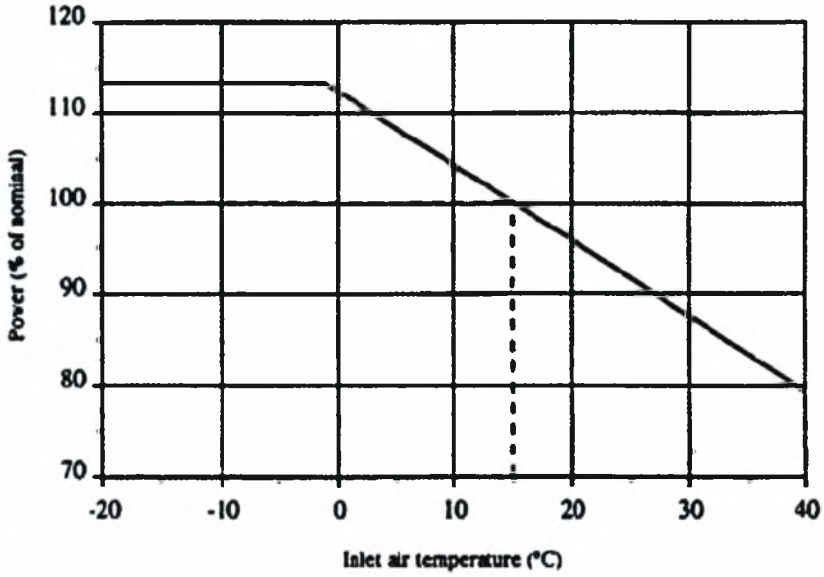

Figure 16 Effect of inlet air temperature on the power output of a gas turbine

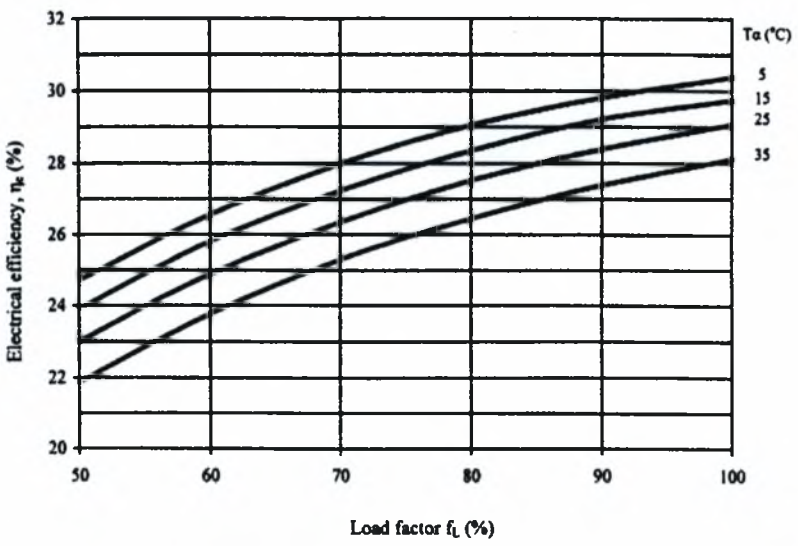

Figure 17 Effect of load and inlet air temperature on the electrical efficiency of gas turbine system

A significant portion of the turbine power output, often exceeding 50%, is consumed to drive the compressor, thus resulting in a relatively low electric efficiency (e.g. in comparison to a reciprocating engine of similar power). In cases of high pressure ratios, intercooling of the air at an intermediate stage of compression can be applied, which reduces the work required for compression. A significant increase in electric efficiency is also achieved by regenerative air preheating, i.e. preheating of air with exhaust gases. In such a case the recoverable heat from the exhaust gases after the regenerative heat

exchanger decreases and the value of PHR increases. In the case of cogeneration, as well as for combined gas-steam cycles, the addition of a regenerative air preheater is not justified.

2.4.1 Combined Cycle Cogeneration Systems

The term combined cycle is used for systems consisting of two thermodynamic cycles, which are connected with a working fluid and operate at different temperature levels. The high temperature cycle (topping cycle) rejects heat, which is recovered and used by the low temperature cycle (bottoming cycle) to produce additional electrical (or mechanical) energy, thus increasing the electrical efficiency. The most widely used combined cycle systems are those of gas turbine - steam turbine (combined Joule - Rankine cycle). They so much outnumber other combined cycles that the term combined cycle, if nothing else is specified, means combined Joule - Rankine cycle (see for example [18]). A simplified diagram of such a system with the main components only is given in Figure 18. Double or triple-pressure steam boilers enhance the heat recovery (Figure 19) and increase the efficiency, but make the system more complex; they are used in large systems [19]. In Figure 18**Σφάλμα! Το αρχείο προέλευσης της αναφοράς δεν βρέθηκε.**, the steam turbine is a backpressure one. Of course this is not the only configuration. Condensing turbine is also possible, while extraction can also be used with either the backpressure or the condensing turbine [20].

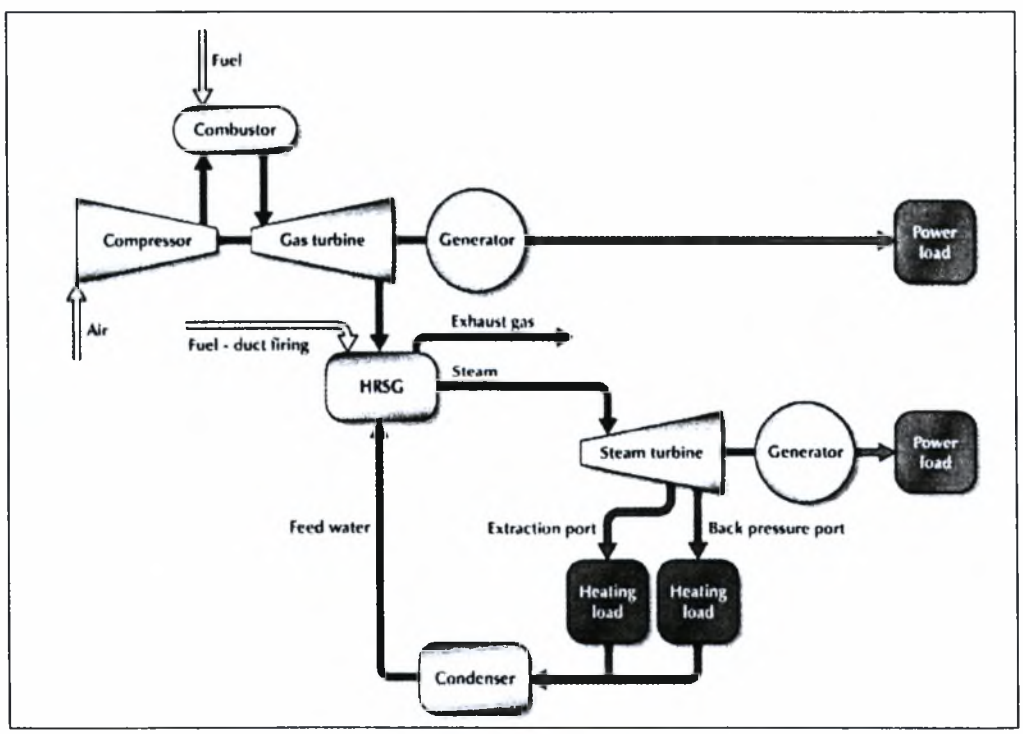

Figure 18 Joule-Rankine combined cycle cogeneration system with back pressure steam turbine

The maximum possible steam temperature with no supplementary firing is by 25-40°C lower than the exhaust gas temperature at the exit of the gas turbine, while the steam pressure can reach 80 bar. If higher temperature and pressure is required, then an exhaust gas boiler with burner(s) is used for firing supplementary fuel. Usually there is no need of supplementary air, because the exhaust gases contain oxygen at a concentration of 15-16%. With supplementary firing, steam temperature can approach 540°C and pressure can exceed 100 bar. Supplementary firing not only increases the capacity of the system but also improves its part-load efficiency. Initially, combined cycle systems were constructed with medium and high power output (20-400 MW). During the last years, also smaller systems (4-15 MW) are being constructed, while there is a tendency to further decrease the power limit. The power concentration (i.e. power per unit volume) of the combined cycle systems is higher compared to the simple gas turbine (Brayton - Joule) or steam turbine (Rankine) cycle [21].

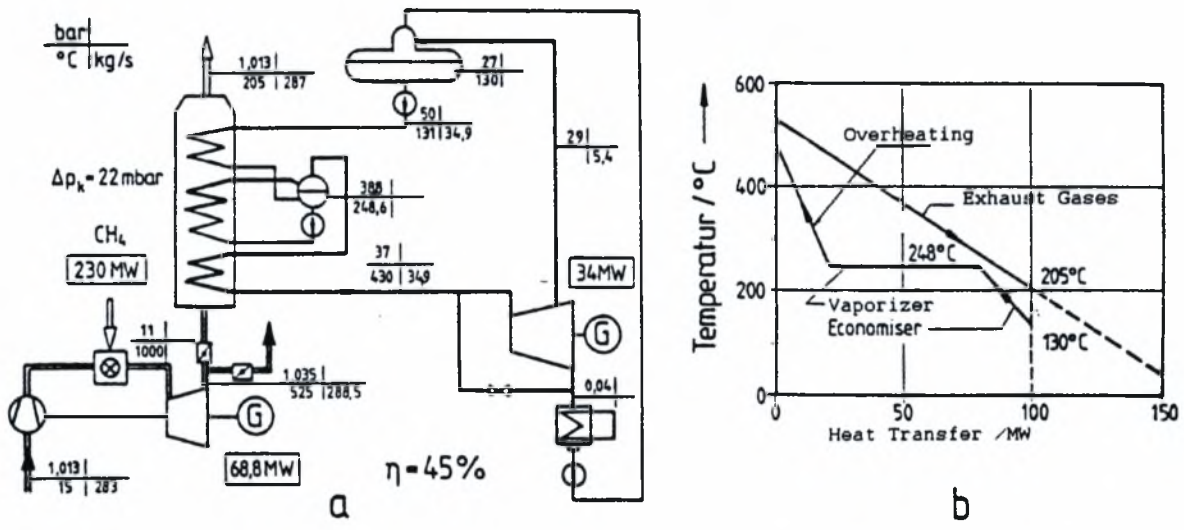

Figure 19 Heat recovery steam generator operation in combined cycle

The installation time is 2-3 years. It is important to note that the installation can be completed in two phases: the gas turbine subsystem is installed first, which can be ready for operation in 12-18 months. While this is in operation, the steam subsystem is installed.

The reliability of (Joule - Rankine) combined cycle systems is 80-85%, the annual average availability is 77-85% and the economic life cycle is 15-30 years. The electrical efficiency is in the range 40-55%, the total efficiency is 70-90% and the power -to- heat ratio is 0.6-2.0 [22].

Many basic industrial products require for their production very high quantities of electricity and heat as shown in the examples of typical uses of the produced electricity and heat in various industrial processes are shown in Table 6

Table 6 Required specific electricity and heat consumption for the production of various industrial products of everyday use with cogeneration systems

Product	Heat Energy Input (kWh/t)	Pressure (bar)	Electrical energy Input (kWh/t)
Paper	5000	5	1100
Packing Paper	2500	2.5	450
Rice	500	3.5	70
Sugar	3000	3	175

2.5 The TRNSYS simulation environment

TRNSYS [23] is a complete and extensible simulation environment for the transient simulation of systems, including multi-zone buildings. It is used by engineers and researchers around the world to validate new energy concepts, from simple domestic hot water systems to the design and simulation of buildings and their equipment, including control strategies, occupant behaviour, alternative energy systems (wind, solar, photovoltaic, hydrogen systems), etc.

One of the key factors in TRNSYS' success is its open, modular structure. The source code of the kernel as well as the component models is delivered to the end users. This simplifies extending existing models to make them fit the user's specific needs.

The DLL-based architecture allows users and third-party developers to easily add custom component models, using all common programming languages (C, C++, PASCAL, FORTRAN, etc.). In addition, TRNSYS can be readily connected to other applications, for pre- or post-processing or through interactive calls during the simulation (e.g. Microsoft Excel, Matlab, COMIS, etc.).

TRNSYS applications include: Solar systems (solar thermal and PV), Low energy buildings and HVAC systems with advanced design features (natural ventilation, slab heating/cooling, double façade, etc.), Renewable energy systems, Cogeneration, fuel cells etc

A TRNSYS project is typically setup by connecting components graphically in the Simulation Studio. Each component is described by a mathematical model in the TRNSYS simulation engine and has a set of matching Proforma's in the Simulation Studio The proforma has a black-box description of a component: inputs, outputs, parameters, etc. TRNSYS components are often referred to as Types (e.g. Type 1 is the solar collector). The multizone building model is known as Type 56.

The Simulation Studio generates a text input file for the TRNSYS simulation engine. That input file is referred to as the deck file.

2.5.1 TESS Libraries

Thermal Energy System Specialists (TESS) was founded in early 1994 by a group of engineers dedicated to providing engineering software and programming expertise to companies and individuals in the energy field. Relying heavily on TRNSYS [23] and other popular simulation tools, TESS provides analyses of a variety of thermal systems. They have experience in developing simulations and analyses for a multitude of different components and systems used in today's energy engineering field, including, Geothermal Heat Pump Systems, Combined Heating, Cooling and Power Systems, Solar Thermal Processes, Building Load Evaluation, Heating, Ventilating and Air Conditioning Systems, Refrigeration Systems, Photovoltaics, etc.

2.5.2 STEC Libraries

STEC [24] is a collection of TRNSYS models especially developed to simulate solar thermal power generation. It is a supplement to the standard TRNSYS routines featuring components from solar thermal power plants like concentrating collectors, steam cycles, gas turbines and high temperature thermal storage systems. It was developed as a SolarPACES activity and is steadily used, updated and completed by users within the SolarPACES group. The STEC simulation models are intensively used in feasibility studies for solar thermal power projects as well as in research programmes for new solar thermal power technologies.

The STEC model library was initiated in 1998 in a joint effort by DLR (German Aerospace Centre), Sun*Lab/SANDIA (USA) and IVTAN (Institut for High Temperatures of the Russian Academy of Science, Russia). TRNSYS and the STEC were envisioned as a potential replacement for the SOLERGY code, up to then the quasi-standard for estimating the annual performance of solar thermal power plants, which was no longer up to date with modern standards of computing power and user friendliness. SOLERGY is limited to energy flow calculations of fixed (hard wired) plant configurations. Consequently, various code adaptations arose for different plant designs and detailed modelling of plant thermodynamics was not possible. TRNSYS was chosen for the simulation environment because of its modularity, user friendliness and the simplicity in adding new component models. Moreover, the availability of the TRNSYS source code together with its reasonable price gave rise to hope for a rapidly increasing acceptance and usage of the STEC software developments.

In 2000 the STEC models were updated to be fully compatible with the new TRNSYS15 and Iisibat3. In early 2001, parts of the STEC library were successfully validated with measurement data from the SEGS VI plant, a commercial solar thermal power plant in the Californian dessert. While agreement between the simulation and actual plant data was generally within 10%, there was difficulty in modelling solar field flow rate during transients. Later that year, Thorsten Stuetzle, Prof. Beckman and colleagues at the University of Wisconsin performed a ground-up analysis of the problem and developed a dynamic solar field model and new control algorithms that can both better model existing plant behaviour and offer the possibility of more stable field outlet temperatures if implemented in place of human control. The latest version 3.0 of the library was released in October, 2006. The German DLR is currently the keeper of the library and is in charge of updating and distributing it [25].

2.6 Use of transient simulation software in cogeneration systems studies

Application of transient simulation software in cogeneration systems studies are limited, as found by an extensive literature search. The following cogeneration HVAC study projects are reported of being carried out by TESS and ORNL using TRNSYS as the simulation engine. They are not yet documented by any published results:

Fort Bragg: Combined Heating, Cooling, Power Simulations: Study of combined heating, cooling and power systems for a central plant application at Fort Bragg. Projections from the simulations of the pre-retrofit steam plant will be calibrated to measured data taken at the site in order to tune the model to better fit the data. The proposed retrofit to the building will be performed in the simulation to determine the energy and demand impacts. Control issues and equipment specifications will be analyzed to determine their impact on performance.

Floyd Bennett Field, Gateway National Recreation Area: Combined Heating, Cooling, Power Simulations: Study of combined heating, cooling and power systems for an application at Floyd Bennett Field, Gateway National Recreation Area. Projections from the simulations of the pre-retrofit heating and cooling systems will be calibrated to measured data taken at the site in order to tune the model to better fit the data. The proposed retrofit to the building will be performed in the simulation to determine the energy and demand impacts. Control issues and equipment specifications will be analyzed to determine their impact on performance.

2.7 Objectives of this study

Traditionally, cogeneration systems are studied and optimized based on their steady-state performance [26-28],[29-34],[35-37]. In a recent assessment of an existing cogeneration facility comprising two 1.6 MWe NG SI reciprocating engines by simplified steady state analysis, [38], it was found that system's performance was not economically viable, mainly due to the degree of exploitation of the produced heat.. This fact negatively affected some thoughts to further invest on the production of cooling. In general, when one shifts to tri-generation, the situation becomes more complex as regards economic analysis. For example, the steady state analysis presented in [27], regarding a hospital tri-generation system based on reciprocating natural gas engines, concluded that, from the exergy point of view, the cooling power consumption of a compression chiller are substantially lower than those of an absorption chiller during the whole cooling season. This was be explained by the fact that the exergy factor of electricity is 1, whereas the exergy factor of heat depends on the temperature levels of taken-off heat. Considering exergy, cooling power costs from May to August for a one-stage hot water absorption chiller (gas engine) were the highest. For mid season, (March, April, September and October) it was observed that the costs of cooling power from a steam absorption chiller (gas turbine) and from a hot water absorption chiller (gas engine) were substantially higher than those from a compression chiller. The reason for this lies in the differences in exergetic efficiencies [39] of the two types of chiller. A comparison between different types of chillers shows that the cooling power costs are much higher when the calculation is based on the exergy analysis than those based on the energy analysis [40, 41]. The sensitivity of the various chiller types on fuel (natural gas) cost in this analysis was also remarkable.

Moreover, the transient performance of systems of this type is highly variable, due to the variation in thermal energy demand that is associated with changes in weather and schedules [42]. See for example the recorded performance of a hospital cogeneration system reported in Figure 20.

In the specific case study, approximately 3000 data points of cogeneration plant logged at 6 min. intervals over a two week period was taken for analyzing the system performance. Various performance parameters of the cogeneration system, such as the energy utilisation factor, artificial thermal efficiency and heat-to-power ratio, are shown in the figure. Total energetic efficiency values stayed around 50%, while the heat energy being recovered from the plant reaches about 85%, indicating that approximately 35% of the recoverable heat was being dumped to the cooling towers. Obviously, steady state performance is not the best way to assess and optimize cogeneration systems

[43-45]. For this reason, during the recent years, energy systems simulation software is increasingly employed in the study of transient operation of cogeneration systems.

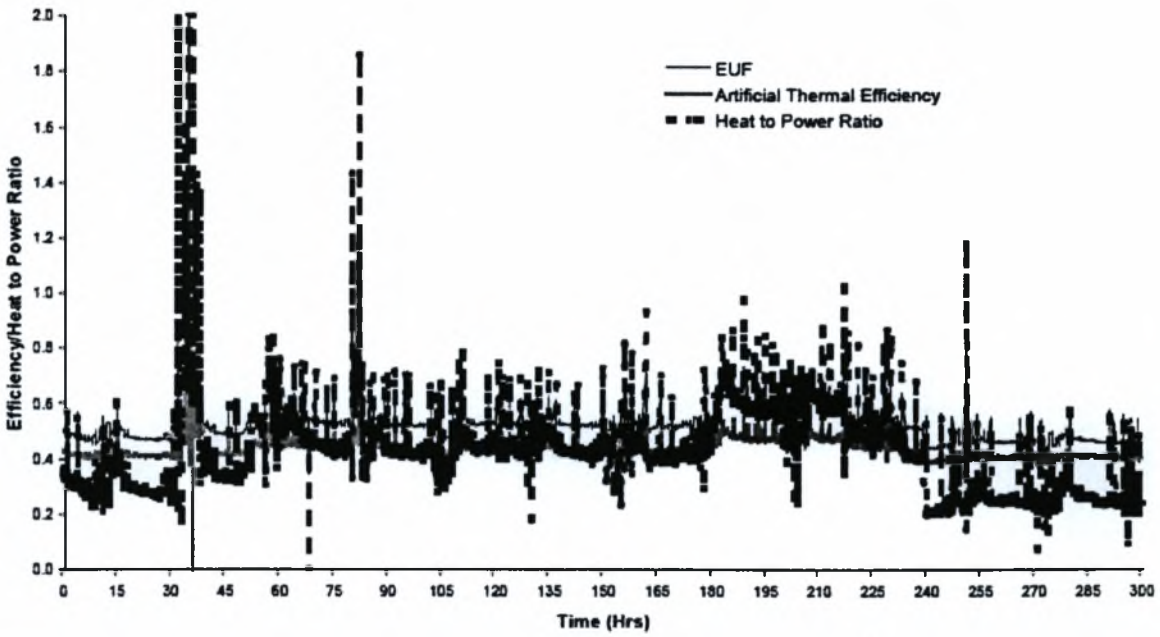

Figure 20 Recordings of hospital cogeneration system performance (adapted from [42])

However, the study of transient operation faces numerous challenges due to the complexity of the systems, and research continues in an exploratory manner, in a search for novel optimization methodologies.

Based on the above the main objectives of this thesis are the following:

- To develop a transient simulation model of a tri-generation system in the TRNSYS environment
- To understand and study system's transient operation based on the simulation tool, and
- To perform system's size optimization, based on a simplified economic analysis.

The specific trigeneration system selected and studied for retrofitting to the Volos Public Hospital, is based on a combined cycle and produces electricity, steam, hot water and chilled water.

The size of the specific installation is of the order of a few MW, but it can be readily scaled up to fit much bigger cogeneration installations for commercial buildings, district heating and cooling etc, sized up to and beyond 100 MW. The experience gained by the modelling and sizing process could support the future development of dedicated optimization methodologies, based on the transient system's performance, instead of the standard, steady-state optimization procedures [46, 47].

3 System Simulation Details

3.1 Description of the system studied

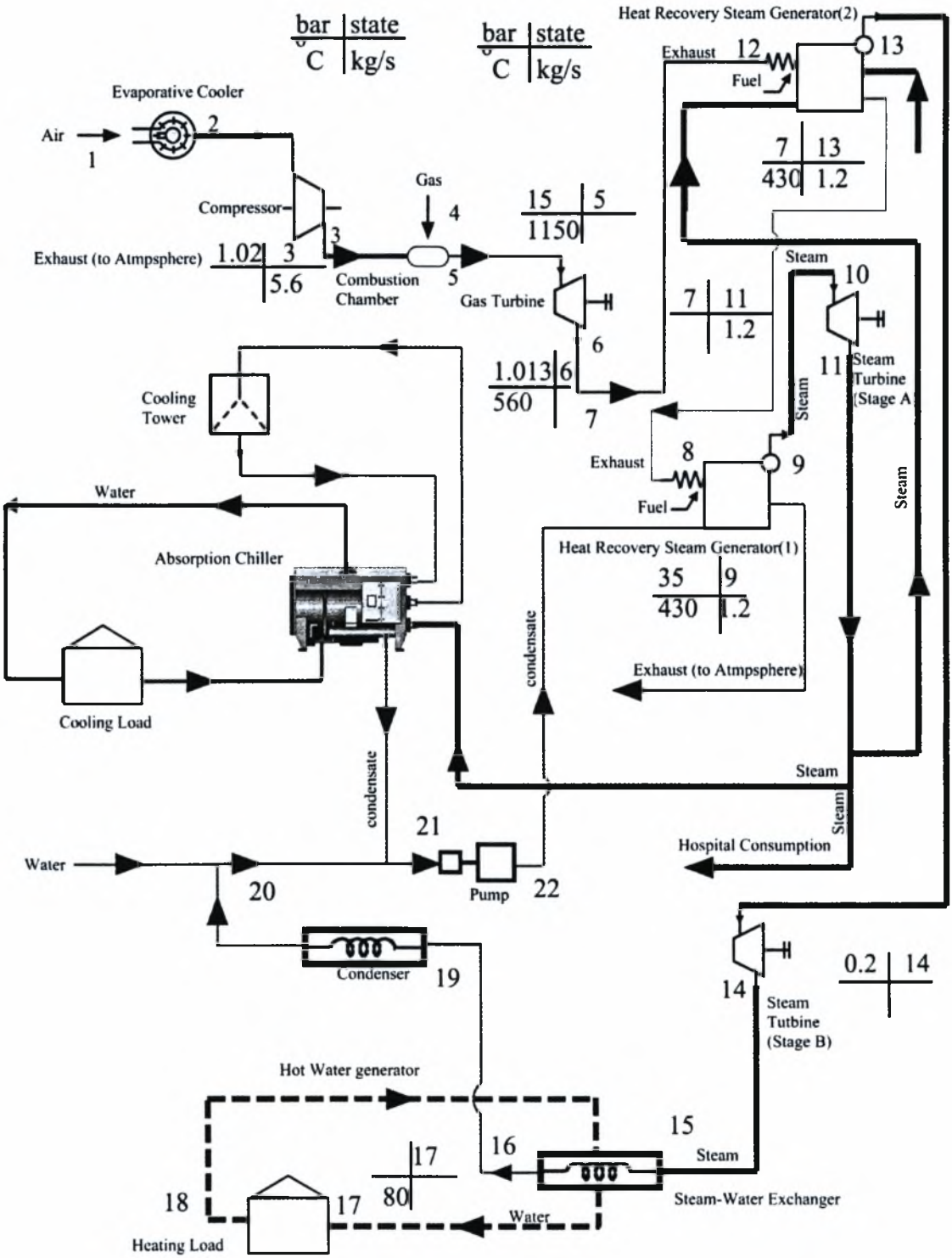

Figure 21 Schematic of the system studied in this work

This study models a combined-cycle tri-generation application with additional hot water loads. A system's schematic is shown in Figure 21. A gas turbine produces power that depends on the (variable) inlet air conditions. The gas turbine exhaust feed the respective heat recovery steam generators 1-2, producing superheated steam at 3500 kPa and 430 °C and at 700 kPa and 430 °C, respectively. The waste heat streams leaving the heat recovery steam generators are exhausted to the ambient, at about 130 °C. The steam exiting the heat recovery steam generator is expanded in a steam turbine (operating at maximum capacity) to 700 kPa. Some of useful exhaust steam from the turbine is then directed to a double-effect absorption chiller to meet the cooling load and hospital's consumption, while the rest is further expanded in a second steam turbine. This is also a backpressure turbine. The steam is exited to a heat exchanger producing hot water for space heating (see Figure 21).

The absorption chiller takes the 700 kPa steam and provides chilled water to the load, rejecting energy to a cooling water flow stream. In this study, the cooling load is specified by a typical load curve. Detailed building models and cooling equipment components could easily be added to the system.

In addition to standard TRNSYS types, certain components are employed from the TESS Library (Thermal Energy System Specialists) [48]. Also, certain Types from the STEC library are employed [24]. Certain codes were slightly modified to better meet the specifications of the particular modelling project.

In addition to the above, one new component was developed in FORTRAN code, namely, the heat recovery steam generator. In the basic configuration of Figure 19, the heat recovery steam generator docs not require additional heating. In our case, we have an additional heat exchanger for the superheating of steam entering turbine Stage A, by supplemental heating by natural gas. A new component was written to calculate the fuel and combustion air consumption as functions of the steam generation rate (see Figure 25). The hot combustion gases transform the feed water to superheated steam in the economizer, which preheats the water, the evaporator, and superheaters (Figure 23). [49], [26].

As regards the fuel, a typical composition of Natural Gas used in Central Europe was assumed (Table 14).

The heating and cooling loads on the building (Hospital of Volos) have already been determined by routine calculations. A standard TNSYS equation component was inserted to simulate the effect of these loads upon the system. This component imposes the variable heating or loads, by heating or

cooling, respectively, the water exiting from the boiler or the chiller. A user-specified load (cooling=positive load, heating = negative load) is calculated based on the following assumptions:

During the heating Season (January-April and October-December) (0-3624hour and 6553-8760hour): the maximum Heating Load is set to 2800000 kJ/h, and the maximum Cooling Load to 1900000 kJ/h

The minimum ambient temperature for the heating season is set to -5°C from the Weather Generator, and the maximum ambient temperature for the cooling season is set to 41°C from the Weather Generator.

Heating and sensible cooling loads are calculated based on the difference of the respective temperatures set-points (21°C for winter and 26°C for summer) from the ambient temperature.

The components employed in the simulation study are summarized in Table 7(see Figure 22).

A cogeneration system for the Public Hospital of Volos is simulated in this study, to assist the design process.

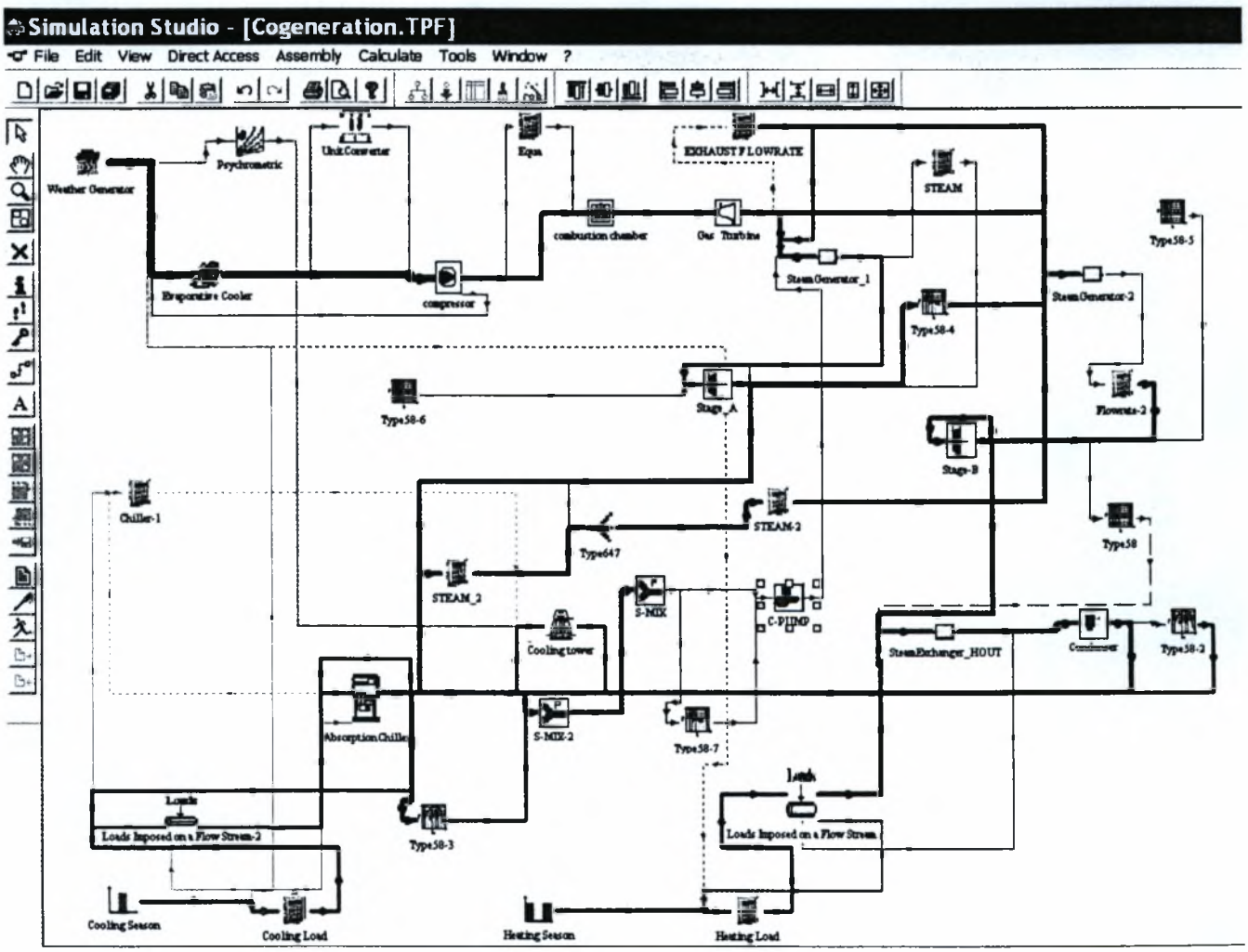

Figure 22 TRNSYS project file

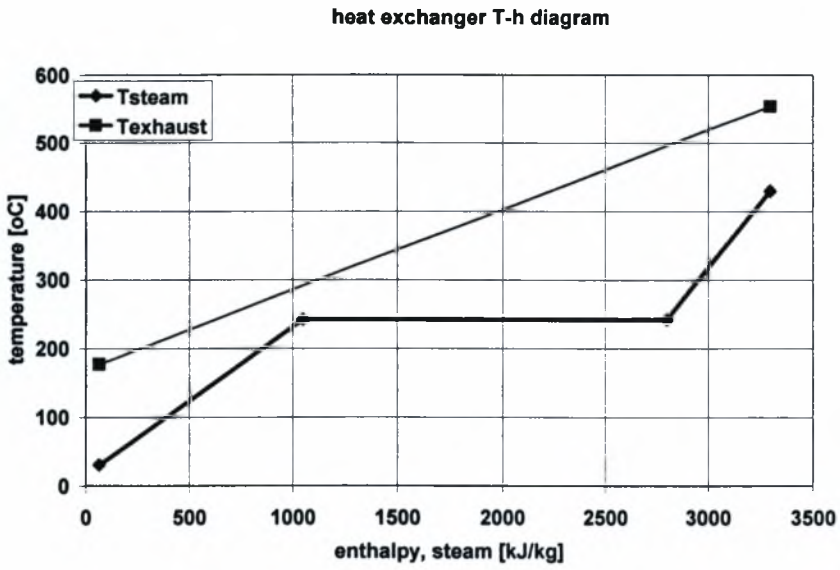

Figure 23 T-h diagram for steam and exhaust from gas turbine

3.2 Components employed in the simulation

Table 7 Modules that are employed in the project

	Name		Library
1	Weather Generator	Type54	Trnsys 16
2	Evaporative Cooling Device	Type506	Tess
3	Unit Conversion Routine	Type57	Trnsys 16
4	Psychrometric	Type33	Trnsys 16
5	Compressor	Type424	StecLib
6	Combustion chamber	Type426	StecLib
7	Gas Turbine	Type427	StecLib
8	Heat Recovery steam generator	Type152	Olympia Zogou
9	Steam Exchanger	Type152	Olympia Zogou
10	Refrigerant Properties	Type 58	Trnsys 16
11	Building Cooling and Heating Load	Type682	Tess
12	Steam-Fired Double-Effect Absorption Chiller	Type686	Tess
13	Cooling Tower	Type51	Trnsys 16
14	Turbine Stage	Type318*	StecLib
15	Condenser	Type383	StecLib
16	Pump used for steam cycle	Type390*	StecLib
17	Mixer	Type330*	StecLib
18	Fluid Diverting Valve	Type647	Tess
19	Online Plotters	Type65	Trnsys 16
20	Simulation Summary	Type28	Trnsys 16
21	Equations		Trnsys 16

3.2.1 Weather Generator

This component generates hourly weather data given the monthly average values of solar radiation, dry bulb temperature, humidity ratio, and wind speed. The data are generated in a manner such that their associated statistics are approximately equal to the long-term statistics at the specified location. The purpose of this method is to generate a single year of typical data, similar to a Typical Meteorological Year. This component allows TRNSYS to be used for any location for which standard yearly average weather statistics are known. However, many of the correlations used in the model were developed from primarily temperate climate data. For other climates, e.g., tropical climates, the generated data are less accurate and the user may wish to make some modifications. In this instance of Type54, predefined random number seeds are used as the basis of the generation of hourly values. It reads monthly average values of temperature, solar radiation, and humidity ratio. If desired, the user may enter values of monthly average wind speed as parameters to the model.

3.2.2 Evaporative Cooling Device

Type506 models an evaporative cooling device for which the user supplies the inlet air conditions and the saturation efficiency and the model calculates the outlet air conditions. The cooling process is assumed to be a constant wet bulb temperature process meaning that air enters and exits at the same wet bulb temperature. The device is not equipped with controls that monitor the conditions of the outlet air.

When the device is ON (based on a user supplied control signal value), Type506 cools the air as much as it can given the entering conditions and the device efficiency.

3.2.3 Unit Conversion Routine

To accommodate users accustomed to working with English or not standard SI units TYPE 57 unit conversion routine is provided. Users must describe the incoming variable type and units (temperature and C for example) and the desired output variable units (F for example) using tables provided at the end of the technical documentation of this component. The conversion routine checks the input to make sure it is of the correct variable type and units, performs the unit conversion, providing the new output type and units to all units depending on this output.

3.2.4 Psychrometric

This component (Type33) takes as input two properties of moist air and calls the TRNSYS Psychrometrics routine, returning the following corresponding moist air properties: dry bulb temperature, dew point temperature, wet bulb temperature, relative humidity, absolute humidity ratio, and enthalpy.

3.2.5 Compressor

This compressor model calculates the outlet conditions from the inlet state by using an isentropic efficiency [50], which can be specified by the user as a function of the flow rate using a variable curve. In this way, the model calculates for a given compressor ratio the outlet- temperature tout, is and - enthalpy hout, is for an isentropic compression by calling the Gas routine (call Gas with the inputs pout and $s_{out,\,is} = s_{in}$). The real outlet conditions are then calculated by using the isentropic efficiency and a new call of the Gas routine (call Gas with the inputs p_2 and h_2).

$\Delta h = (h_{out,is} - h_{in}) / \eta_{sV}$

$h_{out} = h_{in} + \Delta h$

$P_{compressor} = (m_{out} * \Delta h) / \eta_m$

PARAMETER Number	Name	Unit
1	compression ratio	
2	mechanical efficiency	
3	ISO inlet mass flow design	[kg/hr]
4	partial load by mass flow reduction if mode 2 limited the mass flow when it is an input	
5	operating mode mode = 1 : inlet mass flow as a function of the inlet conditions mode = 2 : inlet mass flow as an input	
INPUTS Number	Name	Unit
1	inlet air temperature	[°C]
2	inlet pressure	[BAR]
3	inlet mass flow if mode 2	[kg/hr]
4	isentropic efficiency design to be specified by the user	
5	cooling air mass ratio evaluated by the turbine model (to cool the blades)	
OUTPUTS Number	Name	Unit
1	outlet temperature	[°C]

2	outlet pressure	[BAR]
3	outlet mass flow working air	[kg/hr]
4	outlet mass flow cooling air	[kg/hr]
5	actual compressor power	[kJ/hr]
6	relative compressor power (Pve/mse)	[kJ/kg]
7	outlet enthalpy	[kJ/kg
8	total outlet mass flow	[kg/hr]

3.2.6 Combustion chamber

This model describes an adiabatic combustion chamber for different liquid or gaseous fuels.

The user has to define the fuel by the lower heating value and the mass ratio of the fuel elements: C, H_2, S, O_2, N_2, H_2O, ash and air nitrogen given in the organic analysis. The model allows two different operating modes- in the first case for a given outlet temperature the required fuel mass flow is calculated, in the other way the reached temperature results from the fuel flow used. Beside that a pressure loss is evaluated, based on a user specified reference value as a function of inlet conditions.

PARAMETERS Number	Name	Unit
1	operating mode mode = 1 : outlet temperature as a result of given fuel flow rate mode = 2 : fuel flow rate as a result of given outlet temperature	
2	lower calorific value	[kJ/kg]
3	C mass ratio	
4	H2 mass ratio	
5	S mass ratio	
6	N2 mass ratio	
7	O2 mass ratio	
8	H2O mass ratio	
9	ashes mass ratio	
10	relative pressure drop design	
11	design or off-design (mode 3 or 4) pressure loss independent/dependent from the inlet conditions	
12	inlet temperature design if mode 4	[°C]
13	inlet pressure design if mode 4	[BAR]
14	inlet mass flow design if mode 4	[kg/hr]
INPUTS Number		
1	inlet air temperature	[°C]
2	inlet air flow rate	[kg/hr]
3	fuel flow rate if mode 1	[kg/hr]
4	outlet temperature if mode 2	[°C]
5	inlet pressure	[BAR]
6	inlet enthalpy	[kJ/kg]
OUTPUTS		

Number		
1	outlet temperature	[°C]
2	fuel mass flow	[kg/hr]
3	outlet mass flow combustion air	[kg/hr]
4	outlet pressure	[BAR]
5	air ratio	
6	CO2 mass ratio	
7	H2O mass ratio	
8	SO2 mass ratio	
9	air nitrogen mass ratio	
10	air mass ratio	
11	outlet mass flow CO2	[kg/hr]
12	fuel heat flow	[kJ/hr]
13	specific minimum air quantity	
14	outlet enthalpy	[kJ/kg]
15	Relative pressure drop	

3.2.7 Turbine

This gas turbine model calculates the outlet conditions from the inlet state by using an isentropic efficiency which can be specified by the user. In this way, the model calculates for a given ambient pressure and therefore known turbine outlet pressure first the outlet- temperature tout, is and -enthalpy hout, is for an isentropic expansion by calling the Gas routine (call Gas with the mixture of the combustion air and the inputs pout and $s_{out,\ is} = s_{in}$). The real outlet conditions are then calculated by using the isentropic efficiency and a new call of the Gas routine (call Gas with the mixture of the combustion air and the inputs p_2 and h_2) [50]. For the inlet state the model considers the merge of the combustion- and cooling- air by computation new inlet conditions for the mixture.

$\Delta h = (h_{in} - h_{out,is}) * \eta_{st}$

$h_{out} = h_{in} - \Delta h$

$P_{turb} = m_{in} * \Delta h * \eta_m$

PARAMETERS Number	Name	Unit
1	mechanical efficiency	
2	maximum inlet temperature without cooling	[°C]
3	ambient pressure	[BAR]
4	maximum inlet temperature with cooling [°C]	
INPUTS Number		
1	temperature combustion air	[°C]
2	temperature cooling air	[°C]
3	inlet pressure	[BAR]
4	mass flow combustion air	[kg/hr]
5	mass flow cooling air	[kg/hr]

6	isentropic efficiency	
7	CO2 mass ratio	
8	H2O mass ratio	
9	SO2 mass ratio	
10	air mass ratio	
11	air nitrogen mass ratio	
12	relative pressure drop exhaust silencer	
13	relative pressure drop heat exchanger hot side (optional for a recuperative cycle)	
14	inlet enthalpy working air	[kJ/kg]
15	inlet enthalpy cooling air	[kJ/kg
OUTPUTS Number		
1	outlet temperature	[°C]
2	outlet mass flow	[kg/hr]
3	actual turbine power	[kJ/hr]
4	relative turbine power (Pte/ma)	[kJ/kg]
5	relative turbine power (Pte/ma)	[kJ/kg]
6	outlet enthalpy	[kJ/kg]
7	outlet pressure	[BAR]

3.2.8 Heat Recovery steam generator

This is a new component written to simulate the performance of a HRSG. Basically, it calculates the attainable exhaust gas temperature at the heat exchanger's exit, as function of the required steam generation rate and the required degree of superheating. If the available exhaust enthalpy is not sufficient to cover the heat exchanger duty, additional fuel is injected and burned in the combustion chamber. No additional supply of air is required, since the combustion A/F in the gas turbine is of the order of 50 and the exhaust gases have plenty of oxygen left from the combustion in the gas turbine. Performance tests conducted with natural gas boilers were used to check the accuracy of the model [49].

PARAMETERS Number	Name	Unit
1	Inlet pressure of feed water or steam	[kPa]
2	Outlet Temperature of steam	[kPa]
3	Outlet pressure of steam	[kPa]
4	Maximum steam production of steam	[kg/s]
5	Minimum steam production of steam	[kg/s]
6	Ratio of blowdown in %	
7	Exhaust gas Temperature at maximum load	°C
8	Exhaust gas Temperature at minimum load	°C
9	Exterior boiler surface	m^2
10	Heat transfer coefficiency for interior boiler wall	w/m^2K
11	Temperature difference between exhaust gas inlet and steam outlet	°C
12	Air rate for combustion	
13	Mole fraction of carbon	
14	Mole fraction of hydrogen	

INPUTS Number		
1	Steam production	[kg/s]
2	Ambient temperature	°C
3	Exterior boiler surface	°C
4	Fuel temperature	°C
5	Inlet temperature of feed exhaust gas	°C
6	Inlet exhaust gas mass flow rate	[kg/s]
7	Inlet Temperature of feed water or steam	°C
OUTPUTS Number		
1	Steam production	[kg/hr]
2	Blowdown mass flow rate	[kg/hr]
3	Fuel mass flow rate	[kJ/kg]
4	Fuel energy input	[kW]
5	Outlet exhaust gas temperature	°C
6	Outlet exhaust gas mass flow rate	[kg/s]
7	Exhaust gas temperature	°C
8	Lower heating value	kJ/kg

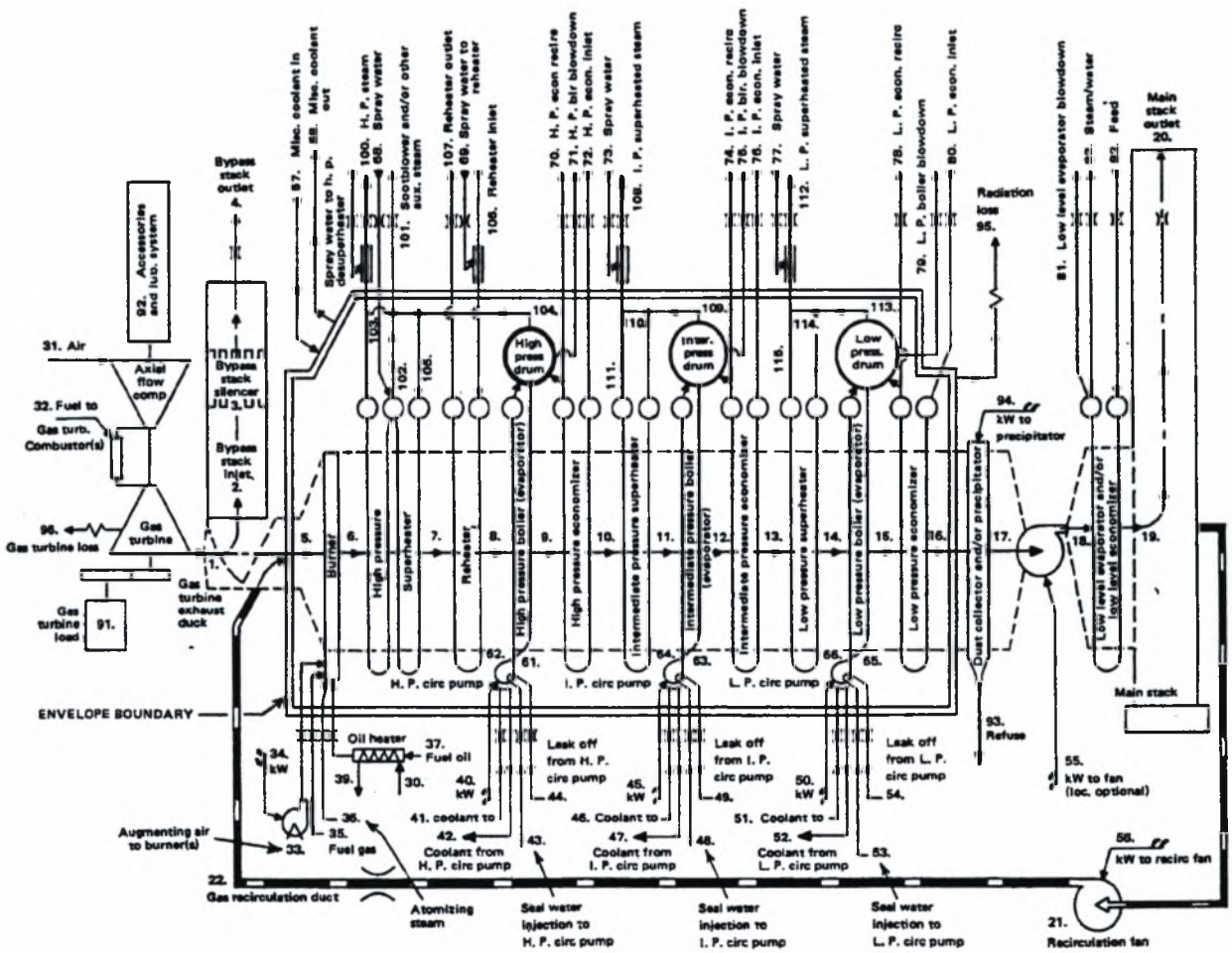

Figure 24 Gas Turbine Hear Recovery Steam Generator Unit Diagram

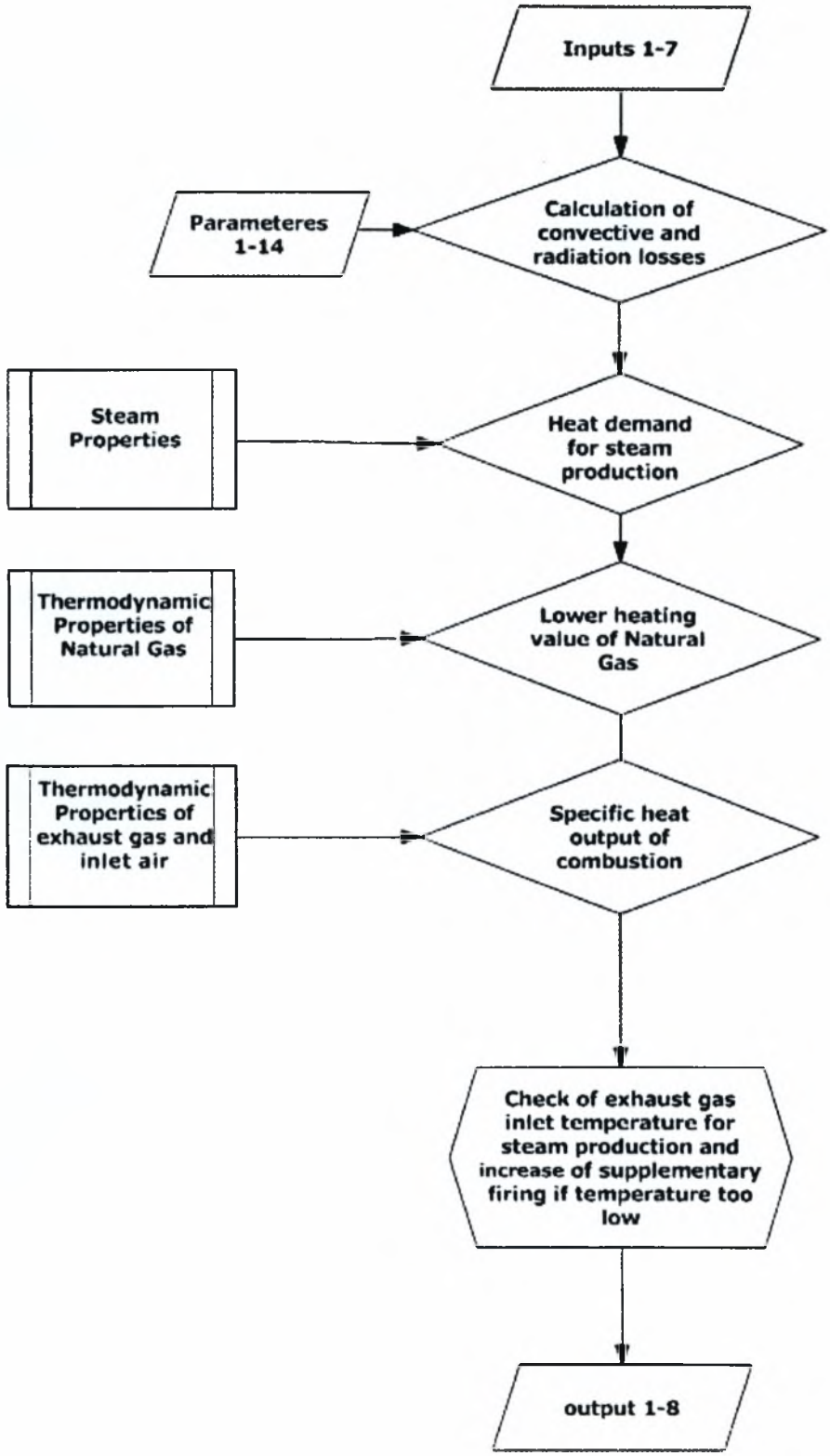

Figure 25 Flow Chart of Heat Recovery Steam Generator

3.2.9 Cross Flow Steam Heat Exchanger

A zero capacitance sensible heat exchanger is modelled in various configurations. Given the hot and cold side inlet temperatures flow rates, enthalpy and pressure, the effectiveness is calculated for a given fixed value of the overall heat transfer coefficient.

This model relies on an effectiveness minimum capacitance approach to modelling a heat exchanger. Under this assumption, the user is asked to provide the heat exchanger's UA and inlet conditions. The model then determines whether the cold (load) or the hot (source) side is the minimum capacitance side and calculates heat exchanger effectiveness based upon the specified flow configuration and on UA. The heat exchanger outlet conditions are then computed, for all flow configurations.

A schematic of the heat exchanger is shown in Figure 26 below.

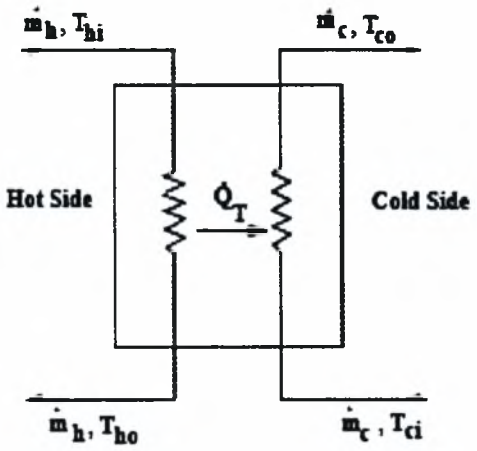

Figure 26 Heat Exchanger Schematic

3.2.10 Refrigerant and Steam Properties

This component takes as input two unique independent state properties of a refrigerant and calculates the remaining state properties. It calls the TRNSYS Fluid Properties routine and the TRNSYS Steam Properties Routine to calculate the thermodynamic properties. The available refrigerants for this routine are: R-11, R-12, R-13, R-14, R-22, R-114A, R-134A, R-500, R-502, ammonia (R-717) and steam (R-718).

3.2.11 Building Cooling and Heating Load

The heating and cooling loads on the building (Hospital of Volos) have already been determined by calculations, the simulation task at hand is to simulate the effect of these loads upon the system. This component allows for there to be an interaction between such pre-calculated loads and the HVAC system by imposing the load upon a liquid flowing through a device. This model simply imposes a user-specified load (cooling=positive load, heating = negative load) on a flow stream and calculates the resultant outlet fluid conditions.

Heating Season (January-April and October-December) (0-3624hour and 6553-8760 hour)

Cooling Season (May-September) (3625-6552 hour)

Max Heating Load 2,800,000 kJ/h

Max Cooling Load 1,900,000 kJ/h

Minimum ambient temperature for heating season (MATHS): -5.(C^o) from Weather Generator

Maximum ambient temperature for cooling season (MATCS): 41 (C^o) from Weather Generator

Tdryheat = min (MATHS, 22) (^oC)

Tdrycool = max (MATCS, 26) (^oC)

Qheat(t)= 2800000*((22-Tdryheat)/26))*Heating Signal [kJ/h]

Qcool(t)= 1900000*((Tdrycool-26)/20))*Cooling Signal [kJ/h]

3.2.12 Double-Effect Steam-Fired Absorption Chiller

In a "conventional" refrigeration cycle, refrigerant returns as low pressure vapor from the evaporator (ideally near the saturated gas line of the vapor dome). This vapour then passes through an electrically driven compressor in which it is turned into a higher pressure gas before being passed to the condenser. Both the work of pressurizing the vapour and the work of pumping the refrigerant through the system is done by the compressor. In a "single effect" absorption machine, the refrigerant (typically water) returning from the evaporator is absorbed in a medium (often aqueous ammonia or lithium bromide) and is cooled to a liquid state, rejecting its heat to a cooling fluid stream. This liquid is then pumped into a device called a generator, where heat is added from an energy source to desorb the refrigerant from its solution. In a "steam fired" chiller, the energy source is steam. Once the

refrigerant is revaporized, it enters the condenser and follows a standard refrigerant cycle (condenser, expansion valve, evaporator). A cooling tower is usually present, but air-cooled condensers are also increasingly employed [51].

In a double-effect machine, two individual absorption cycles are used; a high temperature absorption machine rejects energy from its condenser to the generator of a low temperature machine. A double effect absorption cycle is shown schematically in Figure 28. The benefit of an absorption refrigerant cycles is that the energy required to pump the fluid from a low pressure in the absorber to a higher pressure in the generator is comparatively small and the remainder of the work (vaporizing the refrigerant) can be accomplished with heat instead of electricity. This fact makes absorption chillers especially valuable in cogeneration systems where waste heat from steam and other processes is abundant [52, 53]. Two types of absorption chillers are commercially available: Single effect and Double effect absorption chillers.

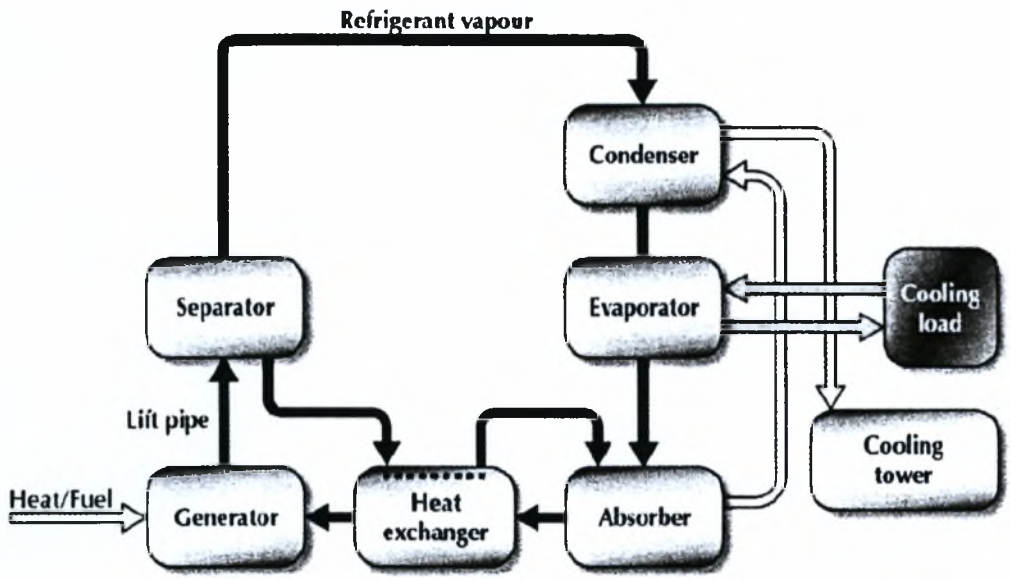

Figure 27 Absorption Cooling System Schematic

Compared to single-effect chillers, double-effect absorption chillers have a higher capital cost but are more energy efficient and thus less expensive to operate. The overall economic attractiveness of each chiller depends on many factors, including the cost of capital and cost of energy. Both types of chillers can be fired with natural gas, or heated with steam.

All absorption chillers consist of the following major components and ingredients: water (as a refrigerant), lithium bromide salt (as an absorbent), an absorber (a vessel in which the absorbent

solution absorbs refrigerant vapour into solution), a condenser (a vessel in which refrigerant vapour is liquefied by removing heat), an evaporator (a vessel in which liquid refrigerant vaporizes by removing heat and thus, producing cooling), at least one generator (a vessel in which refrigerant vapors are produced from the solution of the absorbent and the refrigerant by supplying heat), and at least one heat exchanger (for exchanging heat between two fluid streams).

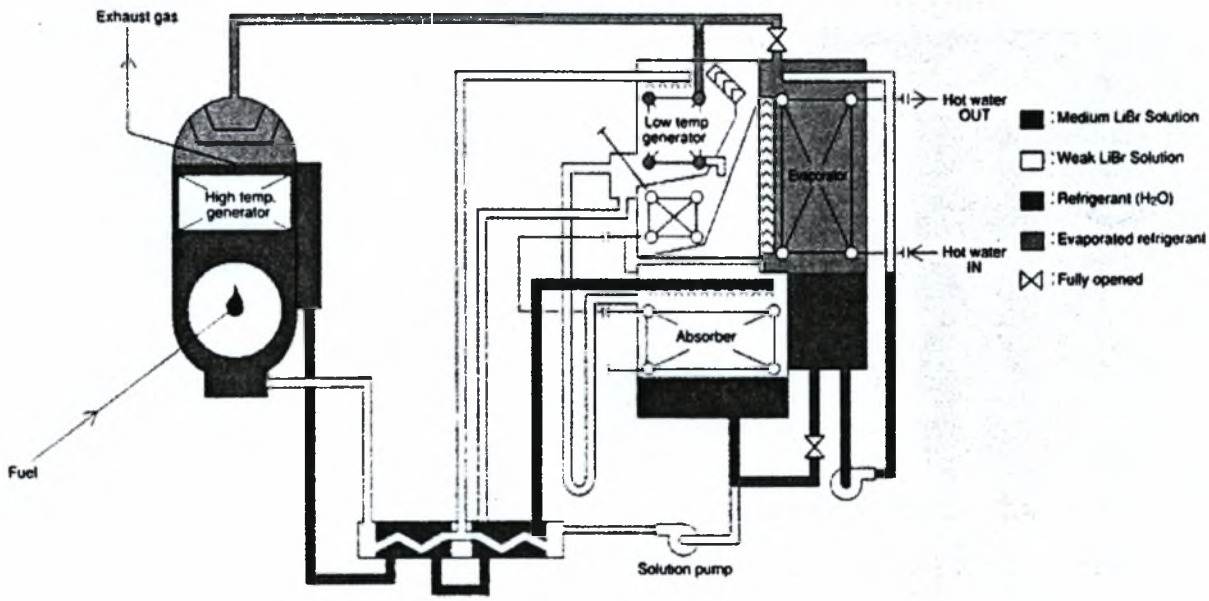

Figure 28 Double-effect LiBr absorption chiller schematic. The high temperature steam (refrigerant) generated in the high temperature generator is moved through valve and condensed in the evaporator, heating up hot water for heating purposes. The refrigerant is then mixed with medium weak solution in the absorber, then pumped up to the high temperature generator by means of the solution pump. The medium weak solution generates steam (refrigerant vapour) in the high temperature generator.

This Type uses a catalog data lookup approach to predict the performance of a double effect, steam water fired absorption chiller. In this design, the heat required to desorb the refrigerant is provided by a steam source. The energy of the refrigerant absorption process is rejected to a cooling water stream and the machine is designed to chill a third fluid stream to a user designated set point temperature. Because of the catalog data lookup approach, the performance of the machine can be predicted and interpolated within the range of available data (e.g. Figure 29) but cannot be extrapolated beyond the range. One beneficial feature to this model is that the data, taken directly from manufacturer's catalogs available online is normalized so that once a data file has been created, it may be used to model absorption machines other than the specific size for which the data was intended. In creating example data files for distribution with this component, the developers noted that there was very little variability between data files once they were normalized. Using normalized data and the model's first two

parameters (design coefficient of performance and design capacity) the user can adjust the size of the machine being modelled to whatever is appropriate to the system being simulated.

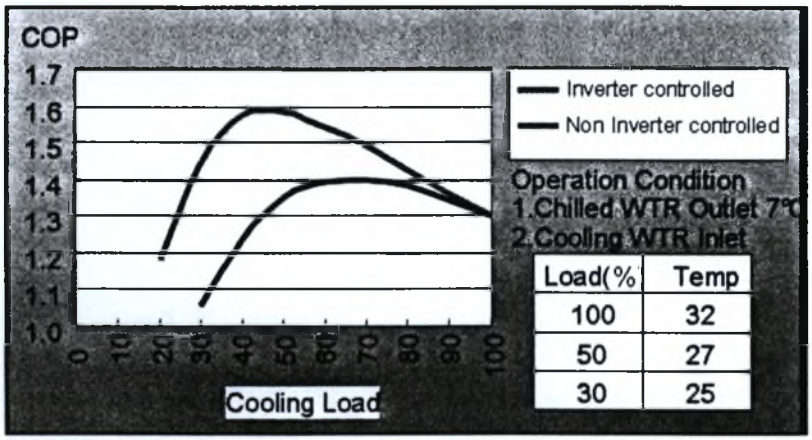

Figure 29 COP characteristics of double effect Absorption Chiller [54]

3.2.13 Cooling Tower

In a cooling tower, a hot water stream is in direct contact with an air stream and cooled by sensible heat transfer due to temperature differences with the air and mass transfer resulting from evaporation to the air. The air and water streams may be configured in either counter flow or cross flow arrangements. Ambient air is drawn upward through the falling water. Most towers contain a fill material which increases the water surface area in contact with the air. A cooling tower is usually composed of several tower cells that are in parallel and share a common sump. Water loss from the tower cells is replaced with make-up water to the sump. This component models the performance of a multiple-cell counter flow or cross flow cooling tower and sump. There are two primary modes. In this instance (MODE 1) the user enters the coefficients of the mass transfer correlation, c and n. Although this data is difficult to obtain, the ASHRAE Systems & Equipment Handbook [55] gives typical data.

Table 8 Typical efficiency of steam turbines

Operating Pressure	Power capacity				
	5000 kW	10000 kW	14000 kW	20000 kW	30000 kW
250 psig (17.2 bar)	74.3%	76.6%	-	-	-
400 psig (27.6 bar)	73.3%	75.7%	76.9%	77.7%	-
600 psig (41.1 bar)	72.0%	74.8%	76.3%	77.2%	77.6%
850 psig (58.6 bar)	-	74.2%	75.8%	76.8%	77.3%
1250 psig (86.2 bar)	-	-	75.4%	76.5%	77.0%

3.2.14 Turbine stage

This turbine stage model calculates the inlet pressure of the turbine stage from the outlet pressure, the steam mass flow rate and reference values of inlet and outlet pressure and mass flow rate using Stodolas law of the ellipse. It evaluates the outlet enthalpy from the inlet enthalpy and inlet and outlet pressure using an isentropic efficiency.

A bypass indicator output is set to 1 if either the input bypass indictor is equal to one or if the flow rate is below a reference fraction given in the parameters. If the bypass flag is set, the steam passes the turbine without doing any work remaining in the same condition. The pressure is assumed to be the same as under minimal flow conditions when the bypass is turned off.

PARAMETERS Number	Name	Unit
1	Reference inlet pressure	[BAR]
2	Reference outlet pressure	[BAR]
3	Reference flow rate	[kg/hr]
4	Reference efficiency	
5	Generator efficiency	
6	Alpha coefficient	
7	Beta coefficient	
8	Gamma coefficient	
INPUTS Number		
1	outlet pressure	[BAR]
2	inlet flow rate	[kg/hr]
3	inlet enthalpy	[BAR]
4	inlet bypass indicator	[kJ/kg]
OUTPUTS Number		
1	Inlet pressure	[BAR]
2	Outlet flow rate	[kg/hr]
3	Outlet enthalpy	[kJ/kg]
4	Turbine power	[kJ/hr]
5	Outlet bypass indicator	
6	Isentropic efficiency	

3.2.15 Condenser

This type models a water cooled condenser.

The cooling water temperature rise is given by parameter (2), the temperature difference between cooling water outlet temperature and condensing temperature is given by parameter (1). Therefore, the

condensing pressure only depends on the feed water inlet temperature and is constant when it is constant.

The transferred power of the condenser is calculated by

$Q_{cond} = h_s * fl_s + h_c * fl_c - (fl_c+fl_h)*h_{sat}$

Using:

h_s main steam inlet enthalpy

fl_s main steam flow rate

h_c additional condensate inlet enthalpy

fl_c additional condensate inlet flow rate

h_{sat} enthalpy of saturated water at p kond

The cooling water flow rate is evaluated by

$fl_{cool} = q_{cond}/(c_{pw} * par(2))$

3.2.16 Pump used for steam cycle

This pump model generates a mass flow rate as output which equals the demand mass flow input. The component can be used in conjunction with an evaporator which demands for a certain mass flow rate. The component also calculated the required pumping power by

$Ppump = (p_{out} - p_{in})*fl / (rho * eta_{pump})$

The outlet pressure is an input of this type and there are two options to evaluate the inlet pressure

if $par(1) = 1$ than $p_{in} = p_{out} - par(2)$

if $par(1) = 2$ than $p_{in} = par(2)$

3.2.17 Mixer

This type models a controlled mixer with two outlets and one inlet which can be used in combination with the turbine stage model and the turbine system controller to allow start-up bypass around the turbine. Enthalpy at inlet 1 and 2 are combined into the outlet enthalpy based on the fractional mass flow rate of each inlet. The pressure is transported opposite to the flow direction. i.e. the pressure at the

output is transported to Input 1 and 2. Therefore, it is obvious that the outlet pressure is an input of this component and the inlet pressures are outputs of this component.

INPUTS Number	Name	Unit
1	Inlet Flowrate 1	[kg/hr]
2	Inlet Enthalpy 1	[kJ/kg]
3	Inlet Flowrate 2	[kg/hr]
4	Inlet Enthalpy 2	[kJ/kg]
5	Outlet Pressure	[BAR]
OUTPUTS Number		
1	Outlet Flowrate 1	[kg/hr]
2	Outlet Enthalpy 1	[kJ/kg]
3	Inlet Pressure 1	[kg/hr]
4	Inlet Pressure 2	[kJ/kg]

3.2.18 Flow Diverter

Type647 models a diverting valve that splits a liquid inlet mass flow into fractional outlet mass flows. One inlet flow may be split into as many as 100 individual streams. The limit of 100 inlet flows can be modified in the Fortran source code.

3.2.19 Online Plotter

The online graphics component is used to display selected system variables while the simulation is progressing. This component is highly recommended and widely used since it provides valuable variable information and allows users to immediately see if the system is not performing as desired. The selected variables will be displayed in a separate plot window on the screen. In this instance of the Type65 online plotter, data sent to the online plotter is automatically printed, once per time step to a user defined external file. TRNSYS supplied unit descriptors (kJ/hr, kg/s, degC, etc.), if available, will be printed along with each column of data in the output file.

3.2.20 Simulation Summary

Type 28 can be conveniently used to generate daily, weekly, monthly or seasonal summaries of information computed in a simulation. Its output can be displayed either in a boxed format or as a table. Type 28 integrates its inputs over the time interval of the summary, performs user specified

arithmetic operations on the integrals, and prints the results. This configuration prints results to an external file and includes an energy balance check.

3.3 Weather data

Standardized meteorological data, in the form of a "Typical Meteorological Year - TMY", [22], were employed in the simulation. The TMY employed is not genuine because of the lack of the required, detailed meteorological data of the last 20 years for Volos. Instead, a TMY was artificially created by a subroutine of TRNSYS, based on the following existing monthly average meteorological data for the city of Volos: monthly average DB temperature, monthly average relative humidity, monthly average wind speed for the years 1956-1988, and monthly average total horizontal radiation for the years 1996-2000.

3.4 Basic calculations for component sizing

3.4.1 Building Description

The health sector is one of the largest users of energy in the Greece. There are approximately 131 Hospitals with 40000 beds.

There are many reasons why the use of CHP in hospitals is favourable. CHP can be one of the best ways to save money, and if less money is being spent on energy, more money could be made available for patient care. As CHP reduces energy waste it can help to reduce health and environment problems.

The Hospital of Volos consists of 6 separate buildings. The main building was constructed in year 1968 and the other 5 small periphery buildings were built later. The main building (basement and three floors) is divided in 5 interconnected sections. It's direction is NW-SE. The other four sections have the shape of "H" and consist of a basement and two floors each.

The total area of the main building is 10160m^2. Out of this area 2600m^2 (25.6%) are patient rooms, 690 m^2 (6.8%) operations rooms, 2200m^2 (21.6%) utility space and 4667 m^2 (45.9%) for other uses.

The energy consumption data employed in this study are based on an energy audit conducted by KAPE in 2000 [56]. They are approximate, since no dedicated measurement or monitoring methodology was carried out in this case (see for example [57, 58]).At present, the Hospital consumes electricity from the grid. Two heating oil-fuelled boilers with nominal power 562500 [kcal/h]

(2355075 [kJ/h]) each, produce heat for space heating and steam for the hospital's needs. Space cooling is provided by means of a compression chiller feeding 5 Air Handling Units with cold water, as well as 93 Split Units powered separately by electricity.

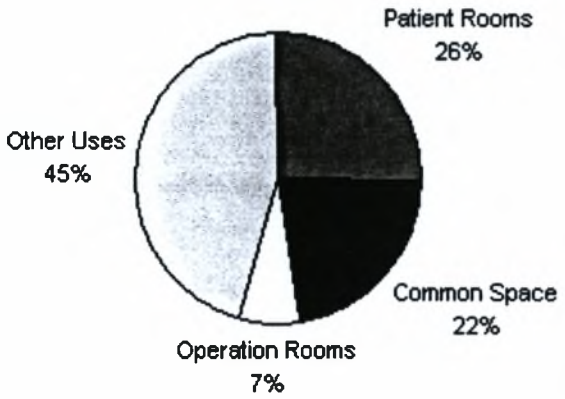

Figure 30 Allocation of Hospital's Area (percentage of total area).

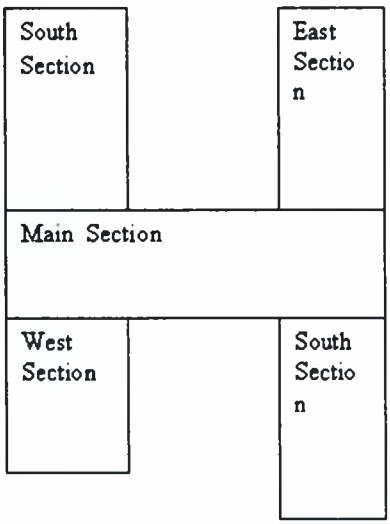

Figure 31 Shape of the central building

Table 9 Steam-consuming equipment of the Volos Public Hospital

Equipment	Number	Steam Load [kg/h]	Steam Properties			Electrical Power[kW]
			p [bar]	θ [°C]	h" [kJ/kg]	
Steam Boiler	4	110	1.5	111.4	2693.4	-
Steam Cauldron	4	110	1.5	111.4	2696.4	-
Steam Washing machine	3	150	4.5	147.9	2737.6	11
Washing machine -Mordant	1	150	4.5	147.9	2737.6	9
Steam Press	6	30	8	170.4	2767.5	0.5
Steam Press	1	500	8	170.4	2767.5	1.2
		1050				21.5

Table 10 Electricity consuming equipment of the Volos Public Hospital

	Equipment		Number	Power [kW]	Function Time [h/d]
Cooking	electric stove	stove	6	16.0	3
		oven	2	16.0	1
	Electric Oven		4	30.0	1
	Electric pan		1	13.2	0.8
	Fryer		2	12.0	0.5
	Steam Boiler		4	70.14	2
	Steam Cauldron		4	70.14	1
	Heating Cambin		2	2.0	2.5
	freezer		3	7.46	12
	Fridge		2	10.0	10
	Fridge		1	0.37	10
	Meat Cutter		1	2.98	0.25
	Vegetable Cutter		1	0.8	1
	Blender		1	0.8	1
	sheller		1	0.5	1
	Kneading Machine		1	0.5	1
	Dishwasher		6	1.12	2
	Fan		4	0.6	4
	Ventilator		1	1.86	8
Washing	Steam Washing Machine		3	108.7	10.3
	Washing machine - Mordant		1	106.7	10.3
	Washing machine		2	19	2
	Mordant		2	8	10.3
	Dryer		2	5	10.3
	Steam Press		6	119	13.7
	Steam Presser		1	330.3	13.7
	Roof fan		5	0.25	13
Cooling	Steam Boiler		3	1962.53	12
	Air Handling Unit 1		2	41.03	24
	Air Handling Unit 2		2	35.17	24
	Air Handling Unit 3		1	20.51	12
	Air Handling Unit 4		2	70.34	20
	Air Handling Unit 5		1	45.17	6
	Split Unit		93	327.07	10
	Incinerator		2	276.68	5
	Water Pump		1	7.5	1
	Gen Set		1	533	-
	Elevator's Motor		2	10.44	5
	Roof fan		240	62.5	10
	Water Cooler		10	3.73	7
	Total			4390	

Table 11 Cooling and Heating Loads of the Volos Public Hospital

	BTU/h	kW	kJ/h	RT	Temperature °C	Pressure (bar)	Consumption
Cooling Load	1770000	519	1867506	148			
Heating Load	660000	768	2763288				
Steam Consumption					170.4	8	1050 kg/hour
Water Consumption					40		38 [m³/day]
Nominal electrical Power of the Hospital is 2.5 MW_{el}							

3.5 Basic Natural Gas combustion calculations

The initial assumption regarding the combustion of NG in the gas turbine is that of a constant air-to-fuel ratio. Thus, the fuel mass flow rate is calculated based on the actual air mass flow rate, assuming an A/F value of 50.

In the present model, natural gas composition is assumed s constant. In a future, improved model, the effect of NG composition variation could be studied, provided that we have access to daily recordings of NG composition at the metering station.

In the following, the basic natural gas combustion calculations are summarized.

Main component combustion reactions:

$C + O_2 \rightarrow CO_2$, ΔH=-393,5 kJ/mol

$H_2 + (1/2)O_2 \rightarrow HO_2$, ΔH=-285.9 kJ/mol

$S_2 + O_2 \rightarrow SO_2$, ΔH=-70 kJ/mol

The exact characterization of gas fuels is being done based on their molar composition.

Table 12 Typical composition of gaseous fuels (%volume)

Fuel	CH_4	H_2	CO	CO_2	N_2	C_2H_4	H (kJ/kg)
Hydrogen		100					10760
Carbon monoxide			100				12640
Methane	100						35795
Natural gas (NL)	80.9	-	-	0.8	14.4	3.9	32000
Lignite distillation gas	25	55	6	2	10	2	17375

For gaseous fuels, as the natural gas, the Lower Heating Value can be estimated based on the volume composition, based on the following relation (H_u in MJ/m^3_N):

$H_{UN} = 10.8\ H_2 + 12.6\ CO + 35.8\ CH_4 + 60 C_2\ H_4 + 71.2\ C_n\ H_m$

This is the usual way of everyday pricing of the natural gas transmitted through the pipelines.

Based on the exhaust gas composition, we can calculate the combustion air-to-fuel ratio, usually with simplified relations for the case of complete combustion:

$$\lambda = \frac{CO_2(max)}{CO_2(measured)} = \frac{1.867C}{V_{min} CO_2(measured)}$$

$$\lambda = \frac{21}{21 - O_2(measured)}$$

The above calculations assume combustion with dry air. More accurate calculations must take into account the air humidity, by multiplying the required air quantity by the factor f

$$f = 1 + \varphi \frac{P_s}{P - P_s}$$

where φ the relative humidity, p the air pressure, p_S the partial pressure of the saturated steam at the specific temperature.

Table 13 Typical exhaust gas composition (m^3/kg)

Component	λ=1	λ>1
CO_2	1.867 C	1.867 C
H_2 O	11.2 H	11.2 H
SO_2	0.7 S	0.7 S
N_2	0.8 N + 0.79 L_{min}	0.8 N + λ0.79 L_{min}
H_2 O	1.22 water	1.22 water
O_2	0	(λ-1)0.21 L_{min}

Calculations based on stoichiometry relations in a combustion chamber are often quite complicated. However, for fast calculations one can employ empirical relations like those presented in Table 13. The error induced does not exceed a few percentage points.

In this project we employed the following typical composition of Natural Gas used in Central Europe.

Table 14 Typical composition of Natural Gas used in Central Europe

CO_2	N_2	CH_4	C_2H_6	C_3H_8	C_4H_{10}	C_5H_{12}	C_6H_{14}
1.2	4.68	90.03	1.14	0.15	0.20	0.08	0.05

4 Results and Discussion

Simulation of system's performance was carried out for the full duration of a Typical Meteorological Year in Volos, aiming at optimum system sizing.

Initially, nominal compressor power was set to 2 MW Sizing the rest of the system based on this figure, we can see that the nominal electric Power of the hospital can be supplied. This is the regular practice followed if the prices of electricity are high with respect to natural gas.

The dry air entering the compressor is approximated by the relation:

$P=m*c_p*\Delta t \rightarrow m=2000000W/(1.1kJ/kg*300\,^{o}C)\,*3600s/h=21800kg/h$

In the following, typical outputs of the simulation will be presented and discussed, aiming at the better understanding of system's operation.

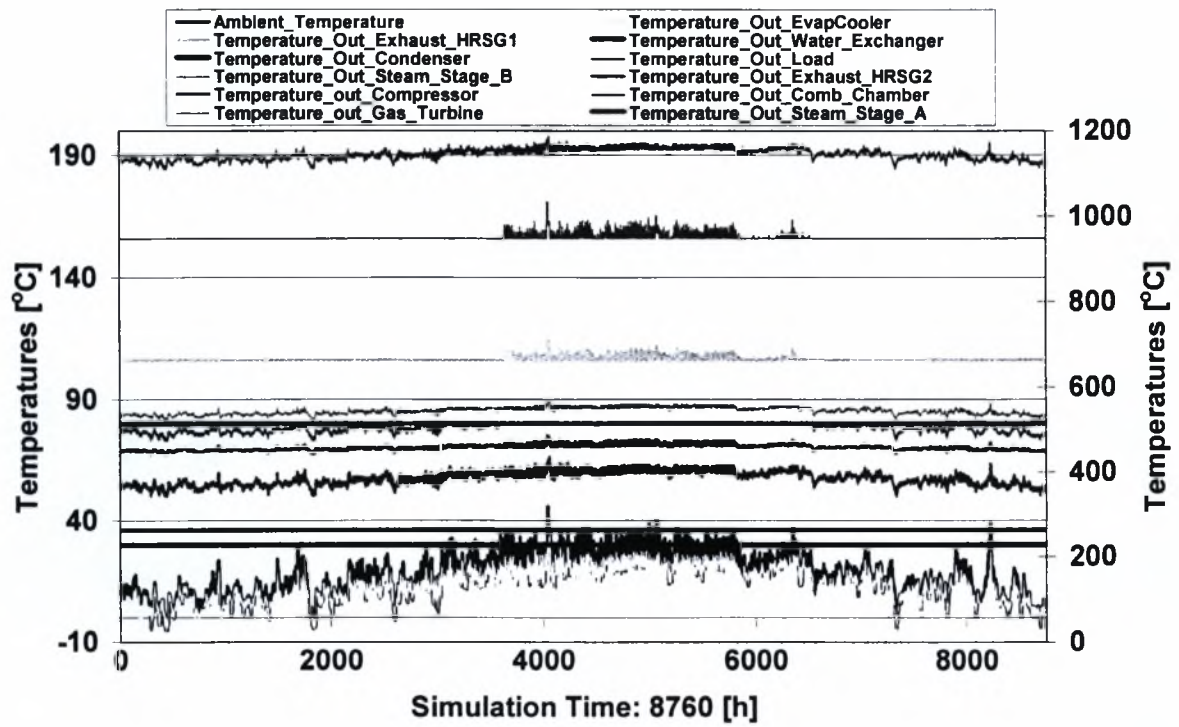

Figure 32 Year round transient system's performance (temperatures)

Simulated performance of the system throughout the typical meteorological year is presented in Figure 32, Figure 35 Figure 36 by means of the variation of characteristic temperatures, flow rates and power figures.

The following remarks pertain here:

The temperature at turbine inlet (Temperature_Out combustion chamber), ranges between 1100 – 1190 °C (for steady state the corresponding Temperature is 1140 °C). The temperature at gas turbine exit (Tout gas turbine), stays between 520 and 570 °C (steady state: 540 °C).

The variation of air temperature at compressor exit (T_out_compressor), follows ambient temperature and humidity variation, ranging from 340 °C (winter) to 430 °C(summer) (for steady state the corresponding Temperature is 379°C) .

The exhaust air from HRSG1 ranges between 106-120 °C and from HRSG2 rages between 420-490 °C (for steady state the corresponding temperature ranges are 106-115 °C and 460 °C).

Thus, there exists plenty of heat from the steam generator exit to heat up pressurized water at temperatures as high as 120 °C. During winter, where there is a significant demand, most of this heat can be exploited at temperatures 50 – 120°C. During summer, it is not useable and a high temperature exhaust gas is discharged to the atmosphere.

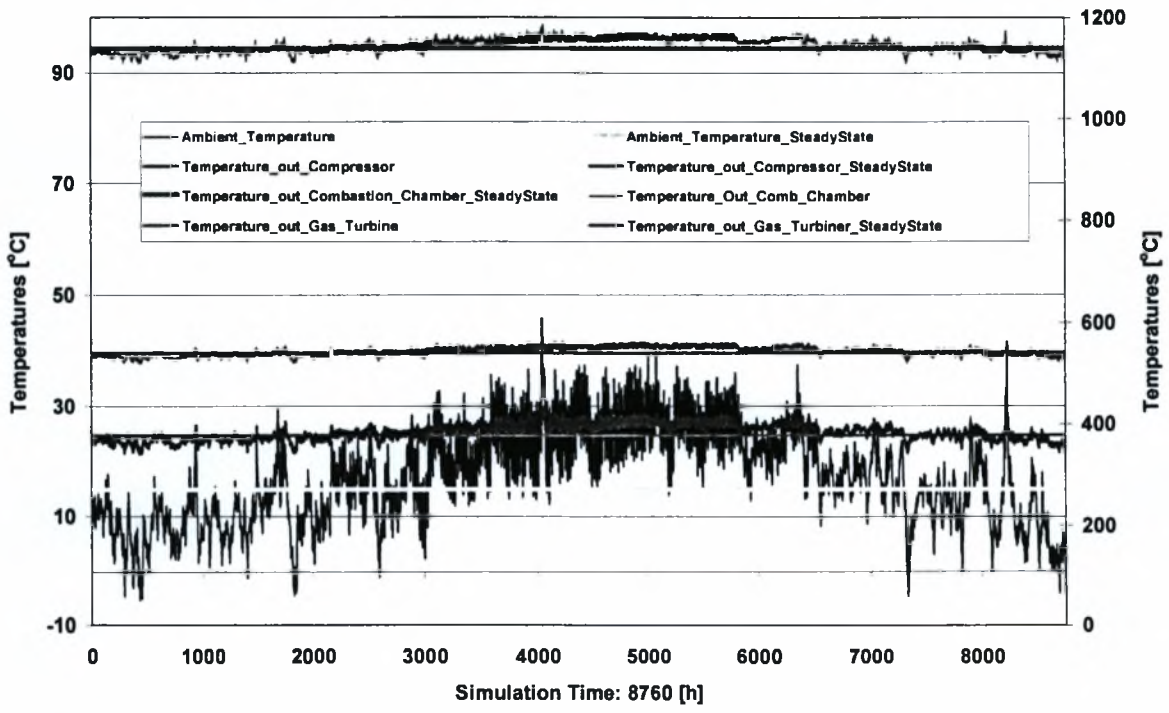

Figure 33 Year round transient system's performance (temperatures) of Gas Turbine – steady state performance of gas turbine.

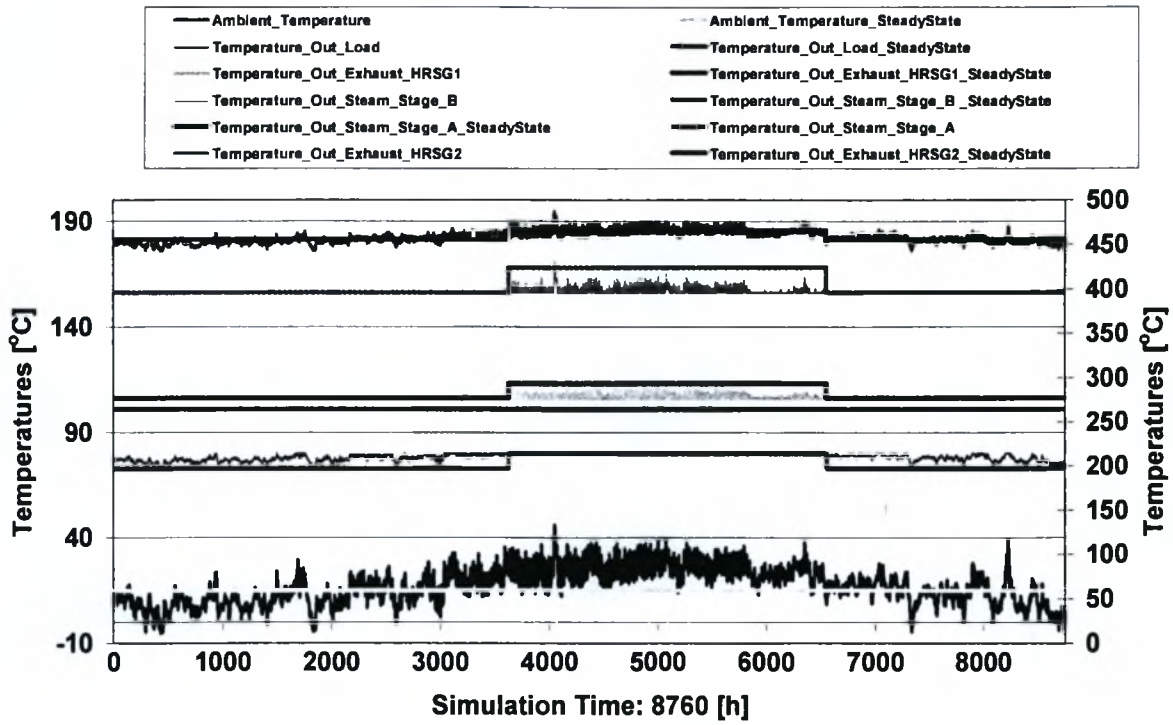

Figure 34 Year round transient system's performance (temperatures) of Steam Turbine, HRSG – steady state performance of Steam Turbine, HRSG

Steady state performance of the system is also presented on the same figures for comparison. For this calculation, ISO standard ambient conditions of 15 °C DB, 60% relative humidity are assumed and all produced heat and chilled water is assumed to be consumed by the maximum respective loads.

The mass flow rate of air entering the compressor via the evaporative cooler is varying in a certain range according to the ambient conditions (see Figure 35). The mass flow rate of steam exiting stage A that is entering in the absorption chiller depends on the cooling load. Thus, during the summer season the steam mass flow rate entering stage B steam turbine varies according to the cooling load.

The total power produced from the turbines stays in the range 2530 (summer) to 2990 kW (winter – high volumetric efficiency due to high air density) (for steady state the corresponding Power is 2734 kW for Summer and 2836 kW for Winter).

Stage A steam turbine gives a constant output of 367 kW during the year. Stage B gives a constant output of 430 kW only during winter and varies between 350 – 470 kW during summer, for the reason explained above (for Steady State 377 kW for winter and 380 kW for summer).

The power absorbed by the compressor stays approximately steady, only a little higher in summer due to the higher volume flowrate – lower density. The power produced by the gas turbine stays

approximately steady in the range 4000 to 4300 kW (for Steady State the corresponding Power is 4130 kW).

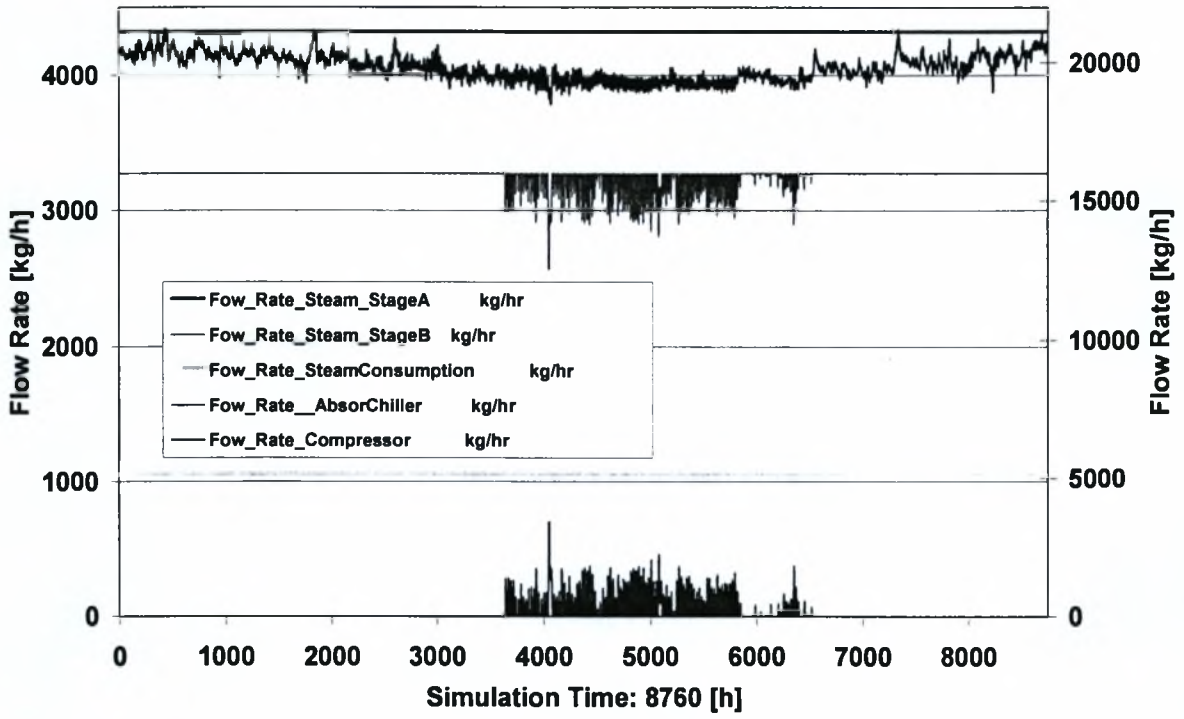

Figure 35 Year - round transient system's performance (flowrates)

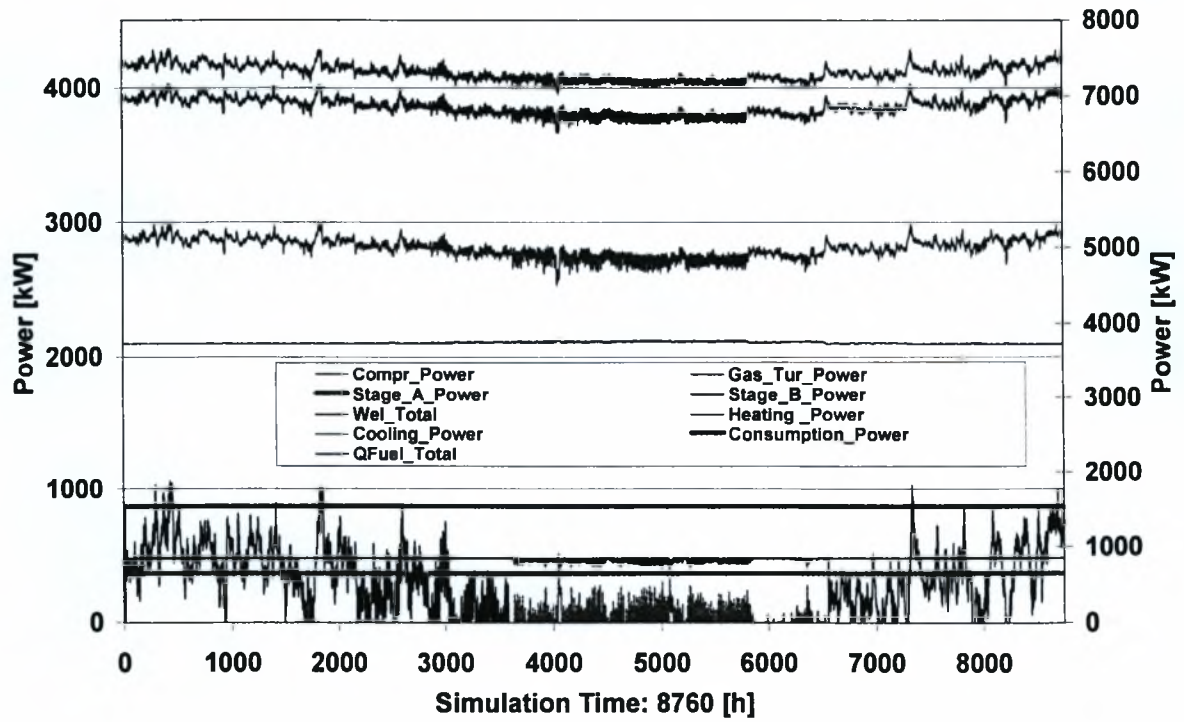

Figure 36 Year - round transient system's performance (power and heat flows)

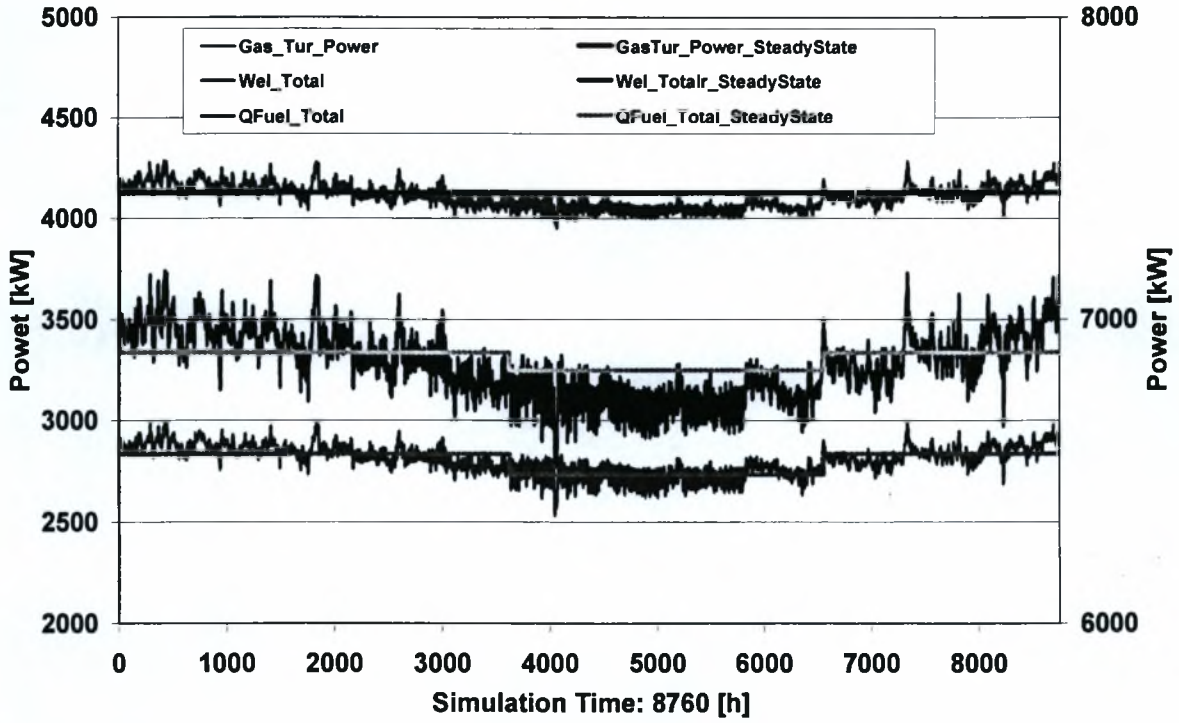

Figure 37 Fuel consumption and power for transient and steady state

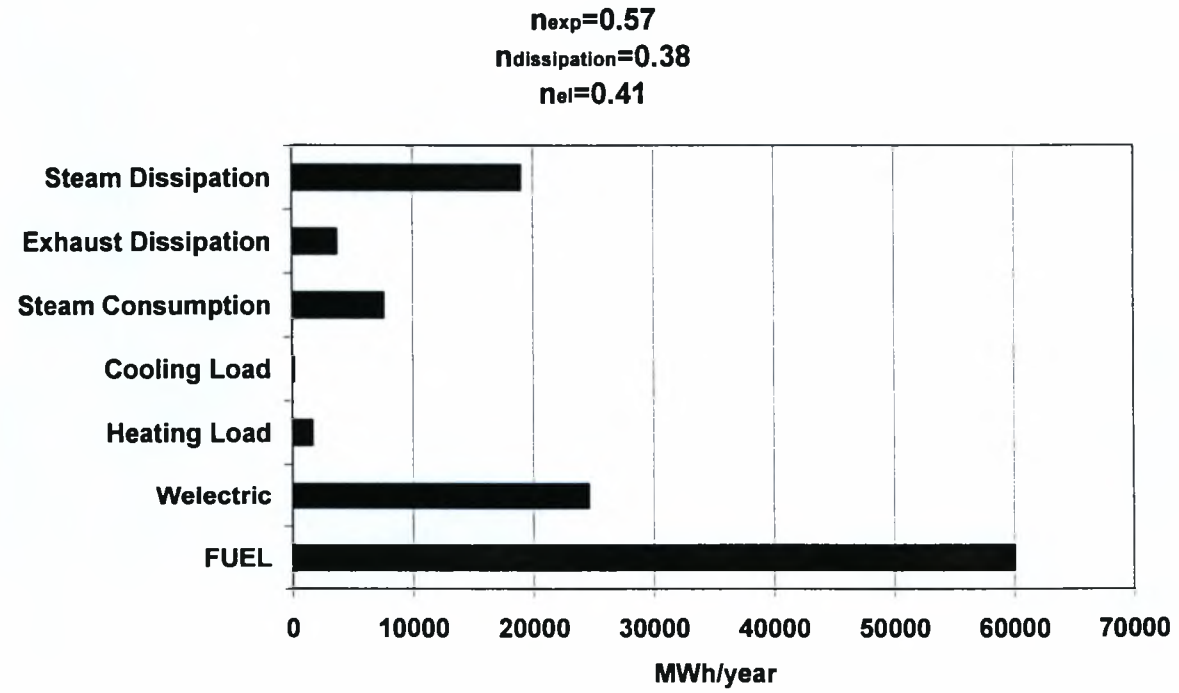

Figure 38 Consumption, electricity production and energy dissipation around a typical meteorological year

The yearly fluctuation of total Natural Gas consumption and the electrical power production is presented in Figure 36. The fuel consumption predicted according to the steady state assumption is less than the transient fuel consumption – (see Figure 37). Obviously, the system's sizing based on the electricity figures resulted in oversizing of the heat exchangers (n_{exp} is higher for steady state Figure 41).

In order to better understand system's operation, in the following, we discuss separately winter and summer operation.

4.1 Winter operation

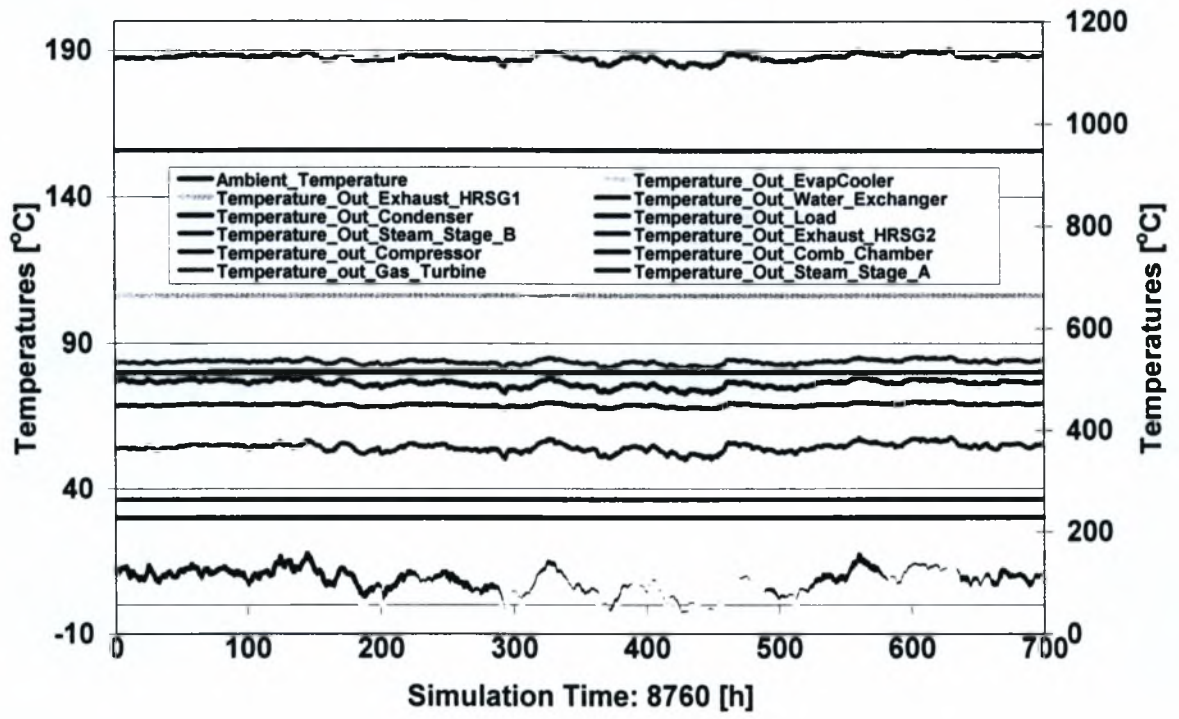

Figure 39 Simulation of winter operation (temperatures)

Typical simulated transient performance of the system during winter (0 to 744h, January) is presented in Figure 39. In the specific simulation, the load fluctuation of the pressurized hot water is set proportional to the indoor-outdoor temperature difference, as if this water were to be used for space heating. Alternatively, one could produce hot water at a lower temperature, as well as steam at 7 bar (for hospital's steam consumption) by taking steam from the exit of Stage_A steam turbine during winter and summer (during summer, we are taking steam from the same point for the adsorption

chiller). However, if we do not exploit the high enthalpy of the heat recovery steam generator's exit, the overall system efficiency will drop.

An inspection of the variation in heat load temperatures (Figure 34) indicates that Tout _Load with the steady state assumption (winter season), is always lower than Tout _Load for transient performance. Again, n_{exp} is higher for steady state due to avoidance of stage B steam dissipation.

Significant yearly variations of the nu1 and nu2 rates during the year are seen in Figure 46 which is due to the respective variation of the space heating load.

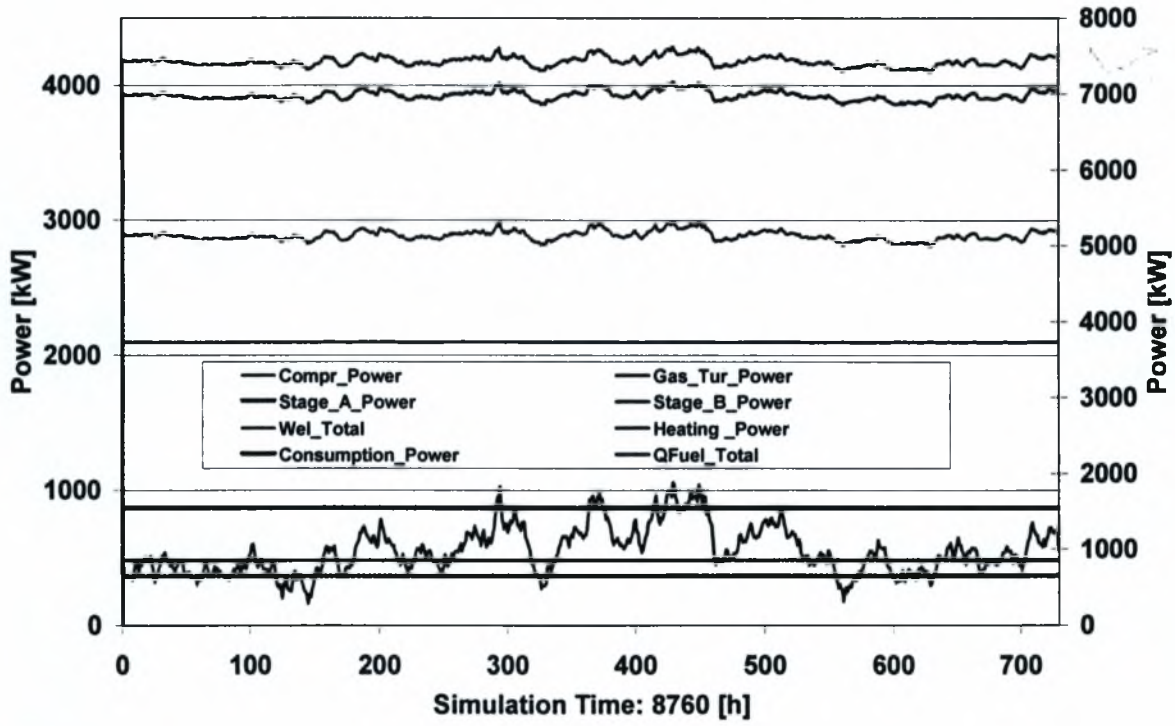

Figure 40 Simulation of winter operation (power and heat quantities)

During winter, the steam flow rate entering Stage A and Stage_B is constant (we assumed constant steam consumption), and thus the electricity production remains constant.

The overall summary for the winter season is seen in the bar-graph of Figure 41. The significant value of $n_{dissipation}$ =0.36 (the ratio of (steam+exhaust dissipation) over (fuel consumption)), point to the fact that the specific system will not be economically affordable.

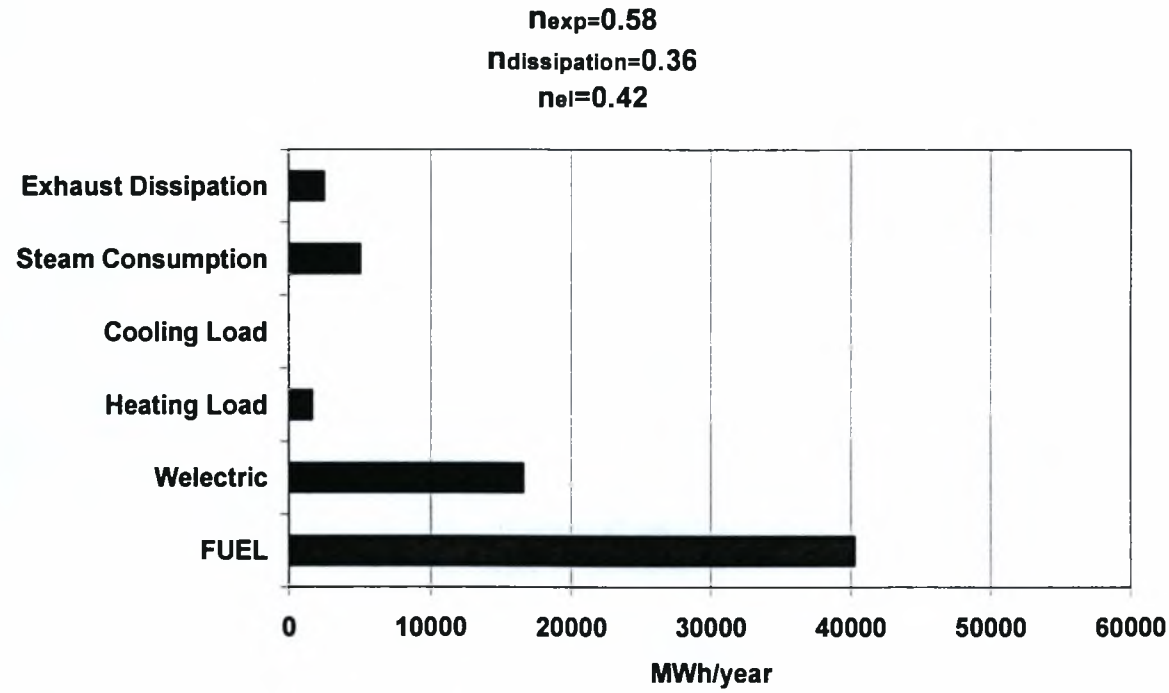

Figure 41 Fuel consumption, electricity production and energy dissipation for winter season

4.2 Summer operation

During the summer, the need for pressurized hot water is assumed to be zero. Steam is taken from the exit of "Stage_A" steam turbine and led to the absorption chiller. For this reason, the power produced by the "stage_B" steam turbine is lower.

An example of the simulation of the system's summer operation is presented in Figure 42, Figure 43. In Figure 44 we focus on the absorption chiller's operation.

A low value for the heat exploitation ratio is observed in Figure 46. Thus, the system's performance can be significantly improved by connecting additional cooling loads to the cogeneration network.

Here we must mention that typical electrical efficiency figures for cogeneration systems of this type are $n_{el} = 0.45$. (see Figure 19) [6].

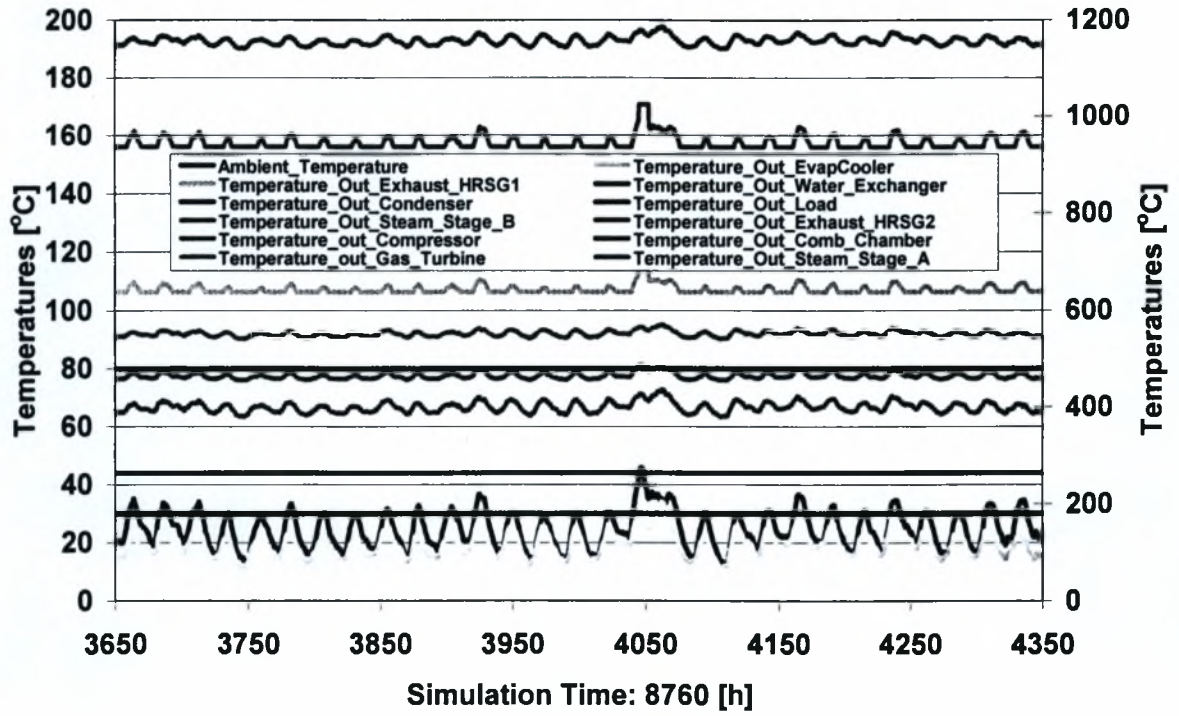

Figure 42 Simulation of summer operation (temperatures)

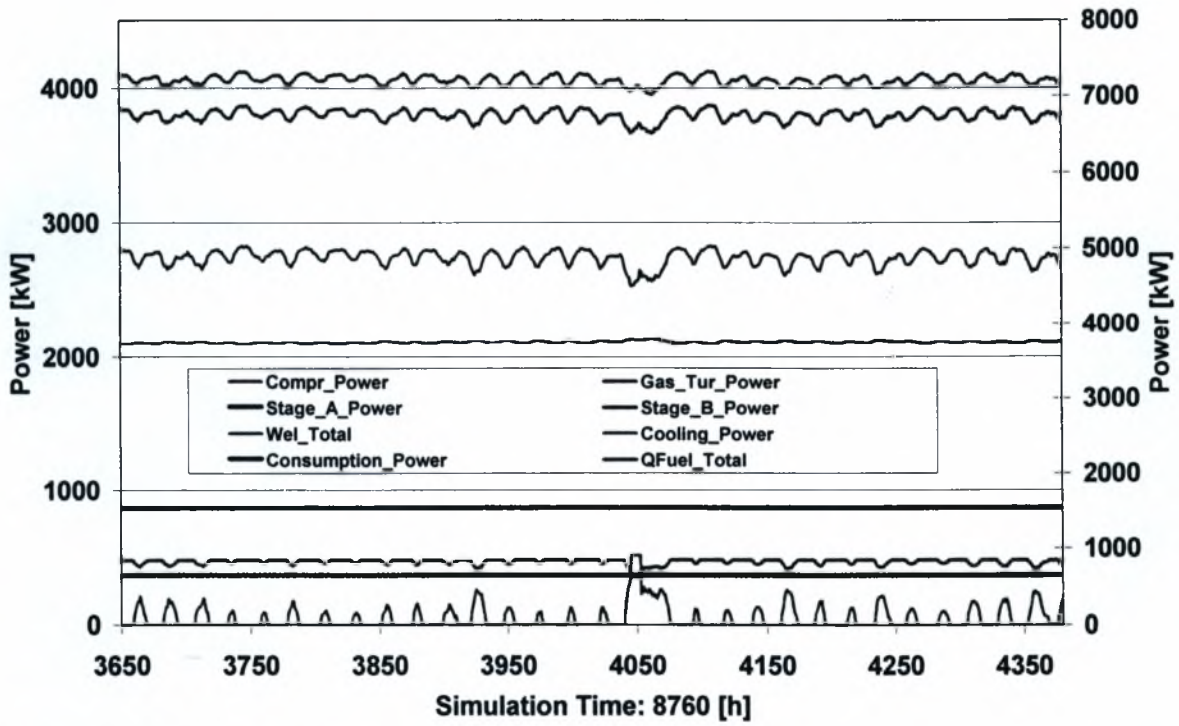

Figure 43 Simulation of summer operation (power and heat quantities)

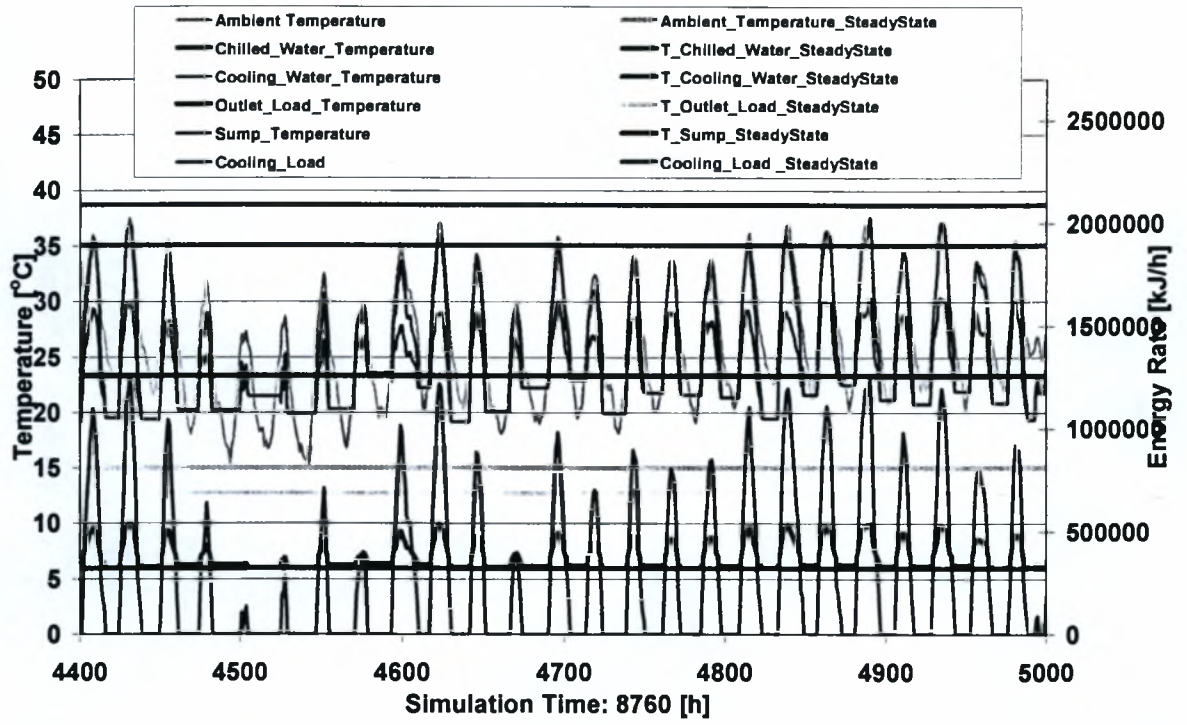

Figure 44 Simulation of absorption chiller (transient and steady state performance)

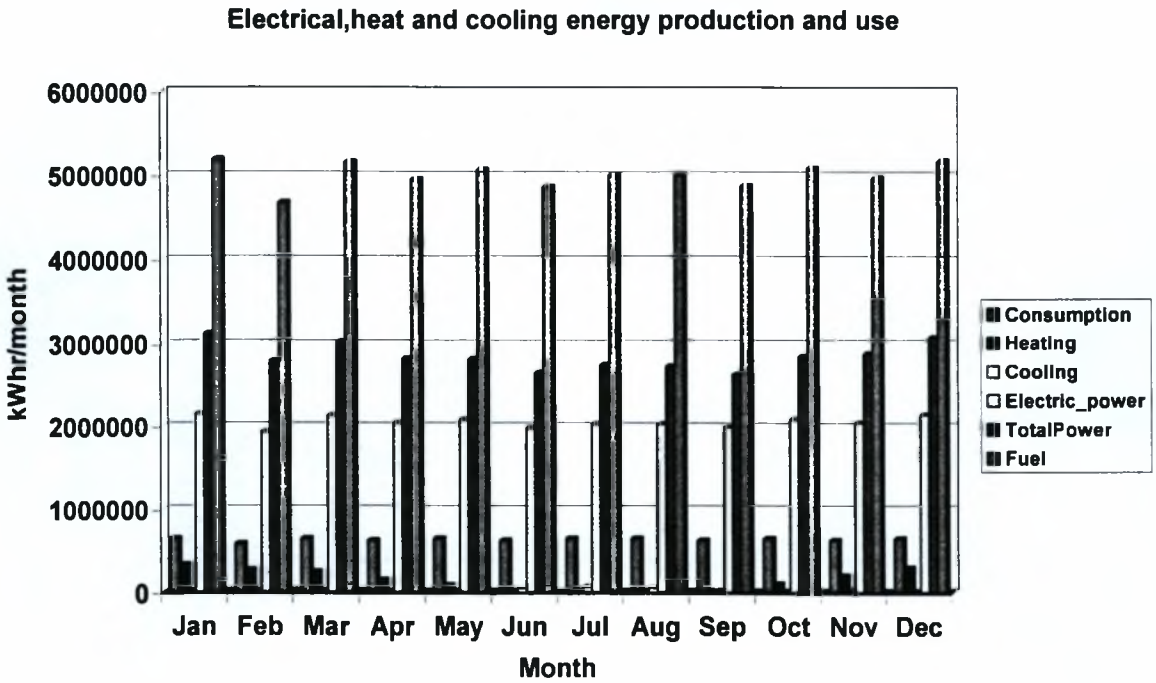

Figure 45 Monthly summary of electrical, heating and cooling energy production and use

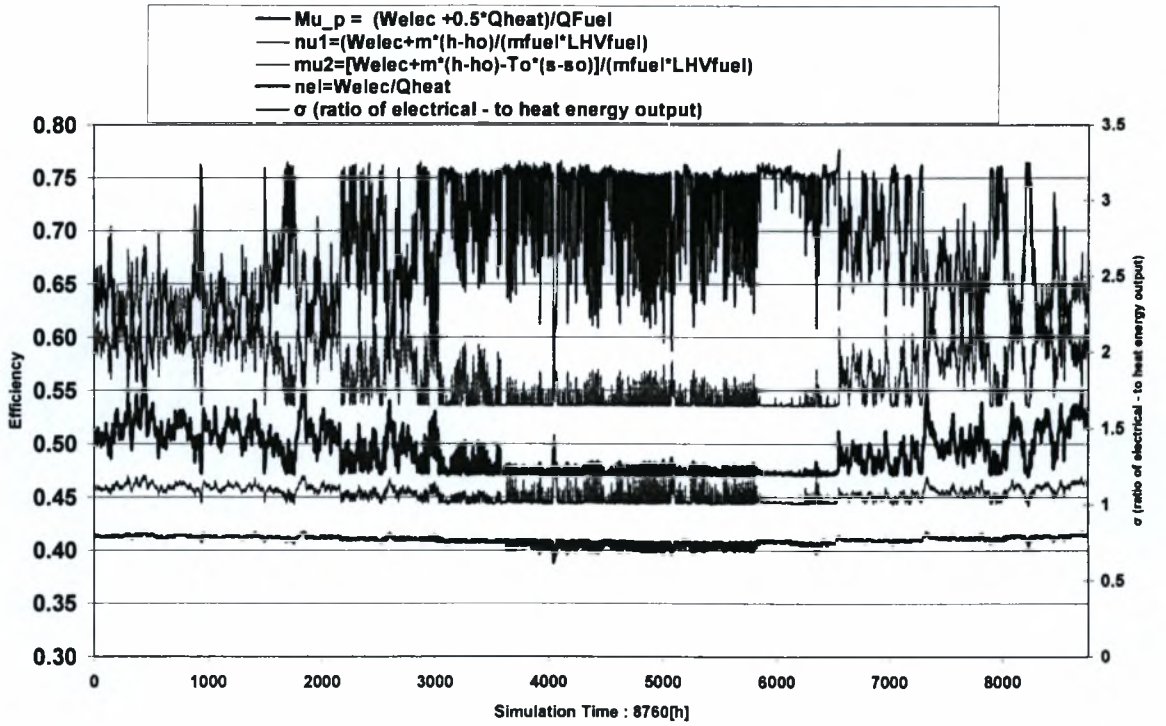

Figure 46 Yearly variation of electricity-to-heat ratio and system's efficiency

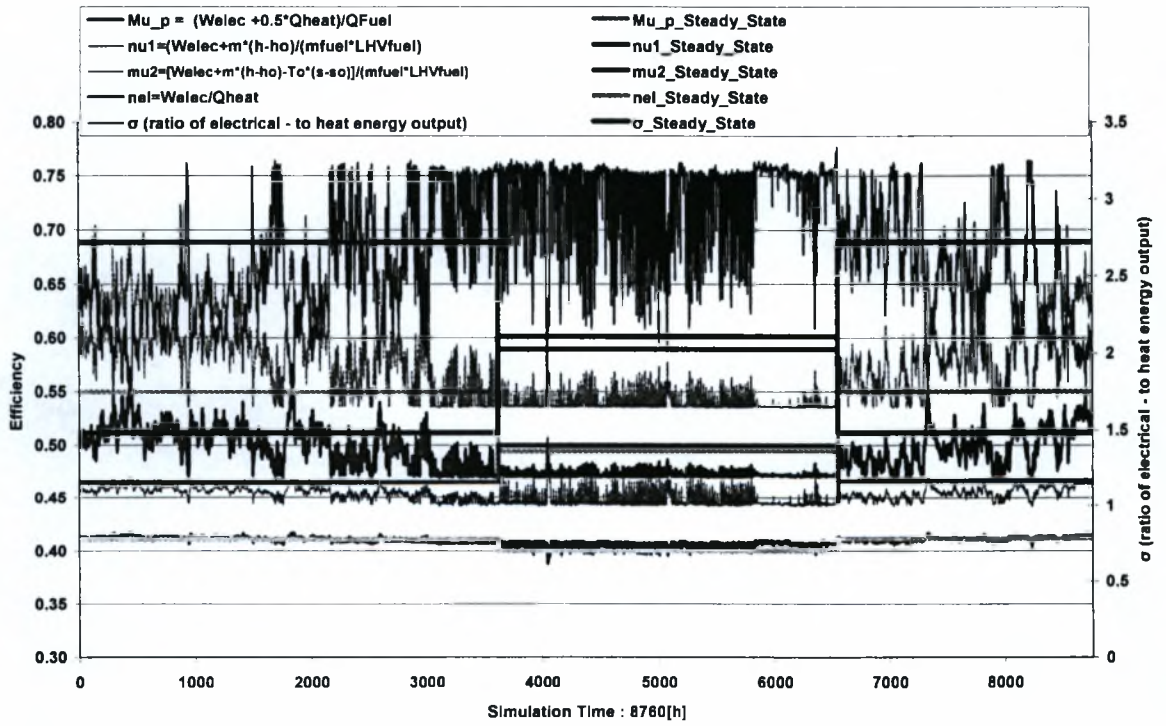

Figure 47 Efficiency for transient Simulation and Steady State

5 Sizing the system

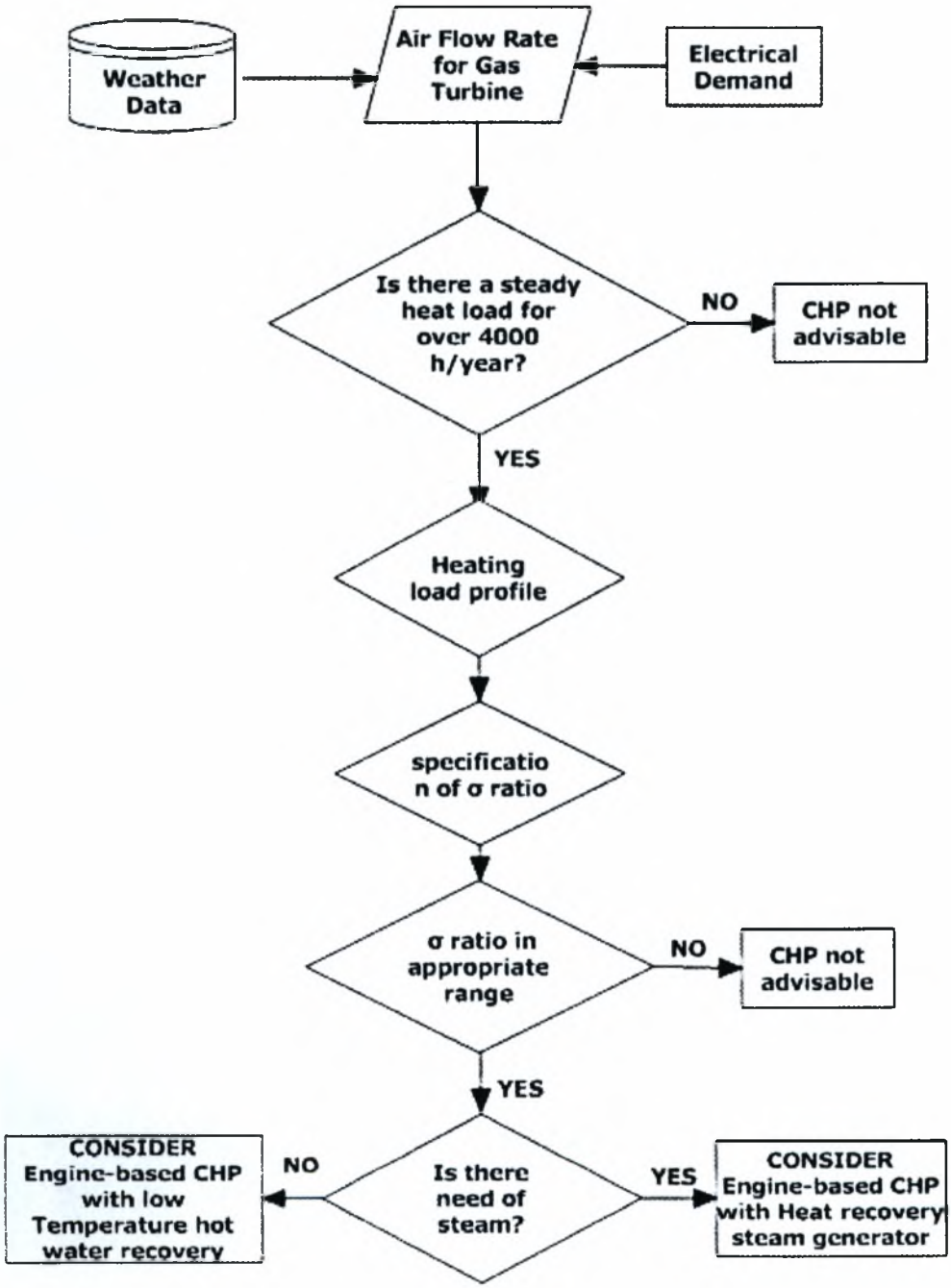

Figure 48 Decision flow chart

After the first simulation based on Nominal Power of the Hospital, following the Decision flow (Figure 48) we simulate the system changing the inlet flow rate of air in gas turbine from 20000kg/ in

14000 kg/h and the steam production from 1.2g/s in 0.6 g/s, so that the electrical output to be about half of the nominal power. The results are present in Figure 49, Figure 50, Figure 51 and Figure 52.

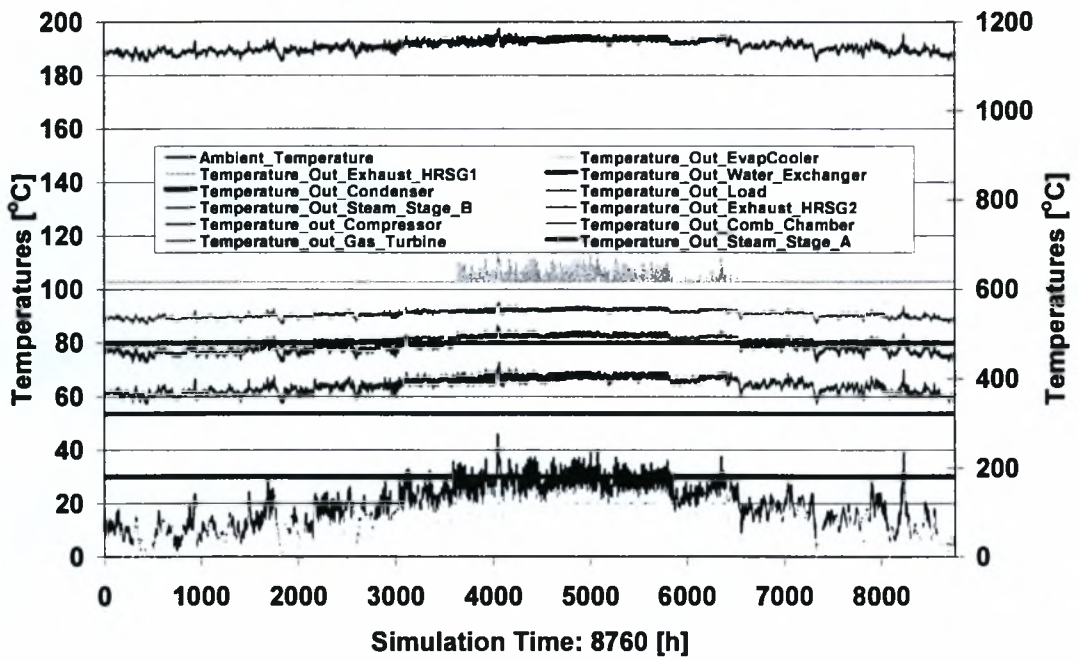

Figure 49 Year round transient system's performance (temperatures)

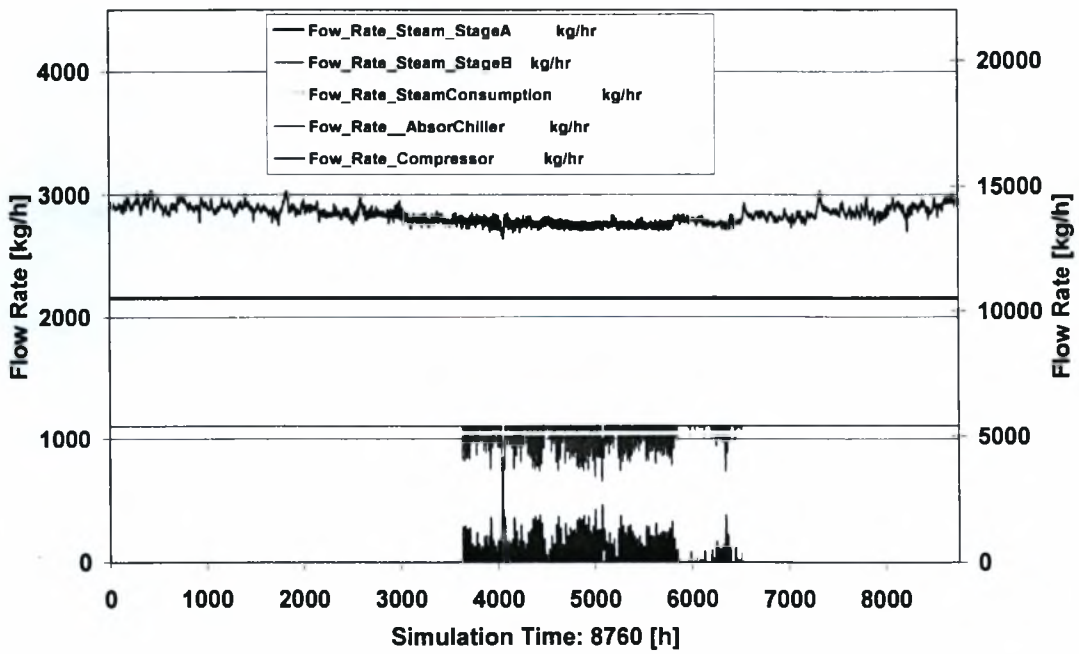

Figure 50 Year - round system performance (flowrates)

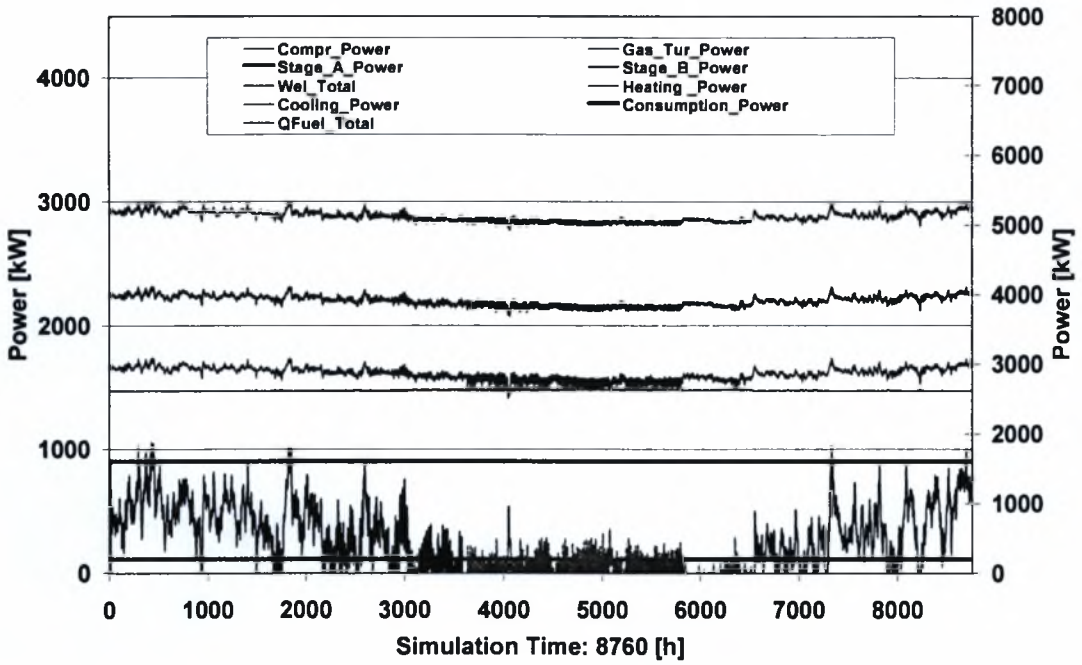

Figure 51 Year - round system performance (power and heat flows)

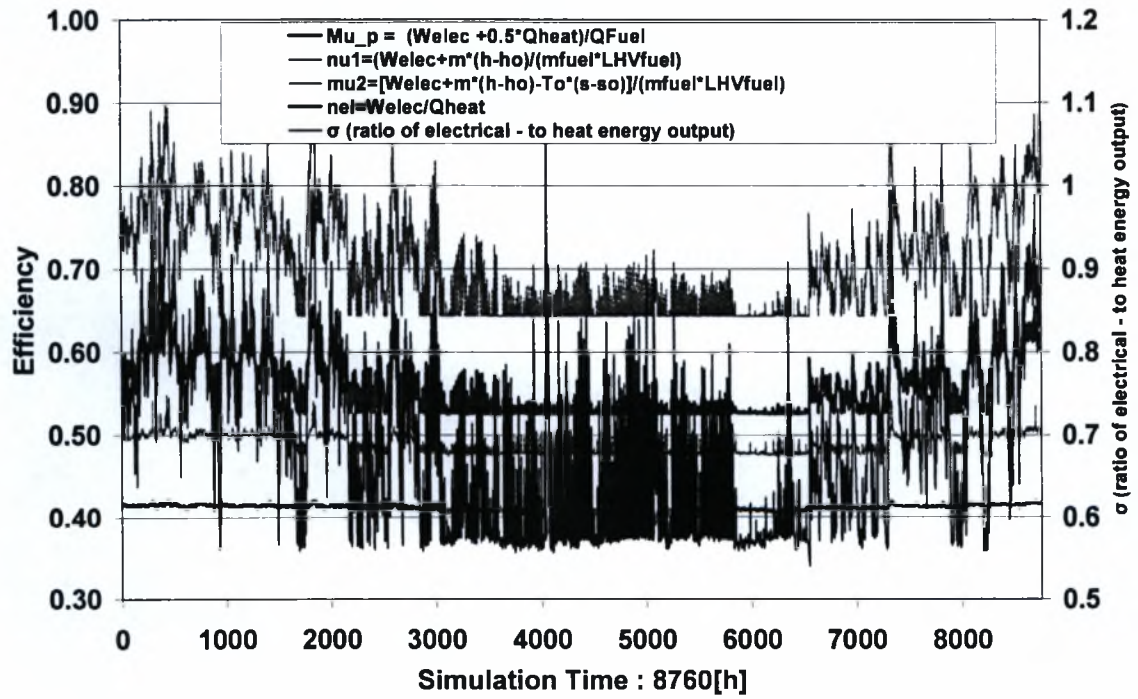

Figure 52 Yearly variation of electricity – to –heat ratio and system's efficiency

As we can see in the above figure the system's efficiency improved significantly and the σ ratio takes now a more appropriate value. The new system's sizing is closer to optimal.

6 Economic Analysis

The economic analysis is the most important and the most difficult part in a techno-economic assessment of a co-generation installation.

The following principal cost factors can be defined [59]:

(a) The gains due to the lower electricity self-production cost, as compared to the normal prices paid by the hospital to the electricity generation facility, taking into account the fact that the electricity produced by co-generation is mainly consumed by the hospital itself.

(b) The purchases of electricity from the external facility (DEH), during the periods that cogeneration does not work, or does not fully cover the hospital's needs.

(c) The gains due to selling to the external facility (DEH) of the surplus quantities of electricity which are not self-consumed.

(d) The fuel expenses of the cogeneration installation.

(e) The additional operation and maintenance costs of the cogeneration installation.

The items (b) and (c) require the selection of a tariff of purchase and a tariff of selling of electricity to the external facility (DEH). This procedure may become complicated in the future, because of the legislative or regulative and company rules on nominal power levels (on purchasing), guaranteed power levels (on the selling quantities), that require a complete and accurate examination of the operating conditions of the cogeneration system year- round, the reliability of the system and the cost of break downs, based on the penalties set by the external facility to the lack of supply or to the increase of required power beyond the nominal levels.

That is, every singular case requires a detailed optimization study, and the role of the transient modeling in this study is essential, as already explained in the previous chapters.

Another especially important factor in Greece is the financial motives offered by the Government to facilitate the penetration of co-generation to the Greek market.

Item (d) (fuel expenses) is calculated based on the difference between the fuel consumed by the cogeneration facility (natural gas in our case) and the fuel(s) that would be consumed to produce the finally exploited quantities of co-generated heat and cold, if co-generation would not exist.

In this case, attention is required to take into account differences in the fuels or other energy sources initially employed, (e.g. heavy oil, electricity etc for space heating, steam production or cooling), compared to the natural gas that is the sole fuel consumed by the cogeneration facility.

That is, we must carry out a detailed financial calculation based on the transient system's operation during the year, with and without co-generation, in order to estimate the value of item (d).

Moreover, this situation frequently changes, mainly due to the significant fluctuation in the fuel prices, but also in the electricity prices, which are currently considered quite low in Greece and are expected to significantly increase in the near future.

The operation costs (item (e)), principally comprise the additional operation and maintenance costs of the cogeneration installation that can be quantified. But here it could also be added additional costs, like the following [60]:

Insurance costs, either normal (insurance of equipment and facilities), or specific (accidents, fail to fullfill the guaranteeing of power levels to DEH etc);

General costs and margins if an external client is added;

Local, professional and other taxes;

Provisions for renovation of damaged equipment and materials [61].

Based on the above cost factors, on can deduce a raw exploitation gain:

E = a-b+c-d-e

Capital investment costs

The calculation of the capital investment costs requires, of course, multiple calculations depending on the equipment size and details, the number and power level of machines, the quality of materials, the investment details etc.

If we know the investments I, the duration and interest rates of the loans, we can deduce the annuities of reimbursement (or cost of money P4). For example, for an interest rate of 10 % for a duration of 12 years, the annuities (P4) reach 14.7 %.

6.1 Profitability

In this work, we judge the profitability of the co-generation installation project by the simplest available formulas:

— the simple payback period, which is calculated by dividing the additional initial investment of cogeneration to the raw exploitation gain of cogeneration:

SPP=I/E

— the net annual financial gain

G= E-P4

An energy investment's simple payback period is the amount of time it will take to recover the initial additional investment. While simple payback is easy to compute, it fails to take into account the time value of money, inflation, the true project lifetime or detailed operation and maintenance costs. To take these factors into account, a more detailed life-cycle cost analysis must be performed. The calculated values allow the decision makers to assess the feasibility of the project [62]. Once the initial assessment looks promising, one proceeds to detailed financial calculations [63].

The economics of cogeneration greatly depend upon the local utility rates, particularly demand charges (EUR per kilowatt) and natural-gas prices, as well as system capital costs. The aforementioned simulation of a cogeneration system energy savings must be extended to the economics of the system, assuming that the prime-mover technologies meet their R&D performance goals. It has been reported that advanced -IC-engine cogeneration systems (generation efficiency = 42% [LHV]) would have a simple payback period (SPP) of between one and three years for large office buildings in New York or Los Angeles, but the SPP would exceed 15 years in Miami and Phoenix. In contrast, the SPP for a standard or advanced microturbine (generation efficiency = 26% or 31% [LHV], respectively) increased to between two and five years [64].

Clearly, high electric generation efficiency is a key to good economics as well as energy savings—the greater heat production of less-efficient generation technologies cannot compensate for their reduced electric output.

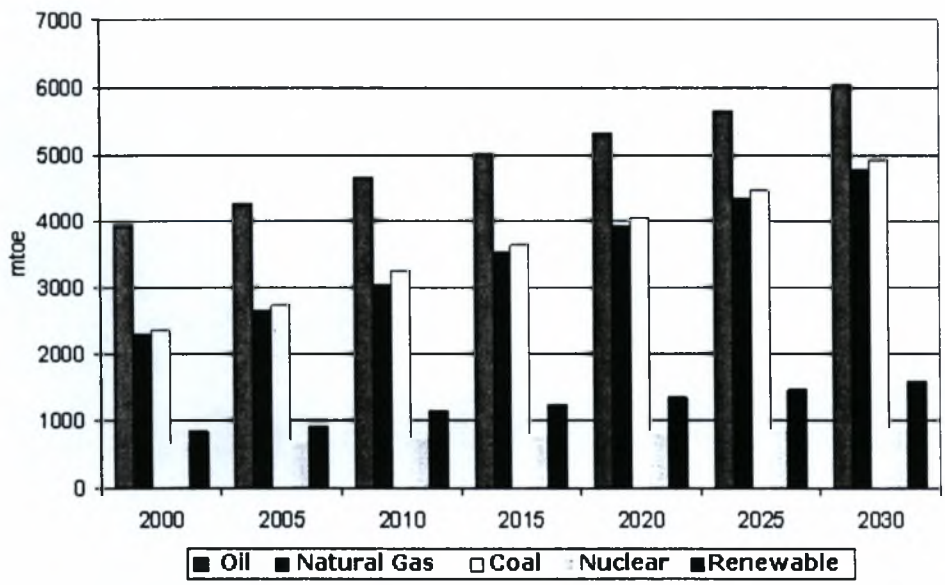

Figure 53 Projected evolution world of energy demand (million tons oil equivalent/year).

The clean combustion advantages of the Natural Gas, along with its favorable pricing with respect to Diesel fuel, have led to its widespread use in many developed countries in America, Europe and Asia. Globally, fossil fuels will remain the dominant source of energy to 2030 in all scenarios. Their share of world demand edges up, above 80%. The share of natural gas also rises, even though gas use grows less quickly than projected in the past, due to higher prices [65].

Moreover, the rate of penetration of Natural Gas in the Energy Market clearly surpasses that of the other traditional fuels (Figure 53). In the period 1995-2005, oil consumption increased 18%, whereas NG consumption increased 28%.

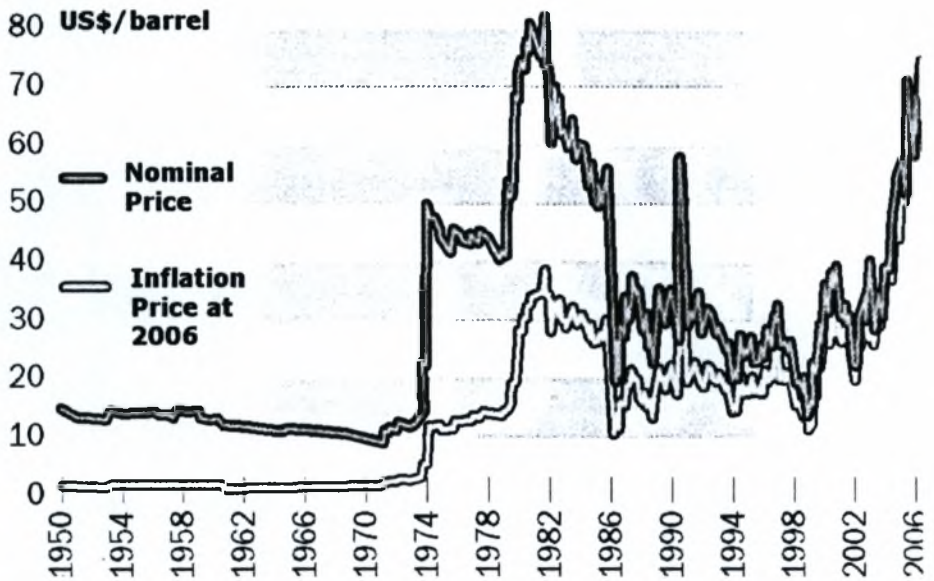

Figure 54 Evolution of oil prices during the last 56 years (red curve in US dollars, white curve after inflation correction).

On the other hand, the economics of Natural Gas use, as compared to the prices of electricity and of other alternative fuels and energy sources, are essential to the sizing of the cogeneration equipment [66].

In order to better explain the situation, one should begin with an analysis of the evolution of oil prices during the last 50 years, like that of Figure 54.

According to above figure, since year 2000, we have entered a period of increasing oil and energy prices. Most economic analysts predict that the high oil prices will be maintained in the future due to the increasing consumption of economic giants as China and India, followed by other developing countries.

As regards the prices per kWh of Natural Gas, the monthly pricing system in Greece is based on the assumption that the NG should be kept 20% cheaper than the heating Diesel oil (including VAT, which is 9% for NG compared to 19% for Diesel fuel).

In an international context, gas-fired power remains the default option for new power generation. Demand for new gas-fired power generation capacity continues to grow as political commitments in some countries to avoid or phase out nuclear and reduce carbon emissions have left gas as the default option. There are large numbers of new coal and nuclear plants planned, but construction start is delayed. Renewables cannot fill the gap in the meantime; to the contrary, increasing shares of intermittent renewables such as wind may increase the need for flexible gas-fired power as back-up. The growing interdependence of gas and electricity is raising concerns about security, reliability and competition because gas increasingly meets electricity demand peaks, notably in summer, where an increasing number of IEA countries are experiencing peak power demand. In many regions, gas-fired plant sets the price of electricity a significant proportion of the time. Expensive gas therefore means expensive electricity [67].

In order to better understand the situation, one should keep in mind the following figures:

1 l. Diesel oil is 0.83 kg

1 Nm^3 Natural Gas averages 11.2 kWh Gross Heating Value (Brennwert).

Using May 2007 as a reference, we may record the following typical prices for large industrial clients in the Greek Energy Market:

1 l. heating Diesel fuel is priced 0.36 EUR

1 MWh NG is priced about 39. EUR for heating, or 36. EUR for other uses (incl. cogeneration).

1 kWh electricity (medium voltage supply to private switchgear station) is priced about 0.04 EUR

With an average NG price of 0.4762 €/kg			
	Natural Gas	Gasoline	Heating oil
Price	0.4762 €/kg	1 €/l.	0.55 €/l.
Higher heating value	13.16 kWh/kg	8.77 kWh/l.	9.86 kWh/l.
Price / energy output	0.036 €/kWh	0.11 €/kWh	0.056 €/kWh
One kg NG produces the same energy as 1.5 l. Gasoline or 1.33 l. oil			

Traditionally, electricity is low-priced in Greece, since it is mainly produced by a public corporation, (DEH) based on a locally available fuel (lignite). However, during the recent years, a high penetration of imported Natural Gas as fuel in power stations is observed, along with an increase in electricity imports (13% of 2006 demand). This resulted in a severe increase of the power system limiting

electricity cost, from 43 EUR/MWh in 2005 to 64 EUR/MWh in 2006, mainly due to the respective increase in oil and gas prices. Thus, electricity prices are expected to further increase in the near future.

For comparison it should be mentioned that the price of Natural Gas for China's fertilizer makers is currently (May 2007) about 0.10 USD / Nm^3 (0.8 yuan). (8.9 $ for 1 MWh of NG).

For calculating the cost of natural gas and electricity, we employed the official prices in the Greek market in May 2007. (See Annex I).

6.2 Profitability comparison of the three alternative sizing scenarios

Next we compare the total cost of the hospital's electricity and heat consumption during the year with three different cogeneration system sizing scenarios: Case 1, 2 and 3.

Table 15 The three alternative scenarios (cases) examined in this study

	Case 1	Case 2	Case 3
Electricity production - General remarks	No cogeneration	Cogeneration sized by nominal electric power	Cogeneration sized by 50% of nominal electric power
Heating	Boiler fuelled By NG, n=0.85	Steam-Water heat exchanger	Steam-Water heat exchanger
Cooling	Cooling with compressor chiller, COP=3	Double effect Absorption chiller, steam fired	Double effect Absorption chiller, steam fired
Flow rate of gas turbine	-	20000 kg/h air	20000 kg/h air
HRSG steam production	-	1.2 kg/s steam	0.6 kg/s steam

Table 16 Comparison of operating hours for the three alternative cases

	Hours	Start	End
Electricity production	8760	-	-
Steam production	8760	-	-
Heating	5830	1 October	31 May
Cooling	2930	1 June	30 September

Table 17 Cogeneration system investment and operation cost comparison for the three cases

	case 1	Case 2	Case 3
Average cogeneration investment cost (€/kW)	-	700	700
Nominal Power produced by cogeneration (kW)	-	2500	1500
Additional investment cost of cogeneration (€)	-	2,100,000	1,050,000
Average additional operating and maintenance cost (€/kWh)	-	0.005	0.005
Cogeneration electricity kWh /year	-	24,602,904	14,075,537
Electricity purchased from DEH (kWh)	24,602,904	-	-
Total operating and maintenance cost (€/year)	-	184,521	105,565

Table 18 Calculation of raw exploitation gain, E for the three cases

	case 1	Case 2	Case 3
(a) Electricity purchase costs	1,711,422	0	646,144
(b) Cogeneration fuel expenses	0	2,387,739	1,361,099
(c) Gains from selling electricity to DEH	0	303,838	0
(d) Heat production cost without cogeneration (with boiler fuelled by NG)	500,472	0	0
(e) cooling production cost without cogeneration (compressor chiller, COP=3.)	6,650	0	0
(f) additional operation and maintenance costs	0	123,015	70,378
E (Euro)=a+b-c+d+e+f	2,218,544	2,206,915	2,077,621
Raw exploitation gain (cogeneration) E-E_1	0	11,629	140,923
Simple payback period SPP (years)	0	180.58	7.45

Table 19 Cost calculation of Natural Gas for heating (case 1) based on Annex I Table 27

Natural Gas for heating					
	Total Heat Demand	n boiler 0.85	Energy	Power	Nm^3
			0.039 €/kWh	26 €/month	
	kWh /month	kWh /month			
Jan	973,528	1,216,910	47,313	26	109,014
Feb	853,207	1,066,509	41,466	26	95,540
Mar	894,267	1,117,834	43,461	26	100,138
Apr	774,927	968,659	37,661	26	86,775
May	726,509	908,137	35,308	26	81,353
Jun	668,550	835,688	32,492	26	74,863
Jul	709,632	887,040	34,488	26	79,463
Aug	696,192	870,240	33,835	26	77,958
Sep	635,598	794,497	30,890	26	71,173
Oct	748,351	935,439	36,370	26	83,799
Nov	821,405	1,026,757	39,920	26	91,979
Dec	939,447	1,174,309	45,657	26	105,197
		Sum	458,862	286	948,240
			Total	459,148	
			with VAT	500,472	

As we can see in Table 18 the total cost with 100% cogeneration (case 2) is 99% of the cost of case 1. This is due to the low total n_{exp}, nu_l and the large σ rate that is out of the recommended range. But the

total cost in case 3 is about 93% of the cost of case 1. With an average investment cost of 700 €/kW the total investment is 1,050,000 €, that means a simple pay back period about 7.45 years for case 3. This payback period would be even smaller, because every NG consumer has a discount of 5.5-7.5 €/MWh depending on the type of supply contract and the NG consumption level and government financial support max 50% of initial cogeneration investment cost.

Table 20 Cost calculation of electricity (EURO) based on Annex I Table 24 (case 1)

A	B	C	D	E	F	G	H	I	J
Month		Max Wel month	Total Wel			Energy	Energy	Energy	Power
		kWh	kWh/month			0.060 €/kWh	0.040 €/kWh		10.18 €/kW
				400*C*(B/30)	D-E	E*0.06064	F*0.04017	G+H	(C-1000)*10.18
Jan	31	2992	2150998	1236559	914439	74,497	36,733	111,230	20,279
Feb	28	2972	1933449	1109626	823823	67,532	33,093	100,625	20,080
Mar	31	2983	2128176	1232970	895205	73,889	35,960	109,849	20,190
Apr	30	2948	2035410	1179176	856235	70,740	34,395	105,135	19,833
May	31	2916	2074638	1205438	869199	70,957	34,916	105,873	19,512
Jun	30	2831	1975677	1132391	843286	68,118	33,875	101,992	18,642
Jul	31	2808	2025483	1160756	864726	70,511	34,736	105,247	18,411
Aug	31	2813	2027822	1162772	865050	72,140	34,749	106,889	18,461
Sep	30	2878	1986981	1151271	835709	70,195	33,570	103,766	19,123
Oct	31	2894	2084734	1196160	888574	74,880	35,694	110,574	19,283
Nov	30	2987	2044757	1194997	849760	72,240	34,135	106,375	20,236
Dec	31	2978	2137674	1231006	906668	0	36,421	36,421	20,142
					sum	785,699	418,277	1,203,976	234,194
								Total	1,438,170
								with VAT	1,711,422

Table 21 Cost calculation (EURO) for case 2 (Annex I Table 26)

Natural Gas for heating and electricity					
	Max Qfuel	Total Qfuel	Energy	Power	Nm^3
	kW	MWh /month	36.19€/MWh	232€/maxMW month	kWh/Nm^3
Jan	7161	5,200	188,198	1,661	466,540
Feb	7127	4,679	169,346	1,653	419,804
Mar	7146	5,159	186,720	1,658	462,874
Apr	7085	4,952	179,219	1,644	444,280
May	7030	5,070	183,479	1,631	454,840
Jun	6884	4,863	175,991	1,597	436,277
Jul	6847	5,002	181,038	1,588	448,790
Aug	6855	5,004	181,087	1,590	448,911
Sep	6965	4,875	176,409	1,616	437,315
Oct	6991	5,086	184,076	1,622	456,320
Nov	7154	4,968	179,793	1,660	445,703
Dec	7136	5,176	187,315	1,656	464,350
		Sum	2,172,671	17,915	4,919,467
			Total	2,190,586	
			with VAT	2,387,739	

Table 22 Gain due to selling to the external facility (DEH) (EURO) for case 2 (Annex I Table 25)

Month	kWh/month	Energy
		0.05639€/kWh
		0.05639
Jan	443,069	24,985
Feb	393,466	22,188
Mar	423,173	23,863
Apr	385,399	21,733
May	369,638	20,844
Jun	325,675	18,365
Jul	320,491	18,072
Aug	322,819	18,204
Sep	336,983	19,002
Oct	379,724	21,413
Nov	394,763	22,261
Dec	432,667	24,398
	Total	255,326
	with VAT	303,838

Table 23 Cost calculation (EURO) for electricity supplying by the grid (case 3)

A	B	C	D	E	F	G	H	I	J	K	L	M	N
Month		Max Wel month	Total Wel	Max Wel month	Total Wel	Max Wel month	Total Wel			Energy	Energy	Energy	Power
		kWh	kWh/month	kWh	kWh/month	kWh	kWh/month			0.06064€/kWh	0.04017€/kWh		10.1817€/kW
								400*G*(B/30)	H-I	I*G*0.06064	J*0.04017	K+L	(G-1000)*10.18170
Jan	31	2992	2150998	1735	1236772	1256	914226	519247	394978	31,341	15,866	47,207	2,609
Feb	28	2972	1933449	1722	1112340	1250	821109	466818	354291	28,381	14,232	42,613	2,550
Mar	31	2983	2128176	1729	1222819	1254	905356	518171	387185	31,158	15,553	46,712	2,582
Apr	30	2948	2035410	1705	1166493	1243	868917	497249	371668	29,924	14,930	44,853	2,475
May	31	2916	2074638	1683	1185343	1234	889295	509911	379384	30,279	15,240	45,519	2,379
Jun	30	2831	1975677	1623	1123689	1208	851988	483214	368774	29,137	14,814	43,951	2,118
Jul	31	2808	2025483	1607	1149485	1201	875997	496507	379491	30,145	15,244	45,389	2,049
Aug	31	2813	2027822	1610	1151357	1203	876465	497111	379354	30,634	15,239	45,872	2,064
Sep	30	2878	1986981	1656	1132326	1222	854655	488878	365777	29,760	14,693	44,453	2,262
Oct	31	2894	2084734	1667	1192410	1227	892324	507128	385196	31,456	15,473	46,929	2,310
Nov	30	2987	2044757	1733	1173036	1255	871721	501996	369725	30,374	14,852	45,226	2,596
Dec	31	2978	2137674	1726	1229468	1252	908206	517582	390624	31341	15,691	15,691	2,568
									sum	332,588	181,827	514,415	28,563
												Total	542,978
												with VAT	646,144

6.3 Further remarks on the economics of CHP systems

In the above calculations, it was assumed that the cogeneration system runs according to the electric power demand, which is assumed fairly constant for the 24h period since this is a hospital.

However, in other situations, (factories etc), cogeneration system runs according to the heat demand, which could be of the order of 6000 h/a or less [69]. Heat demand is 100% only during the peak hours (usually about 2000 h/a). Heat demand then varies between 10-100% during the rest of the operating hours.

By assuming that the specific powerplant is designed to operate for several thousand hours a year, it is considered to be a supplier of the energy market. However, additional legislative measures in the future may modify the size optimization constraints. For example, according to the US Federal Energy Commission order 888, (April 1996), an ancillary service market of electricity is also open for competition in the US. It includes regulation and frequency response services; spinning and non-spinning reserve markets, supplementary and reactive reserves as well as black start services. Ancillary services help network operators to keep the balance between production and consumption within seconds. Thus, they are crucial to avoid blackouts. The design criteria for the power systems are currently planned in such a way that the reliability of electricity is 99.99% at the consumer's site. This means that the utilities should have 15-20% of reserve capacity. They should withstand a trip of the largest unit in the system and thus have primary, secondary and tertiary frequency control system and operating reserve [69].

The US markets enable electricity generators to monetize the value of operational flexibility. States that have enacted retail generation choice usually become a part of a regional Independent System Operator (ISO), whose purpose is to monitor and control the generation and transmission system over a service area.

To balance the supply and demand for generation in a deregulated environment, each ISO acts as a clearinghouse for two wholesale markets: the day-ahead and the hour-ahead market. Once it receives all the bids for both supply and demand, the ISO schedules generation. Each generator company is paid the clearing price of the marginal unit which gets dispatched. The clearing price is determined by classical supply and demand economics.

The ISO has a pool of resources that can be called upon at a moment's notice to either increase or decrease the amount of delivered MW. Several important ancillary services definitions are listed below:

Regulation up: the control center sends a real-time signal to the generator to control frequency (by adding stepwise MW).

Regulation down: the control center sends a real-time signal to the generator to control frequency (by reducing stepwise MW).

Spinning reserve: requires generator synchronization to the grid with 10-minute ramp-up time to full load.

Non-spinning reserve: non-synchronized generator that can start, synchronize to the grid and ramp-up to full load within 10-minutes.

Out-of-market energy: energy that is dispatched at a marginal cost above the market price, in order to provide reliability to a sub-region [70]

As an example, in the area serviced by the Pennsylvania ISO (PJM), which is a major ISO in the US energy market, the ancillary service markets and energy market are evaluated simultaneously one day before. The highest process are a result of market conditions, when all power plants sell their output first in the day-ahead markets and there is nothing left for the regulation markets. The regulation prices can fluctuate greatly (see for example the fluctuation of hourly locational marginal prices in the PJM ISO in 4 August 2004) and the extra incomes from the regulation markets are uncertain. The highest fluctuations of demand and prices happen, when the power consumption changes because of unexpected changes in ambient temperatures. The size of the regulation reserve markets is about 2% of peak capacity. The offered regulation reserve should be delivered within 5 minutes from the AGC signal given by the Pennsylvania ISO dispatch center.

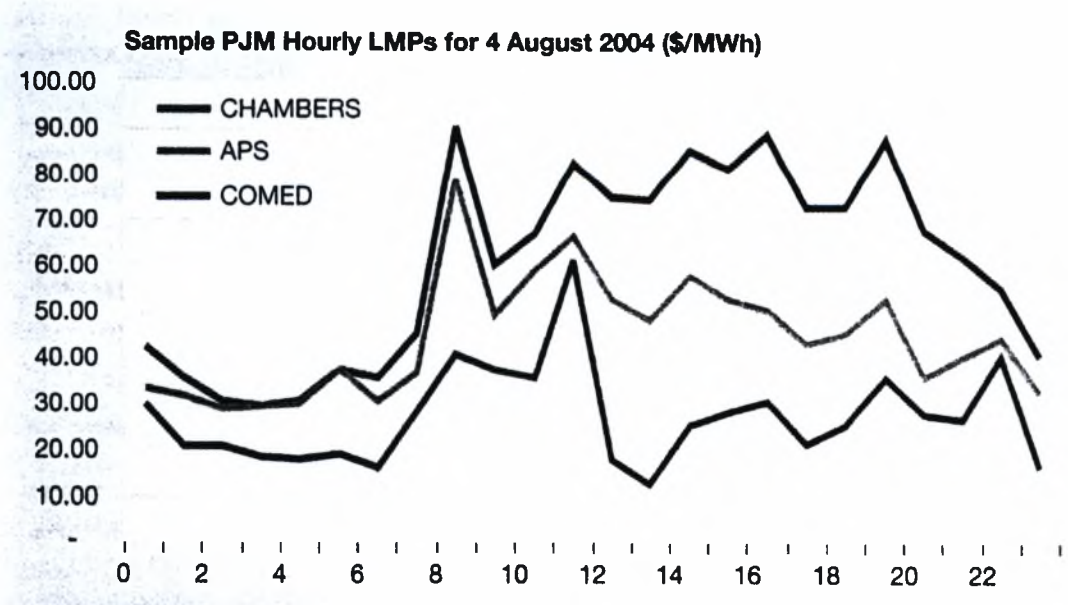

Figure 55 Hourly locational marginal prices in Pennsylvania (PJM) during the 4th of August 2004 [70].

Ancillary service markets are currently opened also in continental Europe. The sizing of fast- load - response cogeneration systems based on aeroderivative gas turbines and reciprocating engines should gradually take into account the possibility of marketing ancillary services as well. The role of transient modeling and study of transient operation characteristics is expected to increase in this area.

7 Concluding Remarks

This study demonstrates the use of transient simulation in the design of tri-generation systems.

Following a literature study of in-use methodologies for the design of cogeneration systems, it was concluded that system design is usually based on the system's steady state operation characteristics.

However, due to the nature of cogeneration systems' thermal and cooling loads, there exists a significant seasonal and daily variation that cannot be taken into account in steady state calculations.

Based on this observation, an objective is set in this study to develop transient modelling as a means of supporting an improved cogeneration system design and optimization methodology.

A hospital tri-generation system, based on a combined cycle, is selected as a case study for the development and application of the transient simulation.

The development of the transient simulation model was carried out in the TRNSYS simulation environment, mainly using existing components of the TRNSYS, TESS and STEC libraries.

A yearly simulation of a tri-generation system which produces the nominal electric power of the hospital (2.5 MW) was carried out. The analysis of the simulation results indicated that a low degree of exploitation of the produced heat was attained. Thus, the economics of this initial sizing were not favourable.

Next, a second simulation was carried out, with a reduced size of the cogeneration system, which now produced only a nominal electric power of 1.5 MW. The analysis of the simulation results for this new version indicates a more favourable economic situation.

The discussion of the simulation results corresponding to the two different system's sizes allows good understanding of the real system operation and its dependence on the ambient conditions, load variations and schedules.

The exploitation of the system's modelling in the development of an optimization methodology is expected to be the subject of future activity.

REFERENCES

1. Onovwionaa, H.I. and V.I. Ugursalb, *Residential cogeneration systems: review of the current technology* Renewable and Sustainable Energy Reviews, 2006. **10**: p. 42.
2. Horlock, J.H., Cogeneration: Combined Heat and Power Dynamics Thermodynamics and Economics. 1987, United Kingdom: Pergamon Books Ltd.
3. Frangopoulos, *CA. EDUCOGEN, The European Educational Tool on Cogeneration*, E. Commission, Editor. 2001, http://www.cogen.org/projects/educogen.htm.
4. HESSAMI, A.W.a.M.A., *Two Case Studies of Cogeneration Systems Design and Economic Feasability.* Heat Recovery Systems & CHP, 1993. **13**(2): p. 19.
5. Kolanowski, B.F., *Small-Scale Cogeneration Handbook* 2nd ed. ed. 2003, New York: Fairmont Press.
6. Wu, D.W. and R.Z. Wang, *Combined cooling, heating and power: A review.* Progress in Energy and Combustion Science, 2006. **32**: p. 459-495.
7. Kugeler and Phlippen, *Energietechnik.* 1998: Springer Verlag.
8. Mattingly, J.D., *Elements of Gas Turbine Propulsion.* 1996, New York: McGraw Hill.
9. Levy, C., Les techniques de cogeneration, in Les Techniques de l' Ingenieur. 2002: Paris.
10. Klimstra, J., The future for reciprocating engines in cogeneration installations in Europe, in 2nd CHAPNET Conference. 2004: Brussels.
11. Klimstra, J. Natural Gas Fuelled Cogeneration - An Overview of the Emission Aspects. in Intersociety Energy Conversion Engineering Conference. 2001.
12. Cardona, E., A. Piacentino, and F. Cardona, *Energy saving in airports by trigeneration. Part I: Assessing economic and technical potential.* Applied Thermal Engineering, 2006. **26**: p. 1427-1436.
13. Cardona, E., et al., Energy saving in airports by trigeneration. Part II: Short and long term planning for the Malpensa 2000 CHCP plant. Applied Thermal Engineering, 2006. **26**: p. 1437-1447.
14. Hoggarth, M.L., Reseach and development by British Gas into the effective use of gas in industry. Energy combustion sience, 1979. **5**: p. 169-192.
15. Bassols, J., et al., *Trigeneration in the food industry.* Applied Thermal Engineering, 2002. **22**: p. 595-602.
16. Magloire, P., T. Heteu, and L. Bolle, *Economie d'énergie en trigénération.* International Journal of Thermal Sciences 2002. **41** p. 1151–1159.
17. Boyce, M.P., *Gas Turbine Engineering Handbook.* 2 ed. 2002, Houston, Texas: Gulf Professional Publishing.
18. Peltier, R., Brooklyn Navy Yard Cogeneration Facility Power, 2006. **150**(6).
19. Beer, J.M., Combustion technology developments in power generation in response to environmental challenges. Progress in Energy and Combustion Science 2000. **26**: p. 301–327.
20. Boyce, M., Handbook for Cogeneration and Combined Cycle Power Plants. 2004: ASME Publications.
21. Beer, J.M., *High effeciency electric power generation : The enviroment role.* Progress in Energy and combustion science, 2007. **33**: p. 107-134.
22. WECC, Northwest Power Planning Council: New Resource Characterization for the Fifth Power Plan:Natural Gas Combined-cycle Gas Turbine Power Plants. 2002.
23. NN, *TRNSYS 16 Manual.* 2005, Solar Energy Laboratory, University of Wisconsin - Madison: Wisconsin - Madison.
24. NN. *STEC library.* 2006 [cited; Available from: http://elib.dlr.de/1754/.
25. Schwarzbözl, P. A TRNSYS Model Library for Simulation of Solar Thermal Electric Power Generation Systems. in III. International TRNSYS User Days. 2004. Barcelona, 29.03.2004.

26. Chmielniak, T., W. Kosman, and G. Kosman, Simulation modules of thermal processes for performance control of CHP plant with a gas turbine unit. Applied Thermal Engineering, 2007. **27**: p. 2181–2187.
27. Ziher, D. and A. Poredos, *Cooling power costs froma trigeneration system in a hospital.* Forsch Ingenieurwes 2006. **70**: p. 105–113.
28. Yilmaz, T., Optimization of cogeneration systems under alternative performance criteria. Energy Conversion and Management, 2004. **45**: p. 7.
29. Cardona, E., et al., Energy saving in airports by trigeneration. Part II: Short and long *term planning for the Malpensa 2000 CHCP plant.* Applied Thermal Engineering 2006. **26**: p. 1437–1447.
30. Cardona, E., A. Piacentino, and F. Cardona, Energy saving in airports by trigeneration. Part I: Assessing *economic and technical potential.* Applied Thermal Engineering 2006. **26**: p. 1427–1436.
31. O'Brien, J.M. and P.K. Bansal, Modelling of cogeneration systems Part 2: development of a quasi-static cogeneration model (steam turbine cogeneration analysis). Proc Instn Mech Engrs Part A, 1999. **214**.
32. O'Brien, J.M. and P.K. Bansal, *Modelling of cogeneration systems Part 1: historical perspective.* Proc Instn Mech Engrs Part A, 1999. **214**.
33. O'Brien, J.M. and P.K. Bansal, Modelling of cogeneration systems Part 3: application of steam turbine cogeneration analysis to Auckland Hospital cogeneration utility system. Proc Instn Mech Engrs Part A, 1999. **214**.
34. Zheng, L. and E. Furimsky, *ASPEN simulation of cogeneration plants.* Energy Conversion and Managment, 2002. **44** p. 7.
35. Zhen Huang, W., M. Zaheeruddin, and S.H. Cho, *Dynamic simulation of energy management control functions for HVAC systems in buildings.* Energy Conversion and Management, 2006. **47** p. 926–943.
36. Cardona, E. and A. Piacentino, *A methodology for sizing a trigeneration plant in mediterranean areas.* Applied Thermal Engineering, 2003. **23**: p. 1665-1680.
37. Hinojosa, L.R., et al., *A comparison of combined heat and power feasibility models.* Applied Thermal Engineering 2007. **27**: p. 2166–2172.
38. Παππάς, Θ., Ανάλυση και Βελτιστοποίηση Παραμέτρων Λειτουργίας του Σταθμού Συμπαραγωγής Ηλεκτρισμού και Θερμότητας των Εργοστασίων ΒΙΟΚΑΡΠΕΤ Α.Ε.-ΕΞΑΛΚΟ Α.Ε. Μεταπτυχιακή Εργασία, in Τμήμα Μηχανολόγων Μηχανικών. 2006, Πανεπιστήμιο Θεσσαλίας: Βόλος.
39. Temir, G. and D. Bilge, *Thermoeconomic analysis of a trigeneration system.* Applied Thermal Engineering, 2004. **24**: p. 2689-2699.
40. Tsatsaronis, G. and M. Winhold, Exergoeconomic analysis and evaluation of energy-conversion plants - I. A new general methodology. Energy, 1985. **10**: p. 69–80.
41. Frangopoulos, C.A., Thermal-economic functional analysis and optimization. Energy 1986. **12**: p. 563–71.
42. Misa, T., et al., *Thermodynamic Analysis of an in-situ Cogeneration plant.* Proc Instn Mech Engrs Part A, 2007.
43. Cardona, E. and A. Piacentino, *Optimal design of CHCP plants in the civil sector by thermoeconomics.* Applied Energy, 2007. **84**: p. 729-748.
44. Silveira, J.L. and C.E. Tuna, *Thermoeconomic analysis method for optimization of combined heat and power systems. Part I.* Progress in Energy and combustion science, 2003. **29**: p. 479-485.
45. Silveira, J.L. and C.E. Tuna, *Thermoeconomic analysis method for optimization of combined heat and power systems—part II.* Progress in Energy and combustion science, 2004. **30**: p. 673-678.

46. Rong , A. and R. Lahdelma, An efficient linear programming model and optimization algorithm for trigeneration. Applied Energy, 2005. **82**: p. 40-63.
47. Arcuri, P., G. Florio, and P. Fragiacomo, A mixed integer programming model for optimal design of trigeneration in a hospital complex. Energy, 2005. **32**: p. 1430-1447.
48. NN, T.E.S.S. Component Libraries for TRNSYS, version 2.0. User's Manual, . 2004, Madison WI.
49. Drake, F.D., Evaluating Cogeneration Operations for a Campus Heating and Cooling Plant, in Mechanical Engineering, Solar energy Lab. 1988, WISCONSIN MADISON
50. Dixon, S.L., *Fluid Mechanics and Thermodynamics of Turbomachinery*. 4 ed. 1998: Butterworth - Heinemann.
51. Liao, X. and R. Radermacher, Absorption chiller crystallization control strategies for intergrated cooling heating and power systems. International journal of Refrigeration 2007. **30**: p. 904-911.
52. Marantan, A. and R. Radermacher, Optimization of Microturbines and Absorption Chillers in CHP for Buildings Applications, in CHP Consortium Meeting. 2002: Univ. of Maryland.
53. Casals, X.G.a., Solar absorption cooling in Spain: Perspectives and outcomes from the simulation of recent installations. Renewable Energy, 2006. **31**: p. 1371-1389.
54. LS. *Double effect absorption chillers*. LS Katalog 2006 [cited; Available from: www.lsaircondition.com.
55. NN, *ASHRAE Handbook* Vol. 4: Systems and Equipment. 2000.
56. CRES, Energy audits - Volos Public Hospital. 2000: Athens.
57. Cardona, E. and A. Piacentino, A measurement methodology for monitoring a CHCP pilot plant for an office building. Energy and Building, 2003. **35**: p. 919-925.
58. Lin, L., et al., *An experimental investigation of a household size trigeneration.* Applied Thermal Engineering, 2007. **27**: p. 576-585.
59. Levy, C. and J.-P. Tabet, Cogeneration en Genie Climatique, in Les Techniques de l' Ingenieur. 2002: Paris.
60. Horngren, C., G. Foster, and S. Datar, *Cost Accounting: A Managerial Emphasis*. 10 ed. 2000, Upper Saddle River, NJ: Prentice Hall.
61. Plinke, W., *Industrielle Kostenrechnung fuer Ingenieure*. 1989, Berlin: Springer Verlag.
62. Jones, T., Business Economics and Managerial Decision Making. 2005: John Wiley and Sons, Ltd.
63. Anderson, P.L., *Business Economics and Finance with MATLAB, GIS, and Simulation Models*. 2005, Boca Raton, FL: Chapman & Hall/ CRC Press LLC.
64. Zogg, R., K. Roth, and J. Brodrick, *Using CHP Systems In Commercial Buildings.* ASHRAE Journal, 2005.
65. NN, *World Energy Outlook 2006*. 2006: OECD/IEA.
66. RETSCREEN. *RETScreen Software Online User Manual.* [cited; Available from: http://www.retscreen.net.
67. NN, Natural Gas Market Review 2007. 2007: OECD/IEA.
68. Huamani, M.M. and A.F. Orlando, Methodology for generating thermal and electric load profiles for designing a cogeneration system. Energy and Buildings 2007. **39**: p. 1003–1010.
69. Vuorinen, A., *Planning of Optimal Power Systems*. 2007, Espoo, Finland: Ekoenergo Oy.
70. Lytikainen, E., Ancillary Services: more added value to the customers in Wartsila Energy News. 2005. p. 24-26.

ANNEX I Prices of electricity and Natural Gas in the Greek Market (May 2007)

Table 24 Electricity pricing (DEH): medium voltage (20 kV)

ELECTRICITY TARIFFS (medium voltage)	
Monthly charges	
A. GENERAL USE TARIFFS	
1 Tariff B1	
Power: charged demand (XZ)	10,1817 €/kW
Energy: the first 400 kWh per kW (MZ) The remaining kWh	0,06064 €/kWh 0,04017 €/kWh
Minimum charges for XZ<= 5 kW	233,26 €
Minimum charges for XZ> 5 kW	2,3272*(XZ-5)+233,26 €

Table 25 Selling of electricity produced by cogeneration and alternative energy sources.

ELECTRICITY TARIFFS (FROM COGENERATION AND RENEWABLES TO DEH)				
	NON-INTERCONNECTED SYSTEM	INTERCONNECTED SYSTEM		
		LOW VOLTAGE	MEDIUM VOLTAGE	HIGH VOLTAGE
Surplus of self-production from cogeneration installations with conventional fuels (renewables exluded)		0,05639 €/kWh	0,04561 €/kWh	Energy (€/kWh): Peaking: 0,02978 Intermediate load: 0,02063 Minimum load: 0,01531
Independent producer with conventional fuels (renewables exluded)			Energy: 0,05321 €/kWh Power: 1,75645 €/kW	Energy (€/kWh): Peaking: 0,03475 Intermediate load: 0,02407 Minimum load: 0,01786
Surplus of self-production from renewables (with or without cogeneration)	From renewables: 0,06579 €/kWh From cogeneration: 0,05639 €/kWh	0,06579 €/kWh	0,05321 €/kWh	Energy (€/kWh): Peaking: 0,03475 Intermediate load: 0,02407 Minimum load: 0,01786
Independent producer from renewable sources (with or without cogeneration)	0,08458 €/kWh		Energy: 0,06842 €/kWh Power: 1,75645 €/kW	Energy: 0,06842 €/kWh Power: 1,75645 €/kW

Table 26 Cogeneration – HVAC Tariffs: business-to-business

Cogeneration – HVAC Tariffs: B2B 1st quarter 2007	
ATTIKI GAS SUPPLY COMPANY	
112, Pireos Str., 11854 Athens, Tel. 210-3406000, Fax.210-3406040	
	Cogeneration – HVAC Yearly consumption > 100.000 Nm3
Power charges	232 €/MW of maximum hourly consumption per month
Energy charges (€/MWh)	36.19
Discount for equipment modification	7.5 €/MWh to 5.5 €/MWh depending on the total equipment power. Maximum amount of discount for the period of contract: from 188 to 138 €/kW MTD

Table 27 Large commercial sector tariffs

Large commercial sector tariffs May 2007			
ATTIKI GAS SUPPLY COMPANY			
112, Pireos Str., 11854 Athens, Tel. 210-3406000, Fax.210-3406040			
	Space heating Yearly consumption> 100.000 Nm3	Large commercial sector Yearly consumption > 100.000 Nm3	
Power charges	160 - 650 m3/h €47,50/month Greater than 650 m3/h €85,00/month	232 €/MW of maximum hourly consumption per month	
Energy charges (€/MWh)	38,88	The first 180 MWh/month	42,86
		The remaining MWh/month	41,07
Discount for equipment modification for shift to NG	60% of non-subsidized cost of modification of burners and internal installation (up to 1.5 €/MWh)